

UC Merced

UC Merced Electronic Theses and Dissertations

Title

Impact of Locally-Sourced Biochar Amendments on Soil Hydrology and Ecosystem Services: A Study of Moisture Retention, Plant Uptake Dynamics, Nutrient Retention, and Greenhouse Gas Emissions in Agroecosystems

Permalink

<https://escholarship.org/uc/item/62x2w3gs>

Author

Thao, Touyee

Publication Date

2023

Peer reviewed|Thesis/dissertation

UNIVERSITY OF CALIFORNIA, MERCED

Impact of Locally-Sourced Biochar Amendments on Soil Hydrology and Ecosystem Services: A Study of Moisture Retention, Plant Uptake Dynamics, Nutrient Retention, and Greenhouse Gas Emissions in Agroecosystems

DISSERTATION

submitted in partial satisfaction of the requirements  
for the degree of

DOCTOR OF PHILOSOPHY

in Environmental Systems

by

Touyee Thao

Dissertation Committee

Teamrat A. Ghezzehei (Chair)  
Rebecca Ryals  
Gerardo C. Diaz  
Ruth Dahlquist-Willard

2023

© 2023 Touyee Thao

---

Rebecca Ryals

---

Gerardo C. Diaz

---

Ruth Dahlquist-Willard

---

Teamrat A. Ghezzehei (Chair)

## **Dedication**

This PhD dissertation is dedicated to my wife Kalneng Xiong and son Liyeng Kyro Thao. Thank You both for your unconditional love, support, and for being patient with me. To my parents Cheryia Thao and Chong Vang. Thank You both for your unconditional love, care, and guidance. To my nine siblings (Cha, Vang Lue, Chia, Mai Zoua, Mai Chue, Tou Pao, Tou Bee, Tou Ger, and baby brother Neng). I hope I make you all proud.

## TABLE OF CONTENTS

<b>List of Figures.....</b>	<b>viii</b>
<b>List of Tables .....</b>	<b>x</b>
<b>Acknowledgements .....</b>	<b>xii</b>
<b>Vita .....</b>	<b>xiii</b>
<b>Abstract of the Dissertation .....</b>	<b>xviii</b>
<b>Chapter 1. Introduction .....</b>	<b>1</b>
<b>1.1 Research Objectives.....</b>	<b>2</b>
<b>1.2 Organization of the Dissertation.....</b>	<b>2</b>
<b>1.3 References .....</b>	<b>2</b>
<b>Chapter 2. Seven biochars and their impact on moisture retention and respiration rate of a coarse -textured soil, exclusively at the mid to dry water regions .....</b>	<b>5</b>
<b>Abstract.....</b>	<b>5</b>
<b>2.1 Introduction.....</b>	<b>5</b>
2.1.1 Water Film Approach to Determine Specific Surface Area .....	6
2.1.2 Research Objective .....	7
<b>2.2 Materials and Method .....</b>	<b>7</b>
2.2.1 Biochar .....	7
2.2.2 Soil Water Retention (Mid to Dry Region) & SSA .....	8
2.2.3 5% Biochar Mass-based Moisture Retention Model & Application Rates.....	8
2.2.4 Incubation Experiments .....	9
2.2.5 CO <sub>2</sub> Measurements .....	10
2.2.6 Statistical Analysis.....	10
<b>2.3 Results .....</b>	<b>10</b>
2.3.1 Biochar WRC and 5% Application Model .....	10
2.3.2 WRC for 5% and 10% Application Rates.....	11
2.3.3 CO <sub>2</sub> Respiration from Incubation Experiments .....	11

<b>2.4 Discussion</b> .....	<b>12</b>
2.4.1 Biochar and Mixtures SSA estimated using WSI Approach .....	12
2.4.2 Biochar Influence on SWRC .....	13
2.4.3 Biochar Influence on Soil Respiration under Different Moisture Conditions. ....	13
<b>2.5 Conclusion</b> .....	<b>14</b>
<b>2.6 Reference</b> .....	<b>15</b>

**Chapter 3. Impact of biochar amendments on soil water and plant uptake  
dynamics under different cropping systems.....25**

<b>Abstract</b> .....	<b>25</b>
<b>3.1 Introduction</b> .....	<b>25</b>
<b>3.2 Materials and Method</b> .....	<b>27</b>
3.2.1 Modeling Strategy.....	27
3.2.2 Model Setup .....	28
3.2.3 Biochar & Soil Water Retention Curves (SWRC).....	28
3.2.4 Cropping Systems .....	29
3.2.5 Meteorological Forcing.....	30
3.2.6 Crop Yield and WUE.....	30
<b>3.3 Results</b> .....	<b>30</b>
3.3.1 Impact of Biochar Application to Rainfed Pasture .....	30
3.3.2 Pasture Yield and WUE.....	31
3.3.3 Impact of Biochar Application to Irrigated Fresh-market Tomato .....	31
3.3.4 Tomato Yield and WUE .....	32
3.3.5 Tomato Economic Trade-off.....	32
<b>3.4 Discussion</b> .....	<b>33</b>
3.4.1 Biochar Application under Rainfed versus Irrigated Systems .....	33
3.4.2 Comparison across Biochar Types.....	33
3.4.3 Indirect Benefits of Biochar Application .....	34
3.4.4 Model Limitations.....	34
<b>3.5 Conclusion</b> .....	<b>35</b>
<b>3.6 Reference</b> .....	<b>35</b>

<b>Chapter 4. The effects of different biochar-dairy manure co-composts on soil hydraulic properties, nutrients retention, greenhouse gas emissions, and tomato productivity; observations from a soil column experiment .....</b>	<b>51</b>
<b>Abstract.....</b>	<b>51</b>
<b>4.1 Introduction.....</b>	<b>51</b>
4.1.1 Research Objectives.....	52
<b>4.2 Materials and Methods.....</b>	<b>52</b>
4.2.1 Tomato Column Experiment.....	52
4.2.2 Column Measurement.....	53
4.2.3 Soil Hydrological Properties.....	54
4.2.4 Greenhouse Gas Emissions.....	54
4.2.5 Nutrient Retention and Soil Analysis .....	54
4.2.6 Statistical Analysis.....	55
<b>4.3 Results .....</b>	<b>55</b>
4.3.1 Crop Productivity.....	55
4.3.2 Soil Hydrological Properties.....	56
4.3.3 Nutrient Retention.....	56
<b>4.4 Discussion.....</b>	<b>57</b>
4.4.1 Influence on Crop Productivity.....	57
4.4.2 Crop Productivity under Irrigation Schemes .....	57
4.4.3 Influence on Soil Hydrological Properties.....	58
4.4.4 Influence on Soil Nutrient Retention .....	59
4.4.5 Influence on GHGs .....	59
4.4.6 Offset between Agroecological based Soil Management vs Crop Productivity.....	59
<b>4.5 Conclusion .....</b>	<b>60</b>
<b>4.6 Reference .....</b>	<b>61</b>
<b>Chapter 5. Conclusion .....</b>	<b>73</b>
<b>Appendices.....</b>	<b>74</b>
<b>Appendix A: Supplemental for Chapter 2.....</b>	<b>74</b>
<b>Appendix B: Supplemental for Chapter 3 .....</b>	<b>75</b>
<b>Appendix C: Supplemental for Chapter 4.....</b>	<b>82</b>

## LIST OF FIGURES

Figure 2-1 Film model used to determine materials specific surface area. Assuming a Hamaker constant of $1.90E-19$ J and one monolayer of film water is $3.50E-10$ m. ....	19
Figure 2-2 WRC for seven different biochar. Mean of three replications with standard error bar. ....	19
Figure 2-3 Modeled Atwater loamy-sand SWRC for 5% biochar application rate. ....	20
Figure 2-4 SWRC for 5% application rate, derived using WP4C. Mean of three replications with standard error bar. ....	20
Figure 2-5 SWRC for 10% application rate, derived using WP4C. Mean of three replications with standard error bar. ....	21
Figure 2-6 CO <sub>2</sub> flux for both MC and MD experiments taken throughout the incubation period. Mean of four replications with standard error bar. ....	21
Figure 2-7 Labile carbon fraction (a), total CO <sub>2</sub> loss (b), and initial rates (fast and slow pools, c and d) of carbon loss for Moisture Constant incubation. ....	22
Figure 2-8 Rate of carbon loss for Moisture Dynamic incubation, y-axis is CO <sub>2</sub> flux in mgC/gC/d and x-axis is moisture content in g/g. ....	23
Figure 3-1 Conceptual diagram of HYDRUS 1-D simulation domain demonstrating control and biochar amendment scenarios for two cropping systems. ....	42
Figure 3-2 Soil Water Retention Curves for control and individual biochars, AS-2, WS-2, and ATC-1. ....	42
Figure 3-3 Moisture profile over time for rainfed control (A) and rainfed AS-2 (B). Solid black line represents the initial soil moisture content (day zero), and solid red line is moisture content in August for the 5th year. All other curves represent yearly moisture content for the month of August. ....	43
Figure 3-4 Seasonal moisture comparison between rainfed control and rainfed AS-2 biochar for the topsoil (A) and bottom soil layer (B). ....	44
Figure 3-5 Cumulative evaporation (A) and Cumulative surface and drainage fluxes (B). ....	45

Figure 3-6 Seasonal moisture comparison between irrigated control and irrigated AS-2 biochar for the topsoil (A) and bottom soil layer (B). .....	46
Figure 3-7 Moisture profile over time for irrigated control (A) and irrigated AS-2 (B). Solid blue line represents the initial soil moisture content (day zero), and solid red line is post-season soil moisture content (August) for the 5th year. All other curves represent yearly post-season (August) moisture content. ....	47
Figure 3-8 Moisture profile over time for irrigated control (A) and irrigated AS-2 (B). Solid blue line represents the initial soil moisture content (day zero), and solid red line is post-season soil moisture content (August) for the 5th year. All other curves represent yearly post-season (August) moisture content. ....	48
Figure 3-9 WUE Comparison in ton/hectare/mm of water, for rainfed grassland and irrigated tomato system. ....	49
Figure 4-1 Tomato fruit yield (a) and sugar content (b). Mean of three replications with standard error bar. ....	66
Figure 4-2 Tomato water use efficiency (WUE). Unit is expressed as ton/hectare/m. Mean of three replications with standard error bar .....	67
Figure 4-3 Moisture retention curves for soil treatments in the tomato column, where x-axis is gravimetric water content and y-axis is suction potential. Mean of three replications with standard error bar. ....	67
Figure 4-4 Post flushed soil $\text{NO}_3^-$ -N and $\text{NH}_4^+$ -N with depth for 100% $\text{ET}_c$ (a, c) and 75% $\text{ET}_c$ (b, d). Mean of three replications with standard error bar.....	68
Figure 4-5 $\text{NO}_3^-$ -N (a) and $\text{NH}_4^+$ -N (b) concentration in leachate collected at the end of tomato study. Mean of three replications with standard error bar. ....	69
Figure 4-6 Fruit-set count taken throughout the season, x-axis is soil organic treatments and y-axis is replications. ....	70
Figure 4-7 Summary of tomato column experiment. An increase, decrease, or equal is in response to soil organic amendments.....	70

## LIST OF TABLES

Table 2-1. R134a absorbance, bulk density, and hydrophobicity of biochar and mixtures.....	23
Table 2-2. Initial Moisture for Incubation Experiments .....	24
Table 2-3. Carbon and nitrogen content of soil and biochar.....	24
Table 2-4. Specific surface area for biochar, 5%, and 10% rates .....	24
Table 3-1. Physical Characteristics of soil layers used in model simulations .....	49
Table 3-2. Chemical Characteristics of soil layers used in model simulations .....	49
Table 3-3 van Genuchten Parameters used in model simulations .....	50
Table 3-4 Annual ET <sub>o</sub> and precipitation .....	50
Table 3-5 Non-Irrigated Pasture Water Applied & Yield.....	50
Table 3-6 Irrigated Tomato Water Applied &. Yield Comparison.....	50
Table 3-7 Irrigated Tomato Economic Comparison .....	50
Table 4-1 Mean greenhouse gas emissions (n = 3), measured with Picarro Gas Analyzer. Data analyzed using a two-way ANOVA, followed by Tukey-HSD test given statistical significance detected. Value with letters indicate statistically significant (p < 0.10) among soil treatments, whereas value with the * asterisk indicates statistical significance across irrigation level.....	71
Table 4-2 Relationship between yield vs mean chlorophyll content and fractional green canopy.....	72
Table S4-1. Tomato yield. Dataset analyzed using a two-way ANOVA, followed by Tukey-HSD test given statistical significance detected. Value with letter's indicate statistically significant (p < 0.10) among soil treatment, whereas value with the * asterisk indicate statistical significance across irrigation level. ....	82
Table S4-2 Water Droplet Penetration Test.....	83
Table S4-3 Mean fractional groundcover (n = 3), measured with the Canopeo Apps. Data analyzed using a two-way ANOVA, followed	

by Tukey-HSD test given statistical significance detected. Value with the \* asterisk indicate statistical significance across irrigation level.....85

Table S4-4. Mean plant chlorophyll content (n = 3) measured throughout the season using the SPAD 502 meter. Data were analyzed using a two-way ANOVA, followed by Tukey-HSD test given statistical significance detected. Value with letter's indicate statistically significant ( $p < 0.10$ ) among soil treatment, whereas value with the \* asterisk indicate statistical significance across irrigation level.....86

## ACKNOWLEDGEMENTS

This work was supported by the Mobile Biochar Production for Methane Emission Reduction and Soil Amendment project funded by California Strategic Growth Council, Climate Research Program under Grant Agreement #CCR20014, the University of California Office of the President under the Global Food Initiative Fellowship, Secure Water Future Fellowship, and Central Valley Graduate Fellowship. The author would like to express his sincere gratitude to Dr. Asmeret A. Berhe for her mentorship and role as a committee member before she was confirmed by the US Senate to serve as the Director of the DOE Office of Science. The author also acknowledged several individual including Dr. Hugh McLaughlin for providing the seven tested biochars, Mya Star Tabares (FACTs student mentee) for her assistance in the tomato study, Dr. Si Gao, Brendan P. Harrison, and Melinda Gonzalez for their assistance with the different projects.

## VITA

Touyee Thao

### EDUCATION

#### **Doctoral of Philosophy – Environmental Systems**

*University of California, Merced – Expected Graduation Date, May 2023*

- Faculty Advisor: Dr. Teamrat A. Ghezzehei
- **GPA: 4.0**

#### **Master of Science – Plant Science/ Soil-Water Management**

*California State University, Fresno – Graduated May 2017 (With Distinction)*

- **GPA: 4.0.**
- **Thesis title:** Developing Crop Coefficient ( $K_c$ ) for Sugar Beet (*Beta Vulgaris*) under Drip Irrigation System Using Weighing Lysimeter.

#### **Bachelor of Science – Plant Science/ Crop Production Management**

*California State University, Fresno – Graduated May 2014 (Magna Cum Laude)*

- **GPA: 3.74.**

### PROFESSIONAL EXPERIENCE

#### **Graduate Student Researcher**

*University of California, Merced*  
*Advisor: Dr. Teamrat A. Ghezzehei*

*August 2019 - Current*  
*Merced, CA*

#### **LBNL Affiliate**

*Lawrence Berkeley National Lab*  
*Mentor: Dr. Bhavna Arora*

*January 2021 – Current*  
*Berkeley, CA*

#### **Teaching Assistant**

*University of California, Merced*  
*Advisor: Dr. Teamrat A. Ghezzehei*

*August 2018 – July 2019*  
*Merced, CA*

#### **Research Technician**

*Center for Irrigation Technology, Fresno State*  
*Supervisor: Dr. Florence Cassel Sharma*

*May 2017 - August 2018*  
*Fresno, CA*

#### **Graduate Research Assistant**

*Center for Irrigation Technology, Fresno State*  
*Supervisor: Dr. Florence Cassel Sharma*

*August 2014 – May 2017*  
*Fresno, CA*

#### **Undergraduate Research Assistant**

*Center for Irrigation Technology, Fresno State*  
*Supervisor: Dr. Dave Goorahoo*

*August 2011- July 2014*  
*Fresno, CA*

### PUBLICATIONS

#### **Peer-reviewed**

1. S. Gao, B.P. Harrison, **T. Thao**, M. Gonzalez, D. An, T.A. Ghezzehei, G. Diaz, and R. Ryals., 2023. Biochar co-compost improves nitrogen retention and reduces carbon emissions in a winter wheat cropping system. *Global Change Biology, Bioenergy*. <http://doi.org/10.1111/gcbb.13028>

2. B.P. Harrison, S. Gao, M. Gonzalez, **T. Thao**, E. Bischak, T.A. Ghezzehei, A.A. Berhe, G. Diaz, R. Ryals., 2022. Dairy Manure Co-composting with Wood Biochar Plays a Critical Role in Meeting Global Methane Goals. *Environmental Science & Technology*. <https://doi.org/10.1021/acs.est.2c03467>
3. T. Longbottom, L. Wahab, K. Min, A. Jurusik, K. Moreland, M. Dolui, **T. Thao**, M. Gonzales, Y. Perez-Rojas, J. Alvarez, Z. Malone, J. Yan, T.A. Ghezzehei, A.A. Berhe., 2022. What's soil got to do with climate change?. *Geological Society of America*. <https://doi.org/10.1130/GSATG519A.1>
4. T. Wang, F. S. Melton, I. Pôças, L. F. Johnson, **T. Thao**, K. Post, F. Cassel S., 2020. Evaluation of Crop Coefficient and Evapotranspiration Data for Sugar Beets from Landsat Surface Reflectances Using Micrometeorological Measurements and Weighing Lysimetry. *Agricultural Water Management* <https://doi.org/10.1016/j.agwat.2020.106533>

### **Manuscripts in preparation**

1. **T. Thao**, M. Gonzales, R. Ryals, R. Dahlquist-Willard, G. Diaz, and T.A. Ghezzehei., 2023. Seven biochars and their impact on moisture retention and respiration rate of a coarse -textured soil, exclusively at the mid to dry water regions. Manuscript to be submitted *European Journal of Soil Science*
2. **T. Thao**, B.P. Harrison, S. Gao, R. Ryals, R. Dahlquist-Willard, G. Diaz, and T.A. Ghezzehei., 2023. The effects of different biochar-dairy manure co-composts on soil hydraulic properties, nutrients retention, greenhouse gas emissions, and tomato productivity; observations from a soil column experiment. Manuscript submitted to *Agrosystems, Geosciences & Environment*.
3. **T. Thao**, V.D. Lopez, M. Gonzales, G.C. Diaz, and T.A. Ghezzehei., 2023. Evaluating the Effects of Temperatures, Particle Sizes, and Application Rates of Almond Shell Biochar on Soil Physical and Hydraulic Properties. Manuscript to be submitted *Agrosystems, Geosciences & Environment*.
4. **T. Thao**, B. Arora, and T.A. Ghezzehei., 2023. Impact of biochar amendments on soil water and plant uptake dynamics under different cropping systems. Manuscript submitted to *Vadose Zone Journal*
5. **T. Thao**., F. Cassel S., D. Goorahoo, J. Ayars, and Shawn Ashkan., 2023. Crop Water Requirement of Irrigated Sugarbeet Grown in the Central Valley. Manuscript to be submitted to *Journal of Agricultural Water Management*.

### **SELECTED PROCEEDINGS, ABSTRACTS, and PROFESSIONAL PRESENTATIONS**

1. **T. Thao**, T.A. Ghezzehei, and B. Arora. Evaluating the Hydrological Characteristics of Different Biochar and its Influence on Soil Water Dynamic. 2021 Universities Fighting World Hunger Summit. *Best Student Poster Award*.
2. **T. Thao** and T.A. Ghezzehei. Evaluating the Hydrological Characteristics of Different Biochar and its Influence on Soil Water Dynamic. 2020 Biochar: Agronomic and Environmental Uses. ASA-CSSA-SSSA. *1<sup>st</sup> Place Graduate Student Poster Winner*
3. D. Goorahoo., J. Samano-Monroy, F. Cassel S., **T. Thao**, G. Seepersad. 2017. Nitrate leaching index for surface drip- irrigated cauliflower fertilized with organic soybean meal. *HortScience* 52(9): S414-415. Supplement—2017 ASHS Annual Conference.
4. **T. Thao**., F. Cassel S., A. Mele, D. Goorahoo, and J. Ayars. 2017. Influence of Growing Degree Days on Sugarbeet (*Beta vulgaris*) Evapotranspiration and Crop

- Coefficient. Poster presentation at the California Chapter of the American Society of Agronomy, Fresno, CA. 2<sup>nd</sup> Place Graduate Student Poster Winner
5. D. Goorahoo., A.Unc, C. McCall, J. Samano-Monroy, F.Cassel S, **T. Thao**, and G. Seepersad. 2016 AirJection Irrigation Mitigates Denitrification and Leaching. Oral presentation at the Irrigation Show & Education Conference, Las Vegas, NV.
  6. E. R. Kent., R. L. Snyder., J. Clay., C. Little., **T. Thao**., F. Cassel S., B Sanden., D. Zaccaria. Measurement-based Actual Evapotranspiration in Pistachio Orchards Under Varying Soil Salinity. Climate Change, Water, and Society IGERT 2016 State of the Science & Policy Workshop, Davis, CA.
  7. **T. Thao**, F. Cassel S, D. Goorahoo., J. Ayars., and S. Ashkan. Evaluating Crop Water Requirements for Sugarbeet (*Beta vulgaris*) under Drip Irrigation. 2016 California Plant and Soil Conference, Visalia, CA. 1<sup>st</sup> Place Graduate Student Poster Winner
  8. **T. Thao**., F. Cassel S., D. Goorahoo., and S. Ashkan. Lysimetric Measurements of Evapotranspiration for Drip-Irrigated Crops. 2015 ASA-CSSA-SSSA International Conference, Minneapolis, MN. National award winner for student oral presentation

### AWARDS

1. Certificate of Excellence, Best Student Poster Award, Universities Fighting World Hunger Summit, 2021
2. 1<sup>st</sup> Place Graduate Student Poster Competition, Biochar Community, ASA-CSSA-SSSA, 2020
3. University Graduate Medalist, Fresno State, 2017
4. Outstanding Thesis Award, Jordan College of Agricultural Science and Technology, Fresno State, 2017
5. Certificate of Academic Achievement, Education Opportunity Program, Fresno State, 2017
6. All-University Graduate Student Leadership Award, Fresno State, 2017
7. Dean Medalist, Jordan College School of Agricultural Science and Technology, 2017
8. 2<sup>nd</sup> Place Graduate Student Poster Competition, CA Chapter of American Society of Agronomy, 2017
9. Research and Creative Activities Support Award, Fresno State, 2016
10. Gerald O. Mott Meritorious Graduate Student Award, ASA-CSSA-SSSA, 2016
11. 1<sup>st</sup> Place Graduate Student Poster Competition, CA Chapter of American Society of Agronomy, 2016
12. National Award Winner, Evapotranspiration Measurement and Modeling Community, ASA-CSSA-SSSA, 2015
13. Irrigation E3 Learner, Irrigation Association, 2014
14. Assemblyman Jim Patterson's Agriculture Science Students of the Year Award, 2014
15. Certificate of Recognition, Fresno County Farm Bureau, 2014
16. Certificate of Appreciation, United States Department of Agriculture, 2014
17. Undergraduate Student Achievement Award, Department of Plant Science, Fresno State, 2014
18. Standard Bearer, Jordan College of Agricultural Sciences and Technology, Fresno State, 2014
19. Dean's Medalist Nominee, Department of Plant Science, Fresno State, 2014

20. National Student Recognition Award, ASA-CSSA-SSSA, 2014
21. Golden Opportunity Scholar, ASA-CSSA-SSSA, 2013
22. EOP Summer Bridge - Counselor & Peer Mentor, Guardian of the Legacy Award, Fresno State, 2009
23. EOP Summer Bridge - Peer Mentor, Hard Working Award, Fresno State, 2009

**Award received by student mentee:**

1. Mya Starr Tabares: 1<sup>st</sup> place student poster, 2022 UC Merced FACTs symposium,

**SCHOLARSHIPS and GRANTS**

1. Central Valley Graduate Fellowship, 2023
2. Secure Water Future Climate Adaptation Science Academy Fellowship, 2022
3. Environmental Systems Bobcat & Seminar Fellowship, 2022
4. UCOP, Global Food Initiative-Berkeley Lab Fellowship, 2021-2022
5. UCOP, Global Food Initiative-Berkeley Lab Fellowship 2020-2021
6. Environmental Systems Professional Fellowship, 2021
7. UCSC, Climate Engagement Program Fellow, 2019
8. Environmental Systems Bobcat Fellowship, 2019
9. Ag One-25<sup>th</sup> Anniversary Ed Rose Scholarship, 2016
10. Ag One-Fraysher Scholarship, 2016
11. Ag One-Lowell A Jordan & Jorda Scholarship, 2016
12. Ag One-Jack Woolf Scholarship, 2016
13. Student Scholarship, California Irrigation Institute, 2016
14. Graduate Net Initiative Research Fellowship, CSU Fresno, 2015
15. Jensen Scholarship, 2015
16. Ag One-Jack Woolf Scholarship, 2015
17. Jensen Scholarship, 2013
18. Valley Grower Local Sunweet Grant, 2013
19. Ag One-Dr Marinus Van Elswyk Grant, 2013
20. Ag One-Dick Markarian Grant, 2012
21. CA Cotton Alliance Scholarship, 2012
22. Ronald McNair Research Grant, 2012
23. Undergraduate Research Grant, 2011
24. General Dillingham Scholarship, 2011
25. CAST Scholarship, 2011

**MEMBERSHIPS IN PROFESSIONAL SOCIETIES:**

American Geophysical Union, *2020-Present*  
 California Irrigation Institute, *2016-Present*  
 Irrigation Association, *2014-Present*  
 American Society of Agronomy, *2012-Present*  
 Crop Science Society of America, *2012-Present*  
 Soil Science Society of America, *2012-Present*

**Volunteer Experience:**

**Environmental Systems Seminar Committee: 2020-2021**

**Science Fair Judge (Merced City School District): 2018-2019**

- o Science Fair Judge, Hoover Middle School, 2019
- o Science Fair Judge, STEAM Center (Merced County Contest), 2018

- Science Fair Judge, Hoover Middle School, 2018

**Future Farmers of America Contests: 2010-2018**

- Staff Coordinator for Vegetable Contest, Fresno State, 2018
- Judge for Vegetable Contest (Tomato), Fresno State, 2016
- Group Leader for Weed Contest, Fresno State, 2015
- Group Leader for Citrus Contest, Fresno State, 2015
- Judge for Vegetable Contest (Lettuce), Fresno State, 2014
- Student Runner for Citrus Contest, Fresno State, 2014
- Student Coordinator for Vegetable Contest, Fresno State, 2013
- Group Leader for Citrus Contest, Fresno State, 2012
- Judge for Vegetable Contest (Broccoli), Fresno State, 2011
- Group Leader for Agribusiness Contest, Fresno State 2010
- Group Leader for Cotton Contest, Fresno State 2010

**SKILLS:**

- Fluent in **English** and **Hmong** (Interpreter/Translator)
- Proficient in Microsoft Windows, Microsoft Office: Word, Excel, and PowerPoint
- Proficient in Statistical Software: SAS, SPSS, Sigma Plot, and R

**Off-Campus Activities:**

**Treasure Officers for Suab Hmoob Txuj Ci Organization: January 2010-2018**

Responsible for the financial management of the organization. Organize fundraising events and raised over \$10,000 for the organization since 2010. Promote the organization mission and visions to the public. Participant in community events and other volunteer services in the Hmong community. Serve an average of 12-24 hours per week in community activities.

## **ABSTRACT OF THE DISSERTATION**

**Impact of Locally-Sourced Biochar Amendments on Soil Hydrology and Ecosystem Services: A Study of Moisture Retention, Plant Uptake Dynamics, Nutrient Retention, and Greenhouse Gas Emissions in Agroecosystems**

by

Touyee Thao

Doctor of Philosophy in Environmental Systems

University of California, Merced, 2023

Dr. Teamrat A. Ghezzehei, Chair

The transferability of excess wasted organic materials, such as agricultural and forestry residues into materials like biochar and compost, to be used as a nutrient-rich organic soil amendment for food production has been viewed as an ecological approach to enhance soil ecosystem services. In this dissertation a variety of research techniques and experiments were used to investigate the effects of different locally produced biochar and also biochar dairy manure co-composts on soil hydrological properties, GHG emissions, nitrogen leaching, and crop productivity. The dissertation is divided into three main research chapters. In the first chapter, we generated moisture retention curves for seven biochar derived from wasted orchard materials e.g. almond shell, walnut shell, and almond pruning, using a mobile pyrolyzer unit. More specifically, we used the water sorption film approach to determine specific surface area for the different biochar and incorporated the data into a model to assess its influence on soil moisture content. Additionally, three of the biochar (one from each feedstock) were also selected and used in two 109 days incubation studies to investigate biochar influence on soil respiration under different moisture levels. In the second chapter, numerical simulation was performed (5-years impact) on the three selected biochar to assess its impacts on soil hydrological properties and plant uptake dynamic for common cropping systems with dissimilar irrigation practices. Lastly, in the third chapter the three selected biochar were co-composted with fresh dairy manure for 45 days then used as soil amendment in a 133 day outdoor soil-tomato column study. Leaf chlorophyll content, canopy coverage, and GHG measurements were taken throughout the season as proxy for crop productivity and soil emissions as influenced by soil treatments. Results from chapter one show that walnut shell biochar has the greatest surface area while almond shell derived biochar has the most positive effect on moisture retention and soil respiration. Next, our 5-years numerical simulation shows that application of biochar at 5% enhanced water conservation by reducing seasonal soil evaporation loss and allowing for more root water uptake. However this positive effect varied between cropping systems and is substantially greater in the rainfed compared to irrigated system. In the last chapter, results from our soil-tomato study show greater positive effect on soil ecosystem services e.g. nitrogen retention and crop productivity, from biochar-dairy manure co-compost soil treatments compared to the control. However crop yield was constrained by external factors such as plant water stress.

# Chapter 1.

## Introduction

The balance between food production and ecological stewardship is a crucial relationship for the sustainability of agriculture. Though food production is a necessity for human welfare, it is also a major contributor to various environmental issues (e.g. non-point source pollution caused by leaching, field runoff, and soil degradation) and climate change through mass emission of various greenhouse gases (GHG), such as methane (CH<sub>4</sub>), carbon dioxide (CO<sub>2</sub>), and nitrous oxide (N<sub>2</sub>O) (Crippa et al., 2021). In recent years there has been a growing interest aimed at improving farm ecological footprint by closing the different leakages in agricultural settings, hence transforming traditional systems into agroecosystems. One such research area involves the circular uses or conversion of different wasted organic materials (e.g. agricultural residues) into nutrient-rich organic soil amendments, such as biochar (Wang et al., 2019; Xiao et al., 2017; Yin et al., 2021). Biochar, a porous and recalcitrant material (Lehmann et al., 2006) commonly synthesized from different organic wasted streams using thermal pyrolysis has been suggested as an approach to mitigate environmental degradation and alleviate the impacts of climate change. Primarily, biochar recalcitrant and high sorption attributes is believed to promote soil carbon sequestration while enhancing biological activities and reducing GHG emissions (Ghezzehei et al., 2014; Jones et al., 2011; Kameyama et al., 2012; Major et al., 2012). In agricultural systems, biochar plus soil sorption can delay the movement of both water and essential nutrients which give crops and soil microbes more time for uptake (Kameyama et al., 2012; Major et al., 2012), thus increasing farm water and nutrients use efficiency.

The porosity and high surface area of biochar is assumed to allow for more internal and external sites for adsorption of water and nutrients. Hypothetically, once in the soil biochar can influence soil characteristics, e.g. cation exchange capacity (CEC), soil organic matter (SOM), soil porosity and physical structure, which ultimately effect soil hydraulic properties (Masiello et al., 2015; Villagra-Mendoza & Horn, 2018). The change and interaction of these soil characteristics directly related to the diversity and functionality of the microbial community, controlling their role in nutrients cycling and dictating whether nutrients in the soil profile is easily available for plant uptake, susceptible to leaching, or chemically converted into volatilized compounds. This led to the belief that amending soil with biochar stimulates resiliency in soil and soil biota, especially under adverse environmental conditions (e.g. drought) (Manzoni et al., 2012; Wang et al., 2020). A literature review by Ali et al. (2017) on biochar potential to lessen abiotic stress, such as drought and salinity, also linked its resiliency potentials to the material physical and chemical characteristics, and positive interaction with soil microorganisms. Although the mechanisms and relationships between biochar, soil, and biological activities is still unclear. Furthermore, conflicting research observations has led to a continuous dispute in regard to the overall benefits of this organic material once applied to soil. Studies have shown both a beneficial (Abel et al., 2013; Ajayi et al., 2016; Arthur et al., 2015; Kameyama et al., 2012; Liu et al., 2011; Villagra-Mendoza & Horn, 2018; Zhou et al., 2018) and negligible (Jeffery et al., 2015; Lanza et al., 2016; Pressler et al., 2017; Wiersma et al., 2020) effect of biochar on different soil properties (e.g. hydraulic properties), GHG emissions, and crop productivity. More so, the literature has exhibited inconsistency when factoring in feedstock types and environmental interactions

(e.g. soil type and climatic factor). Given this constraints the assertion that biochar opens a holistic pathway toward sustainable agriculture requires more scientific evidence.

## 1.1 Research Objectives

The overall objectives in this dissertation are listed below. Briefly, the research objectives were designed to address four major interrelated research questions. (1) How does biochar influence soil water retention characteristics, especially in the mid to dry range of the water potential spectrum? Hence, can we assess the linkage between different biochar and their physical characteristics, such as specific surface area to its sorption capability, thereby evaluating how soil water retention is altered? (2) Can the addition of biochar extend the biologically active range of soil water potential? (3) Does co-application of biochar with other organic amendment, such as composted dairy manure, alter soil hydraulic properties and influence plant productivity? (4) How does biochar and dairy manure co-compost influence the overall fates of soil nitrogen (N)?

Objective 1. Develop a mathematical model and conduct laboratory measurement to determine the effect of different biochar on soil water retention (5% w/w), specifically at the mid to dry moisture region.

Objective 2. Assess how different biochar (5% w/w) affects soil respiration by altering soil hydrological properties using laboratory incubation experiments.

Objective 3. Quantify the effects of locally-produced biochar (5% w/w) on soil water retention and crop yield under two cropping systems with different irrigation schemes and across climatic years using numerical modeling.

Objective 4. Determine the effect of different biochar and dairy manure co-compost combinations (5% w/w) on soil hydrological properties, GHG emission, and crop productivity.

Objective 5. Evaluate the environmental fates of N from different biochar dairy manure co-composts for a commonly farmed coarse-textured soil.

## 1.2 Organization of the Dissertation

The research objectives stated above are organized into three different chapters and a final conclusion. Here objectives 1 and 2 are investigated in Chapter 2, objective 3 is assessed in Chapter 3, and objectives 4 and 5 are investigated in Chapter 4. Lastly, Chapter 5 is the summary of the main findings from all chapters.

## 1.3 References

Abel, S., Peters, A., Trinks, S., Schonsky, H., Facklam, M. and Wessolek, G. (2013). Impact of biochar and hydrochar addition on water retention and water repellency of sandy soil. *Geoderma*, 202, 183-191. <https://doi.org/10.1016/j.geoderma.2013.03.003>

- Ajayi, A.E., Holthusen, D. and Horn, R. (2016). Changes in microstructural behaviour and hydraulic functions of biochar amended soils. *Soil and Tillage Research*, 155, 166-175. <https://doi.org/10.1016/j.still.2015.08.007>
- Ali, S., Rizwan, M., Qayyum, M.F., Ok, Y.S., Ibrahim, M., Riaz, M., Arif, M.S., Hafeez, F., Al-Wabel, M.I. and Shahzad, A.N. (2017). Biochar soil amendment on alleviation of drought and salt stress in plants: a critical review. *Environmental Science and Pollution Research*, 24(14), 12700-12712. DOI 10.1007/s11356-017-8904-x
- Arthur, E., Tuller, M., Moldrup, P. and de Jonge, L.W. (2015). Effects of biochar and manure amendments on water vapor sorption in a sandy loam soil. *Geoderma*, 243, 175-182. <https://doi.org/10.1016/j.geoderma.2015.01.001>
- Crippa, M., Solazzo, E., Guizzardi, D., Monforti-Ferrario, F., Tubiello, F. N., & Leip, A. (2021). Food systems are responsible for a third of global anthropogenic GHG emissions. *Nature Food*, 2(3), 198–209. <https://doi.org/10.1038/s43016-021-00225-9>
- Ghezzehei, T.A., Sarkhot, D.V., Berhe, A.A. (2014). Biochar can be used to capture essential nutrients from dairy wastewater and improve soil physico-chemical properties. *Solid Earth*, 5(2): 953-962. doi:10.5194/se-5-953-2014
- Jeffery, S., Meinders, M.B., Stoof, C.R., Bezemer, T.M., van de Voorde, T.F., Mommer, L. and van Groenigen, J.W. (2015). Biochar application does not improve the soil hydrological function of a sandy soil. *Geoderma*, 251, 47-54. <https://doi.org/10.1016/j.geoderma.2015.03.022>
- Jones, D.L., Murphy, D.V., Khalid, M., Ahmad, W., Edwards-Jones, G. and DeLuca, T.H. (2011). Short-term biochar-induced increase in soil CO<sub>2</sub> release is both biotically and abiotically mediated. *Soil Biology and Biochemistry*, 43(8),1723-1731. <https://doi.org/10.1016/j.soilbio.2011.04.018>
- Kameyama, K., Miyamoto, T., Shiono, T. and Shinogi, Y. (2012). Influence of sugarcane bagasse-derived biochar application on nitrate leaching in calcareous dark red soil. *Journal of Environmental Quality*, 41(4), 1131-1137. doi:10.2134/jeq2010.0453
- Lanza, G., Rebenburg, P., Kern, J., Lentzsch, P. and Wirth, S. (2016). Impact of chars and readily available carbon on soil microbial respiration and microbial community composition in a dynamic incubation experiment. *Soil and Tillage Research*, 164, 18-24. <https://doi.org/10.1016/j.still.2016.01.005>
- Lehmann, J., Gaunt, J., Rondon, M. (2006). Bio-char sequestration in terrestrial ecosystems - A review. *Mitigation and Adaptation Strategies for Global Change*, 11(2): 403-427. DOI: 10.1007/s11027-005-9006-5
- Liu, Y., Yang, M., Wu, Y., Wang, H., Chen, Y. and Wu, W. (2011). Reducing CH<sub>4</sub> and CO<sub>2</sub> emissions from waterlogged paddy soil with biochar. *Journal of Soils and Sediments*, 11(6), 930-939 DOI 10.1007/s11368-011-0376-x
- Major, J., Rondon, M., Molina, D., Riha, S.J. and Lehmann, J. (2012). Nutrient leaching in a Colombian savanna Oxisol amended with biochar. *Journal of environmental quality*, 41(4), 1076-1086. doi:10.2134/jeq2011.0128

- Manzoni, S., Schimel, J.P. and Porporato, A. (2012). Responses of soil microbial communities to water stress: results from a meta-analysis. *Ecology*, 93(4), 930-938. <https://doi.org/10.1890/11-0026.1>
- Masiello, C.A., Dugan, B., Brewer, C.E., Spokas, K.A., Novak, J.M., Liu, Z. and Sorrenti, G. (2015). Biochar effects on soil hydrology. In *Biochar for Environmental Management*, 575-594. Routledge.
- Pressler, Y., Foster, E.J., Moore, J.C. and Cotrufo, M.F. (2017). Coupled biochar amendment and limited irrigation strategies do not affect a degraded soil food web in a maize agroecosystem, compared to the native grassland. *Global Change Biology, Bioenergy*, 9(8), 1344-1355. <https://doi.org/10.1111/gcbb.12429>
- Villagra-Mendoza, K. & Horn, R. (2018). Effect of biochar addition on hydraulic functions of two textural soils. *Geoderma*, 326, 88-95. <https://doi.org/10.1016/j.geoderma.2018.03.021>
- Wang, Y., Villamil, M.B., Davidson, P.C. and Akdeniz, N. (2019). A quantitative understanding of the role of co-composted biochar in plant growth using meta-analysis. *Science of the Total Environment*, 685, 741-752. <https://doi.org/10.1016/j.scitotenv.2019.06.244>
- Wang, D., Li, C., Parikh, S.J. and Scow, K.M. (2019). Impact of biochar on water retention of two agricultural soils—A multi-scale analysis. *Geoderma*, 340, 185-191. <https://doi.org/10.1016/j.geoderma.2019.01.012>
- Wiersma, W., van der Ploeg, M.J., Sauren, I.J. and Stoof, C.R. (2020). No effect of pyrolysis temperature and feedstock type on hydraulic properties of biochar and amended sandy soil. *Geoderma*, 364, p.114209. <https://doi.org/10.1016/j.geoderma.2020.114209>
- Xiao, R., Awasthi, M.K., Li, R., Park, J., Pensky, S.M., Wang, Q., Wang, J.J. and Zhang, Z. (2017). Recent developments in biochar utilization as an additive in organic solid waste composting: A review. *Bioresource Technology*, 246, 203-213. <https://doi.org/10.1016/j.biortech.2017.07.090>
- Yin, Y., Yang, C., Li, M., Zheng, Y., Ge, C., Gu, J., Li, H., Duan, M., Wang, X. and Chen, R. (2021). Research progress and prospects for using biochar to mitigate greenhouse gas emissions during composting: a review. *Science of The Total Environment*, 798, 149294. <https://doi.org/10.1016/j.scitotenv.2021.149294>
- Zhou, H., Yu, X., Chen, C., Zeng, L., Lu, S. and Wu, L. (2018). Evaluating hydraulic properties of biochar-amended soil aggregates by high-performance pore-scale simulations. *Soil Science Society of America Journal*, 82(1), 1-9. doi:10.2136/sssaj2017.02.0053

## **Chapter 2.**

### **Seven biochars and their impact on moisture retention and respiration rate of a coarse -textured soil, exclusively at the mid to dry water regions**

#### **Abstract**

Here we test the hypothesis that soil water status and soil respiration can be augmented with biochar amendment due to an increase in water affinity, specifically at the mid to dry water spectrum. We tested the wettability of seven biochars, made from different orchard residues e.g. almond shell, walnut shell, and almond pruning, using the water-vapor sorption isotherm (WSI) method. The water-retention characteristics were evaluated using film sorption theory and used to infer the specific surface area (SSA). Results were further extended to infer the implication of biochar addition on moisture retention of a coarse-textured soil at 5% application rate (w/w) and compared with measured data. Additionally, of the seven biochars three were selected for our lab experiments based on feedstock type and non-hydrophobic nature. Two 109 days lab incubation trials were conducted to assess the influence of biochar on soil respiration under different moisture conditions. In the first incubation study, moisture content in all treatments was sustained at 1.01 MPa throughout the experimental duration. In the second incubation, treatments were air dried for six hours after every gas measurement until water content was extremely dry. Soil carbon dioxide (CO<sub>2</sub>) emissions were measured every two-six days consecutively. Findings from our study reveal an increase in soil moisture retention with application rates, particularly noticeable at the wilting point region. Biochar derived from almond shells had the most influence on soil moisture regime. In addition, we also detected higher soil respiration from almond shell biochar amended soil. SSA varies among biochars, with walnut shell biochar yielding the highest SSA. The results indicate that biochar enhancement of water retention can play a significant role in countering moisture stress in drying coarse-textured soils.

#### **2.1 Introduction**

With only limited space and natural resources available, a dramatic increase in both system and resource use efficiency in food production is necessary to sustain a growing human population, especially under adverse climatic conditions. The conversion of wasted organic materials, e.g. agricultural residues, into useful soil organic amendments will be an essential approach to enhance soil ecosystem services and crop productivity. Biochar, a material synthesized from different organic waste streams, e.g. municipal, agricultural, and forestry wastes, using thermal pyrolysis is an option to help alleviate the impacts of climate change and better soil ecosystem services (Lehmann et al., 2006). Primarily, biochar recalcitrant and high sorption attributes is believed to promote soil carbon sequestration while enhancing biological activities and reducing greenhouse gas emissions (GHGs) (Delwiche et al., 2014; Ghezzehei et al., 2014; Kameyama et al., 2012; Jones et al., 2011; Major et al., 2012;). One important hypothesized effect of biochar addition to soil is its potential to increase water retention capacity. The

mechanism for this effect is that biochar provides very large wettable surface area that increases the affinity of biochar treated soils to water (Downie et al., 2012; Laird et al., 2010; Leng et al., 2021).

In cropping systems, biochar plus soil sorption can delay the movement of water and essential nutrients which give plants and soil microbes more time for uptake (Kameyama et al., 2012; Major et al., 2012), thus increasing farm water and nutrient use efficiency. This led to the hypothesis that amending soil with biochar stimulates resiliency in soil and soil biota, especially under adverse environmental conditions (e.g. drought) (Manzoni et al., 2012; Wang et al., 2020). A literature review by Ali et al. (2017) on biochar potential to lessen abiotic stress, such as drought and salinity, also linked its resiliency potentials to the material physical and chemical characteristics, and positive interaction with soil microorganisms. Though, the majority of biochar-soil studies were conducted under conditions where water is not a constrained variable (e.g. at field capacity) and therefore may not truly capture the effect biochar has on soil hydrology (Arthur et al., 2015) and microbes, particularly at the dry end of the soil water curve. Additionally, exposure to unfavorable conditions can influence the overall soil productivity by altering microbial health, e.g. extensive periods of drought (Manzoni et al., 2012). Thus, there is a need to assess the extent to which soil water status and soil respiration is influenced by biochar additives under drier water conditions.

### 2.1.1 Water Film Approach to Determine Specific Surface Area

Determining the specific surface area (SSA) of biochar is a key measurement to understand its sorption capacity and potential effect on soil hydraulic properties. SSA is a physical property defined as the surface area per unit mass of the solid (Pennell, 2002). In soil, adsorption of water to soil at low matric potential (less than -10 MPa) has been well correlated to SSA and clay content (Arthur et al., 2013; Arthur et al., 2016; Leão & Tuller, 2014; Tuller et al., 1999) and is often described as the film water thickness of the soil due to the van der Waals surface force (Tuller et al., 1999; Tuller & Or, 2005). Several methods have been used to measure SSA (e.g. ethylene glycol monoethyl ether (EGME), N<sub>2</sub>-BET, CO<sub>2</sub> adsorption), among them is the water vapor sorption isotherm method. The WSI method was proposed by Tuller and Or (2005) as a more practical means to inversely estimate soil SSA. The approach uses a vapor pressure (relative humidity) measurement of the sample under equilibrium state to infer its water content at a given temperature, using the well-known Kelvin equation (Equation 1) which relates change in vapor pressure to surface curvature. Film water thickness can then be derived using Equation 2, which describes film water thickness as a function of matric potential (Iwamatsu & Horii, 1996) using a Hamaker constant, which represent solid-vapor interaction, while neglecting forces such as electrostatic and hydration (Tuller & Or, 2005). Given that gravimetric water content ( $\theta_m$ ) is also known, SSA can be determined by setting gravimetric water content equal to film water thickness, as described by Tuller and Or (2005) and shown in Equation 3.

$$\psi_w = \frac{RT^* \rho_w}{M_w} \ln \left( \frac{e}{e_0} \right) \quad (2.1)$$

Where ( $\psi_w$ ) is soil water potential,  $\left(\frac{e}{e_0}\right)$  is the relative vapor pressure,  $M_w$  is the molecular weight of water (0.0083 kg mol<sup>-1</sup>),  $R$  is ideal gas constant (8.31 J K<sup>-1</sup> mol<sup>-1</sup>)  $T$  is absolute temperature (K), and  $\rho_w$  is the density of water (1000 kg m<sup>-3</sup>).

$$h = \sqrt[3]{\frac{A_{svl}}{6 \cdot \pi \cdot \rho_w \cdot \Psi}} \quad (2.2)$$

Where  $h$  is the water film thickness,  $A_{svl}$  is the Hamaker constant for solid-liquid-gas (set at  $1.90\text{E-}19$  J),  $\rho_w$  is the density of water, and  $\Psi$  is the matrix potential, assuming that one layer monolayer of water is  $3.50\text{E-}10$  meter.

$$\theta_m = \sqrt[3]{\frac{A_{svl}}{6 \cdot \pi \cdot \rho_w \cdot \Psi}} S \cdot \rho_w \quad (2.3)$$

Where  $\theta_m$  is the gravimetric water content,  $A_{svl}$  is the Hamaker constant for solid-liquid-gas (set at  $1.90\text{E-}19$  J),  $\rho_w$  is the density of water, and  $\Psi$  is the matrix potential, and  $S$  is the specific surface area.

Theoretically, since biochar is a porous media with similar sorption attributes as soil, the relationship between relative humidity and matric potential can also be used to generate the water vapor sorption isotherm for biochar using Equation 2 and biochar SSA using Equation 3. Surprisingly, the use of WSI to evaluate biochar or biochar-soil SSA has been scarcely limited (Arthur et al., 2016; McLaughlin et al., 2012). In the literature the  $\text{N}_2$  BET gas adsorption approach has been the common method used to define biochar surface area, despite its known inadequacy in complex permeable media (Arthur et al., 2013) and costly price.

### 2.1.2 Research Objective

The research objective in this study was to assess the water retention potential of different locally produced biochar and also its effects on soil respiration. Our aim was to infer biochar SSA using the film sorption theory and gauge its influence on soil water retention for a coarse-textured soil commonly found in the Central Valley of California, using a 5% mass-based mixing model. Model validation was performed by comparing model prediction with soil-biochar moisture retention dataset at 5% application rates (w/w). Additionally, a 10% application rate was also assessed. Furthermore, we also conducted lab incubation experiments to evaluate the effects of these biochar on soil respiration under different moisture regimes. We hypothesized that biochar synthesized from different feedstocks, e.g. almond shell and walnut shell, have disparate SSA and water sorption characteristics, but an overall positive influence on soil respiration compared to unamended soil.

## 2.2 Materials and Method

### 2.2.1 Biochar

Seven different biochars were tested for their moisture retention potential. In addition, a Control or unamended soil and two application rates (5% and 10% w/w) were also evaluated, each treatment had three replications for a total of 66 samples. All biochars were derived from local orchard waste materials that underwent slow pyrolysis at 300-350 °C using a mobile rotational pyrolyzer. Of the seven biochars, two were made using almond shell (AS-1 and AS-2), three from walnut shell (WS-1, WS-2, BCW), and two from almond pruning (ATC-1 and ATC-2). Table 1 shows the bulk density of each biochar and its absorbance to 1,1,1,2-tetrafluoroethane (R134a) at 100 °C. As noted bulk density was higher for WS-1 and WS-2, whereas WS-2 and ATC-1 yielded higher

absorbance to R134a. Likewise, Table 1 also shows the hydrophobicity test for each respective treatments and biochar mixtures, measured using the water droplet penetration test (WDPT) (n = 9). Four of the biochar were very repulsive to water, with AS-1 and ATC-2 having extremely repellent nature and WS-1 and BCW being strongly repellent. Note that hydrophobicity disappears in the biochar soil mixture (Table 1). The soil used as the Control and for the biochar mixture were collected from a grassland near the UC Merced Castle Facility (37.3732 °N, -120.577 °W) and classified as Atwater loamy-sand series in the taxonomic class coarse-loamy, mixed, active, thermic Typic Haploxeralfs. This well drained Alfisol soil originated from sandy alluvium created by erosion of granite from the Sierra Nevada (Arkley, 1962).

### 2.2.2 Soil Water Retention (Mid to Dry Region) & SSA

WP4C Dewpoint Potentiometer (METER Group, Pullman, WA) was used to measure the water potential of different biochar samples at the mid to dry moisture region. This instrument uses the chilled-mirror dewpoint method (Gee et al., 2002) to measure the relative humidity of a given sample in equilibrium, at a given temperature and record the matric potential associated. Sample preparation, measurement, and derived water retention curves (WRC) followed a modified procedure described by Tuller and Or (2005) for vapor sorption analysis of soil. Briefly, 1-2 g of biochar was transferred into a disposable plastic sampling cup. The samples were moisturized by adding 2 g of DI water (as uniform as possible), then capped and allowed to equilibrate for 24 hours. The biochar samples were then weighed using a precision scale; this weight served as our initial wet weight. All samples undergo analysis using the “precise mode” from the WP4C unit to allow for a longer equilibrium duration and better accuracy. Once the instrument is finished, the sample was re-weighed and air dried (for 2-5 h) prior to being recapped and again stored away for equilibrium. This procedure was repeated 10-15 times before the biochar samples were oven-dried at 100 °C for 48 hours to determine the gravimetric water content. Similar to Tuller and Or (2005), film water thickness and biochar SSA was calculated using the above Equations 2 and 3 with the driest point measured, assuming a Hamaker constant of 1.90E-19 J (Watanabe & Mizoguchi, 2002) and one monolayer of film water is 3.50E-10 m (Leao & Tuller, 2014). The stated assumptions yielded Figure 1, which shows that SSA can be determined when the water film covering the surface area of the material is around one monolayer

### 2.2.3 5% Biochar Mass-based Moisture Retention Model & Application Rates

Subsequently, biochar WP4C data is incorporated into the Peters (Peters, 2013) and Iden and Durner (Iden & Durner, 2014) or PDI model (Equations 4, 5, 7, and 8) using a 5% application rates (wt/wt) to predict its influence on water retention for the Atwater loamy-sand soil. This PDI model incorporates both the van Genuchten capillaries saturation function (Equations 3) and film adsorption (Equation 4 and 5) aspects of soil water hydrostatics. Next, water potential measurement from soil amended with different biochar at 5% and 10% (wt/wt) application rates was also performed using WP4C potentiometer. The procedure for generating the soil moisture retention curve for the mixtures is similar to that of the pure biochar samples. The main difference is the amount of sample used per sampling cup, which is 5 g for the mixtures (e.g. 4.75 g soil + 0.25 g biochar for 5%, and 4.50 g soil + 0.50 g biochar for the 10%).

$$\theta(h) = (\theta_s - \theta_r)S_{cap} + \theta_r S_{ad} \quad (2.4)$$

Where  $S_{cap}$  is the water stored in capillaries and  $S_{ad}$  refers to the water stored in adsorbed films.  $\theta$  ( $\text{m}^3\text{m}^{-3}$ ) is the total water content,  $h$  (m) is the suction head, and  $\theta_s$  ( $\text{m}^3\text{m}^{-3}$ ) and  $\theta_r$  ( $\text{m}^3\text{m}^{-3}$ ) are the saturated and maximum adsorbed water contents (Iden & Durner, 2014). In order to meet the physical requirement that water content reaches zero,  $S_{cap}$  is substituted by scaled version of the original functions:

$$S_{cap}(h) = \frac{\Gamma(h) - \Gamma(h_0)}{1 - \Gamma(h_0)} \quad (2.5)$$

Where  $h_0$  (m) is the suction head at oven dryness, and is set at  $10^{6.8}$  m (Schneider & Goss, 2012),  $\Gamma(h)$  is the van Genuchten unimodal saturation function (van Genuchten, 1980):

$$\Gamma(h) = \left[ \frac{1}{1 + (\alpha h)^n} \right]^{1 - 1/n} \quad (2.6)$$

where  $\alpha$  ( $\text{m}^{-1}$ ) and  $n$  (-) are shape parameters.

$$S_{ad}(h) = \frac{\ln(h/h_0) - b \ln(1 + [h_a/h]^{1/b})}{\ln(h_0/h_a)} \quad (2.7)$$

The parameter  $h_a$  (m) is the suction head where non-capillary water reaches saturation,  $h_0$  as stated above is the suction head where water content reaches zero at oven dry conditions.  $S_{ad}(h)$  increase linearly from zero at oven dry to a maximum value of 1 at  $h_a$ , and  $b$  is the smoothing parameter (Iden & Durner, 2014) defined as:

$$b = 0.1 + \frac{0.2}{n^2} \left\{ 1 - \exp \left[ - \left( \frac{\theta_r}{\theta_s - \theta_r} \right)^2 \right] \right\} \quad (2.8)$$

## 2.2.4 Incubation Experiments

Of the seven biochars tested, three (AS-2, WS-2, and ATC-1) were selected to be used in the lab incubation experiments. Since soil moisture retention as influenced by biochar additives was a main interest in this study, the surface hydrophobicity of the material was a main criteria used for selecting the biochar. Treatments for the incubation experiments are shown in Table 2, which include the three selected biochars, a 5% application rate (w/w) for each biochar, and Control. All biochars had a slightly repellent nature to water and a pH of 9.42, 9.41, and 7.96, for AS-2, WS-2, and ATC-1 respectively. Chemical characteristics such as C:N ratio, pH, EC, carbon, and nitrogen content of Control and the three biochar are displayed in Table 3. As observed, carbon and nitrogen content were lowest for the unamended soil and highest for biochar. For the incubation studies, 20 g of pure biochar and 100 g of unamended soil or mixture were placed into a plastic jar (8.3 cm in diameter) and gently packed to a depth of 4.6 and 5.8 cm for pure and mixture, respectively. For the mixture, 95 g of soil was mixed thoroughly with 5 g of biochar. Each treatment has four replications for a total of 28 samples (7 treatments x 4 replications) per incubation experiment. Two different incubation experiments were conducted at the same time. The first experiment, termed Moisture Dynamic (MD) from hereafter, 40 g of DI water was applied to all treatments at the start of the incubated period. After each gas measurement, the samples were air dried for six hours (~ 2 g of water loss), capped, and set to equilibrate for two to six days before the next measurements. This process is repeated again until samples moisture content falls below

0.01  $\theta_m$  before raising the moisture back up to the original content. The second experiment, termed Moisture Constant (MC) from hereafter, all treatments were kept at a moisture content equivalent to 1.01 MPa throughout the entire incubation duration. MC samples were checked and moisturized on a weekly basis. The required water was applied using a spray bottle for adequate coverage for each sample. The initial moisture content for treatments in both incubation experiments is displayed in Table 2. The incubation period lasted 109 days for both experiments.

### 2.2.5 CO<sub>2</sub> Measurements

Six K30 FR 10000 PPM CO<sub>2</sub> Sensors (Senseair, Delsbo, Sweden) were attached onto the cap of the sampling jar (Figure S2.1). This CO<sub>2</sub> sensor uses a non-dispersive infrared (NDIR) method to measure the CO<sub>2</sub> concentration (via diffusion) and has a range from 0 to 10,000 ppm. The sensor has an accuracy of  $\pm 30$  ppm  $\pm 3$  % of measured value and repeatability of  $\pm 20$  ppm  $\pm 1$  % of measured value. These low-cost sensors have been shown to be well reliable and accurate for in-situ CO<sub>2</sub> measurement (Brown et al., 2020; Chopda et al., 2020). The sensors are connected to a PC computer and monitored using GasLab™ Software. Gas measurements were conducted for 10 minutes with reading taken every ten seconds. During this time, room temperature (°C), humidity (%), and room pressure (kPa) were also measured (ten minutes duration) using temperature probe, relative humidity sensor, and barometer (Vernier Science Education, Beaverton, OR). After each measurement, the K30 CO<sub>2</sub> sensor is opened, and air is blown onto each sensor to remove any CO<sub>2</sub> residue and potential contamination. All samples were weighed before and after flux measurement to track moisture change. A hole (1.3 cm in diameter) was also drilled into the top of all sample caps in order to avoid anaerobic conditions or build up of CO<sub>2</sub> before the next measurement. In both experiments the first CO<sub>2</sub> measurement was conducted on May 22, 2021 on dry samples, or before water was applied

### 2.2.6 Statistical Analysis

Statistical analysis was performed for appropriate datasets using a one-way Analysis of Variance (ANOVA). Datasets were checked for normality and homogeneity of variance assumption. Tukey-HSD tests were used to distinguish significance among treatments. Additionally, linear regression was also performed on estimated biochar SSA to SSA of both 5% and 10% biochar application rates to evaluate statistical relationships. Confidence interval for both analyses was set at the 95% level or  $p = 0.05$ . Statistical analyses were conducted using the R package (R Core Team, 2020).

## 2.3 Results

### 2.3.1 Biochar WRC and 5% Application Model

Figure 2 shows the mean WRC for the seven biochars ( $n = 3$ ) with standard error bar. As observed, from 0.2 to 0.8  $\theta_m$ , we can see a clear separation of suction potential associated to the same moisture content from the tested biochar. Between this moisture content, AS-1, AS-2, and BCW biochar have substantially higher moisture retention compared to WS-1, WS-1, ATC-1, and ATC-2. However, at suction potential from 10 to 100 MPa (very dry moisture region), WS-2 exhibited more moisture retention than all other biochar.

Figure 3 shows the modeled 5% application rate soil water retention curve (SWRC) for the Atwater loamy-sand soil, using the measured biochar retention data. Similar to the

biochar WRC, the model predicted higher soil moisture retention for AS-1, AS-2, and BCW biochar. The model also projected an increase in soil water available at both field capacity (FC = 0.033 MPa) and permanent wilting point (PWP = -1.5 MPa) regions, for all tested biochar compared to the Control or unamended soil. Again, this increase in plant available water was greatest for AS-1, AS-2, and BCW biochar, ranging from 15% to 25% (Figure 3)

### 2.3.2 WRC for 5% and 10% Application Rates

Figures 4 and 5 show the measured SWRC for 5% and 10% biochar application rates. As observed, the Control had lower moisture retention potential compared to biochar mixtures. For the 5% application rate (Figure 4), AS-1 and AS-2 mixtures show much higher moisture retention than all other biochar mixtures. Surprisingly, the positive effect on moisture retention for the 5% BWC mixture did not align with the WRC of the pure BWC biochar (Figure 3) or what the 5% model predicted (Figure 3). At 10% application rate, all biochar mixtures have substantially higher moisture retention compared to Control (Figure 5), again with the highest retention potential detected for AS-1 and AS-2 biochar mixtures.

Table 4 shows the calculated SSA for all biochars, biochar mixtures, and Control using the WSI method stated above. For the pure biochar, there was a highly statistical difference ( $p < 0.001$ ) in SSA among the biochar, with the highest being WS-2 (159 m<sup>2</sup>/g) followed by BCW (113 m<sup>2</sup>/g). SSA for all other biochar were statistically lower than BCW and WS-2, but not from each other. As for SSA in the 5% and 10% mixtures, we observed that Control yielded the lowest SSA (11 m<sup>2</sup>/g) in both cases, whereas WS-2 held the highest SSA (24 m<sup>2</sup>/g and 35 m<sup>2</sup>/g, respectively). All other biochar mixtures were statistically greater than Control ( $p < 0.001$ ) but lower than WS-2 mixture in each respective rate. Furthermore, we also detected a general increase in SSA with biochar application rates compared to Control (Figure S2.2). The correlation between estimated biochar SSA and mixtures SSA yielded an  $R^2 = 0.8083$  (5%) and  $R^2 = 0.8025$  (10%); both relationships were highly significant, with  $p = 0.0059$  and  $0.0064$ , respectively (Figure S2.2).

### 2.3.3 CO<sub>2</sub> Respiration from Incubation Experiments

Figure 6 shows the CO<sub>2</sub> flux (mmol C m<sup>-2</sup> s<sup>-1</sup>) taken throughout the 109 days incubation period for the two lab experiments. For the incubation experiment where moisture was sustained at 1.01 MPa or MC experiment, we observed that AS-2, both pure (Figure 6c) and 5% mixture (Figure 6a) had the highest CO<sub>2</sub> emission throughout most of the 109 days incubation period. In addition, CO<sub>2</sub> emissions for both pure and mixtures AS-2 followed an exponential decline. CO<sub>2</sub> emissions for pure WS-2 and ATC-1 were similar to each other, whereas 5% WS-2 were slightly greater than Control throughout the first half of incubation. At the end of July or 60 days into the incubation, CO<sub>2</sub> flux was similar for all 5% mixtures (Figure 6a). For the MD experiment, where samples were air dried after each gas measurement, we also observed again that CO<sub>2</sub> flux was highest for the pure AS-2 (Figure 6d) and 5% mixture (Figure 6b) throughout the entire incubation period, although CO<sub>2</sub> flux fluctuated greatly.

Figure 7 shows the fitted respiration parameters for treatments in the MC incubation and is separated into labile carbon pool (a), total CO<sub>2</sub> loss in mgC per gC (b), and rate of decomposition (in mgC/gC/d) for both the fast and slow carbon pools at the initial stage (Figure 7c and 7d). As observed, pure AS-2 biochar and AS-2 biochar mixture are the

only treatments with significantly higher effect on total carbon loss (Figure 7b) and both fast and slow decomposition rates (Figures 7c and 7d) at the start of the incubation. WS-2 and ATC-1 both pure and mixture were similar to each other and to the Control. Figure 8 shows the CO<sub>2</sub> flux, expressed in mgC/gC/d, plotted against moisture content (in g/g) for the MD incubation and is separated by pure biochar and 5% biochar mixtures. For the pure material, AS-2 biochar has the most effect on CO<sub>2</sub> flux at any given moisture content, followed by WS-2 and ATC-1. When comparing the Control and biochar mixtures, again we observed that CO<sub>2</sub> flux was highest for AS-2 biochar, whereas all biochar mixtures yielded a much greater respiration slope compared to Control (Figure 8).

## 2.4 Discussion

### 2.4.1 Biochar and Mixtures SSA estimated using WSI Approach

As observed in Table 4, except for WS-2 and BCW, SSA was similar for most of the tested biochars (~ 72 m<sup>2</sup>/g). This outcome is surprising since these biochar were made using different orchard residues, but at the same time expected because all biochar were created using the same pyrolyzer unit at the same pyrolysis temperature. Note that both WS-2 and BCW are walnut shell derived biochar, similar to WS-1. We suspected the variation in SSA among walnut shell biochar may be linked to the conditions of the original raw feedstock (e.g. moisture content, feedstock age, etc.) prior to pyrolysis. For example, drier biomass exposed to the same temperature, pyrolysis duration, and residence time will undergo more physiochemical changes (via combustion) than wet biomass of the same feedstock (Cha et al., 2016). A literature review conducted by Weber and Quicker (2018) on biochar properties as influenced by different variables (e.g. feedstock, temperature, and process design) also concluded that pyrolysis temperature has the most dominant effect on biochar properties, particularly sensitive at 200 – 400 °C. In this case it is possible that both WS-2 and BCW are walnut shell that have relatively lower moisture content compared to WS-1 and the other orchard wastes. Other factors that could potentially cause this disparity in SSA among the same feedstock is residence time after pyrolysis, which has also been reported to have a major impact on biochar specific area but is feedstock specific (Lu et al., 1995).

The application of these seven biochar to the Atwater loamy-sand soil significantly enhances mixture SSA regardless of biochar type and increases with application rate. This is evidenced by the strong correlation ( $R^2 > 0.8$ ) between biochar SSA and mixtures SSA shown in Figure S2.2, and the statistical difference shown in Table 4. This observation proves that the water sorption isotherm method works well for inverse estimation of biochar and biochar soil mixtures SSA. Similarly, Arthur et al. (2015) also observed significant increase in SSA for coarse-textured soil amended with biochar and manure at different application rates using the WSI approach. However in our study the significant increase in SSA did not translate to an increase in soil moisture retention or more specifically plant available water (discussed more in Section 4.2). The higher SSA detected for WS-2 may be associated with the presence of more micropore which is the main contributor to biochar surface area (Panahi et al., 2020). This could explain why WS-2 retained substantially greater moisture at very dry suction potential (> 10 MPa), compared to the other biochar (Figure 2).

### 2.4.2 Biochar Influence on SWRC

In our study, soil water retention for the Atwater loamy-sand soil was enhanced by biochar amendment. This was observed in both the soil hydraulic model using a 5% application rate (Figure 3) and actual WRC measurement for biochar application rates (Figures 4 and 5). The increase in moisture as predicted by the model ranges from less than 5% to as great as 20% in water content at field capacity and wilting point regions. The influence on SWRC from the 5% WP4C dataset was consistent with the model prediction for most of the biochar but varied for BCW. As stated earlier, measured moisture retention at 5% application rate for BCW biochar is considerably lower than what the model predicted using WRC from the pure BCW. Currently, we don't have an appropriate explanation for this discrepancy. Though in the literature, it has been reported that biochar water holding capacity is affected by multiple factors such as, surface functional groups, total pore volume, porosity structure, and specific surface area (Zhang & You, 2013). However, since we did not assess most of these variables, we are not able to identify the causes for this observation. Another possibility could be the surface hydrophobicity of BCW biochar (determined to be strongly repellent in Table 1) that could prevent pore water sorption (Gray et al., 2014; Jeffery et al., 2015). However AS-1 was also classified as extremely hydrophobic, therefore this assumption is not probable. Nevertheless, from the seven biochar tested, it seems that biochar derived from almond shell using this mobile unit and at this temperature range has the most positive effect on the coarse-textured soil water holding capacity. Similarly, Sánchez et al. (2022) also observed an increase in moisture content for saline affected soil amended with almond shell biochar (derived at 450 °C) using different application rates (5%, 10%, and 15% w/w).

The difference between WS-2 which has higher SSA and greater moisture retention at MPa > 10, and AS-1 and AS-2 biochar (lower SSA but greater moisture retention at MPa < 10) may be linked to the difference in pore size distribution (e.g. macropore, mesopore, and micropore) that makes up total pore volume of biochar (Brewer et al., 2014). As previously stated, the higher SSA detected for WS-2 may be associated with the presence of more micropore, which retained greater moisture in dry conditions by adsorption but is less accessible for plant uptake (Panahi et al., 2020). Meanwhile the greater water retention observed for both AS-1 and AS-2 may be due to the presence of more macropores which allow for more storage of plant-available water due to higher pore volume compared to micropore (Downie et al., 2012). In a lab study, Mollinedo et al. (2015) evaluated five different biochar and its effects on moisture retention also detected a significant increase soil water holding capacity (~25% increase compared to unamended soil) and greater fitted water retention curve parameters corresponding to the macropore and mesopore regions for biochar amended sandy loam soil. Furthermore, the statistical consistency in SSA and moisture retention as observed to amplify with increasing biochar application rate also support our assertion that adding these locally derived biochar to soil can enhance moisture retention for commonly farmed coarse-textured soil in the Central Valley.

### 2.4.3 Biochar Influence on Soil Respiration under Different Moisture Conditions.

Soil water status has been recognized as one of the most important abiotic factors influencing microbial activity and mineralization rates (Ghezzehei et al., 2019; Manzoni et al., 2012). Soil water status is affected by soil physical properties, e.g. porosity, bulk density, aggregation, and surface area, that are key factors in soil aeration, sorption, and

transport of solutes in the soil profile. Hence, changes in these components can cause disturbance in the microbial communities. In the case of biochar, incorporating the material means physically altering soil structure (Blanco-Canqui, 2017), changing its pore connectivity, thus hydraulic conductivity, and impacting water accessibility to soil microorganisms. In our incubation experiments, CO<sub>2</sub> flux shows that the addition of a carbon rich material like biochar enhanced respiration rate for the loamy sand soil, particularly visible for almond shell biochar. In conditions where moisture is not a limiting factor (sustained at 1.01 MPa) we observed that 5% AS-2 biochar application increased the initial rate of decomposition for both fast and slow carbon pools compared to unamended soil (Figure 7c & 7d). However, note that the labile carbon pool of AS-2 mixture is also substantially lower than WS-2 and ATC-1 mixtures (Figure 7a), which implies that only a small fraction of the total C is bioavailable in AS-2 mixture (compared to others). Nevertheless, that small fraction decomposes faster because of the elevated water status (Figure 4) which results in more carbon loss (Figure 7b). This result is astonishing especially since the moisture difference between Control and AS-2 biochar mixture was not that great at 1.01 MPa (Table 2). Similarly, Smith et al. (2010) also detected a substantial increase in cumulative respiration rate for biochar amended soil using lab incubation study. Furthermore, we observed a peak in soil respiration rate after water application followed by a rapid decline in CO<sub>2</sub> flux during the first three weeks of the MC study. Other incubation studies have also observed a significant increase in soil respiration after biochar incorporation especially during the initial incubation period, which implied the present of labile carbon in biochar that affect short-term mineralization rate (Farrell et al., 2013; Smith et al., 2010; Ulyett et al., 2014). For conditions where moisture is a limiting factor, the application of biochar to the coarse-textured soil also enhances soil respiration rate. This is observed by the increases in the CO<sub>2</sub> slope (moisture dependence of flux) relative to Control in Figure 8. These observations support our hypothesis that biochar addition to soil can increase microbial activity by prolonging moisture accessibility to soil microbes (Gul et al., 2015; Lehmann et al., 2011).

## 2.5 Conclusion

In this study we were able to infer the specific surface area of different biochar using water vapor measurement and film sorption theory. The film model shows that walnut shell derived biochar WS-2 and BCW have the highest SSA. However, we observed that at 5% and 10% application rates, almond shell derived biochar has a more remarkable impact on soil water retention, specifically at the mid to dry moisture regions for the loamy sand soil. For the modeled 5% application, the moisture retention predicted were as much as 20-25% increase in water holding capacity for almond shell biochar, compared to unamended soil. Biochar derived from almond tree chip and walnut shell has negligible effect on predicted soil water retention capacity. Change in moisture content at these soil water potential regions can have a profound effect on soil biota, influencing the overall soil respiration rate. CO<sub>2</sub> measurement from the two 109 days incubation experiments shows that almond shell biochar also has the most effect on soil respiration. The application of 5% AS-2 biochar also enhances the initial decomposition rates and total soil carbon loss. Our results reflect the immediate effect of biochar added to a loamy sand soil and is encouraging for the use of locally produced biochar, derived from local agricultural wasted organic materials using small-scale pyrolysis units.

## 2.6 Reference

- Ali, S., Rizwan, M., Qayyum, M.F., Ok, Y.S., Ibrahim, M., Riaz, M., Arif, M.S., Hafeez, F., Al-Wabel, M.I. and Shahzad, A.N. (2017). Biochar soil amendment on alleviation of drought and salt stress in plants: a critical review. *Environmental Science and Pollution Research*, 24(14), 12700-12712. DOI 10.1007/s11356-017-8904-x
- Arkley, R.J. (1962). *Soil Survey, Merced Area, California* (No. 7). The Service.
- Arthur, E., Tuller, M., Moldrup, P. and de Jonge, L.W. (2015). Effects of biochar and manure amendments on water vapor sorption in a sandy loam soil. *Geoderma*, 243, 175-182. <https://doi.org/10.1016/j.geoderma.2015.01.001>
- Arthur, E., Tuller, M., Moldrup, P. and de Jonge, L.W. (2016). Evaluation of theoretical and empirical water vapor sorption isotherm models for soils. *Water Resources Research*, 52(1), 190-205. <https://doi.org/10.1002/2015WR017681>
- Arthur, E., Tuller, M., Moldrup, P., Resurreccion, A.C., Meding, M.S., Kawamoto, K., Komatsu, T. and De Jonge, L.W. (2013). Soil specific surface area and non-singularity of soil-water retention at low saturations. *Soil Science Society of America Journal*, 77(1), 43-53. <https://doi.org/10.2136/sssaj2012.0262>
- Blanco-Canqui, H. (2017). Biochar and soil physical properties. *Soil Science Society of America Journal*, 81(4), 687-711. <https://doi.org/10.2136/sssaj2017.01.0017>
- Brewer, C.E., Chuang, V.J., Masiello, C.A., Gonnermann, H., Gao, X., Dugan, B., Driver, L.E., Panzacchi, P., Zygourakis, K. and Davies, C.A. (2014). New approaches to measuring biochar density and porosity. *Biomass and Bioenergy*, 66, 176-185. <https://doi.org/10.1016/j.biombioe.2014.03.059>
- Brown, S.L., Goulsbra, C.S., Evans, M.G., Heath, T. and Shuttleworth, E. (2020). Low cost CO<sub>2</sub> sensing: A simple microcontroller approach with calibration and field use. *HardwareX*, 8, p.e00136. <https://doi.org/10.1016/j.ohx.2020.e00136>
- Cha, J.S., Park, S.H., Jung, S.C., Ryu, C., Jeon, J.K., Shin, M.C. and Park, Y.K. (2016). Production and utilization of biochar: A review. *Journal of Industrial and Engineering Chemistry*, 40, 1-15. <https://doi.org/10.1016/j.jiec.2016.06.002>
- Chopda, V.R., Holzberg, T., Ge, X., Folio, B., Tolosa, M., Kostov, Y., Tolosa, L. and Rao, G. (2020). Real-time dissolved carbon dioxide monitoring I: Application of a novel in situ sensor for CO<sub>2</sub> monitoring and control. *Biotechnology and Bioengineering*, 117(4), 981-991. <https://doi.org/10.1002/bit.27253>
- Delwiche, K.B., Lehmann, J. and Walter, M.T. (2014). Atrazine leaching from biochar-amended soils. *Chemosphere*, 95, 346-352. <https://doi.org/10.1016/j.chemosphere.2013.09.043>
- Downie, A., Crosky, A. and Munroe, P. (2012). Physical properties of biochar. In *Biochar for Environmental Management*. 45-64. Routledge.

- Farrell, M., Kuhn, T.K., Macdonald, L.M., Maddern, T.M., Murphy, D.V., Hall, P.A., Singh, B.P., Baumann, K., Krull, E.S. and Baldock, J.A. (2013). Microbial utilisation of biochar-derived carbon. *Science of the Total Environment*, 465, 288-297. <https://doi.org/10.1016/j.scitotenv.2013.03.090>
- Gee, G.W., Campbell, M.D., Campbell, G.S. and Campbell, J.H. (1992). Rapid measurement of low soil water potentials using a water activity meter. *Soil Science Society of America Journal*, 56(4), 1068-1070. <https://doi.org/10.2136/sssaj1992.03615995005600040010x>
- Ghezzehei, T.A., Sarkhot, D.V., Berhe, A.A. (2014). Biochar can be used to capture essential nutrients from dairy wastewater and improve soil physico-chemical properties. *Solid Earth*, 5(2): 953-962. doi:10.5194/se-5-953-2014
- Ghezzehei, T.A., Sulman, B., Arnold, C.L., Bogie, N.A. and Berhe, A.A. (2019). On the role of soil water retention characteristic on aerobic microbial respiration. *Biogeosciences*, 16(6). doi:10.5194/bg-16-1187-2019.
- Gray, M., Johnson, M.G., Dragila, M.I. and Kleber, M. (2014). Water uptake in biochars: The roles of porosity and hydrophobicity. *Biomass and Bioenergy*, 61, 196-205. <https://doi.org/10.1016/j.biombioe.2013.12.010>
- Gul, S., Whalen, J.K., Thomas, B.W., Sachdeva, V. and Deng, H. (2015). Physico-chemical properties and microbial responses in biochar-amended soils: mechanisms and future directions. *Agriculture, Ecosystems & Environment*, 206, 46-59. <https://doi.org/10.1016/j.agee.2015.03.015>
- Iden, S. C., & Durner, W. (2014). Comment on “Simple consistent models for water retention and hydraulic conductivity in the complete moisture range” by A. Peters. *Water Resources Research*, 50, 7530–7534. <https://doi.org/10.1002/2014WR015937>
- Iwamatsu, M. & Horii, K. (1996). Capillary condensation and adhesion of two wetter surfaces. *Journal of Colloid and Interface Science*, 182(2), 400-406. <https://doi.org/10.1006/jcis.1996.0480>
- Jeffery, S., Meinders, M.B., Stoof, C.R., Bezemer, T.M., van de Voorde, T.F., Mommer, L. and van Groenigen, J.W. (2015). Biochar application does not improve the soil hydrological function of a sandy soil. *Geoderma*, 251, 47-54. <https://doi.org/10.1016/j.geoderma.2015.03.022>
- Jones, D.L., Murphy, D.V., Khalid, M., Ahmad, W., Edwards-Jones, G. and DeLuca, T.H. (2011). Short-term biochar-induced increase in soil CO<sub>2</sub> release is both biotically and abiotically mediated. *Soil Biology and Biochemistry*, 43(8), 1723-1731. <https://doi.org/10.1016/j.soilbio.2011.04.018>
- Kameyama, K., Miyamoto, T., Shiono, T. and Shinogi, Y. (2012). Influence of sugarcane bagasse-derived biochar application on nitrate leaching in calcaric dark red soil. *Journal of Environmental Quality*, 41(4), 1131-1137. doi:10.2134/jeq2010.0453

- Laird, D.A., Fleming, P., Davis, D.D., Horton, R., Wang, B. and Karlen, D.L. (2010). Impact of biochar amendments on the quality of a typical Midwestern agricultural soil. *Geoderma*, 158(3-4), 443-449. <https://doi.org/10.1016/j.geoderma.2010.05.013>
- Leão, T.P. & Tuller, M. (2014). Relating soil specific surface area, water film thickness, and water vapor adsorption. *Water Resources Research*, 50(10), 7873-7885. <https://doi.org/10.1002/2013WR014941>
- Leng, L., Xiong, Q., Yang, L., Li, H., Zhou, Y., Zhang, W., Jiang, S., Li, H. and Huang, H. (2021). An overview on engineering the surface area and porosity of biochar. *Science of the total Environment*, 763, 144204. <https://doi.org/10.1016/j.scitotenv.2020.144204>
- Lehmann, J., Gaunt, J., Rondon, M. (2006). Bio-char sequestration in terrestrial ecosystems - A review. *Mitigation and Adaptation Strategies for Global Change*, 11(2): 403-427. DOI: 10.1007/s11027-005-9006-5
- Lehmann, J., Rillig, M.C., Thies, J., Masiello, C.A., Hockaday, W.C. and Crowley, D. (2011). Biochar effects on soil biota—a review. *Soil Biology and Biochemistry*, 43(9), 1812-1836. <https://doi.org/10.1016/j.soilbio.2011.04.022>
- Lu, G.Q., Low, J.C.F., Liu, C.Y. and Lua, A.C. (1995). Surface area development of sewage sludge during pyrolysis. *Fuel*, 74(3), 344-348. [https://doi.org/10.1016/0016-2361\(95\)93465-P](https://doi.org/10.1016/0016-2361(95)93465-P)
- Major, J., Rondon, M., Molina, D., Riha, S.J. and Lehmann, J. (2012). Nutrient leaching in a Colombian savanna Oxisol amended with biochar. *Journal of Environmental Quality*, 41(4), 1076-1086. doi:10.2134/jeq2011.0128
- Manzoni, S., Schimel, J.P. and Porporato, A. (2012). Responses of soil microbial communities to water stress: results from a meta-analysis. *Ecology*, 93(4), 930-938. <https://doi.org/10.1890/11-0026.1>
- Masiello, C.A., Dugan, B., Brewer, C.E., Spokas, K.A., Novak, J.M., Liu, Z. and Sorrenti, G. (2015). Biochar effects on soil hydrology. In *Biochar for Environmental Management*. 575-594. Routledge.
- McLaughlin, H., Shields, F., Jagiello, J. and Thiele, G. (2012). Analytical options for biochar adsorption and surface area. In *North American Biochar Conference*, Sonoma, CA.
- Mollinedo, J., Schumacher, T.E. and Chintala, R. (2015). Influence of feedstocks and pyrolysis on biochar's capacity to modify soil water retention characteristics. *Journal of Analytical and Applied Pyrolysis*, 114, 100-108. <https://doi.org/10.1016/j.jaap.2015.05.006>
- Panahi, H.K.S., Dehghani, M., Ok, Y.S., Nizami, A.S., Khoshnevisan, B., Mussatto, S.I., Aghbashlo, M., Tabatabaei, M. and Lam, S.S. (2020). A comprehensive review of engineered biochar: production, characteristics, and environmental applications. *Journal of Cleaner Production*, 270, 122462. <https://doi.org/10.1016/j.jclepro.2020.122462>

- Pennell, K.D. (2002). Specific surface area. In 'Methods of soil analysis. Part 4. Physical methods'. (Eds JH Dane, G Clarke Topp). 295–315. Soil Science Society of America: Madison, WI
- Peters, A. (2013). Simple consistent models for water retention and hydraulic conductivity in the complete moisture range. *Water Resources Research*, 49, 6765–6780. <https://doi.org/10.1002/wrcr.20548>
- R Core Team. (2020). R: A language and environment for statistical computing. R Foundation for Statistical Computing. [www.R-project.org](http://www.R-project.org)
- Rouquerol, J., Rouquerol, F., Llewellyn, P., Maurin, G., Sing, K.S. (2013). Adsorption by Powders and Porous Solids: Principles, Methodology and Applications. Academic press.
- Sánchez, E., Zabaleta, R., Fabani, M.P., Rodriguez, R. and Mazza, G. (2022). Effects of the amendment with almond shell, bio-waste and almond shell-based biochar on the quality of saline-alkali soils. *Journal of Environmental Management*, 318, 115604. <https://doi.org/10.1016/j.jenvman.2022.115604>
- Schneider, M., & Goss, K.-U. (2012). Prediction of the water sorption isotherm in air dry soils. *Geoderma*, 170, 64–69. <https://doi.org/10.1016/j.geoderma.2011.10.008>
- Smith, J.L., Collins, H.P. and Bailey, V.L. (2010). The effect of young biochar on soil respiration. *Soil Biology and Biochemistry*, 42(12), 2345-2347. <https://doi.org/10.1016/j.soilbio.2010.09.013>
- Tuller, M., Or, D. and Dudley, L.M. (1999). Adsorption and capillary condensation in porous media: Liquid retention and interfacial configurations in angular pores. *Water Resources Research*, 35(7), 1949-1964. <https://doi.org/10.1029/1999WR900098>
- Tuller, M. & Or, D. (2005). Water films and scaling of soil characteristic curves at low water contents. *Water Resources Research*, 41(9). <https://doi.org/10.1029/2005WR004142>
- Ulyett, J., Sakrabani, R., Kibblewhite, M. and Hann, M. (2014). Impact of biochar addition on water retention, nitrification and carbon dioxide evolution from two sandy loam soils. *European Journal of Soil Science*, 65(1), 96-104. <https://doi.org/10.1111/ejss.12081>
- van Genuchten, M. T. (1980). A closed-form equation for predicting the hydraulic conductivity of unsaturated soils. *Soil Science Society of America Journal*, 44, 892–898. <https://doi.org/10.2136/sssaj1980.03615995004400050002x>
- Wang, D., Felice, M.L. and Scow, K.M. (2020). Impacts and interactions of biochar and biosolids on agricultural soil microbial communities during dry and wet-dry cycles. *Applied Soil Ecology*, 152, .103570. <https://doi.org/10.1016/j.apsoil.2020.103570>
- Weber, K. & Quicker, P. (2018). Properties of biochar. *Fuel*, 217, 240-261. <https://doi.org/10.1016/j.fuel.2017.12.054>

Zhang, J. & You, C. (2013). Water holding capacity and absorption properties of wood chars. *Energy & Fuels*, 27(5), 2643-2648. <https://doi.org/10.1021/ef4000769>

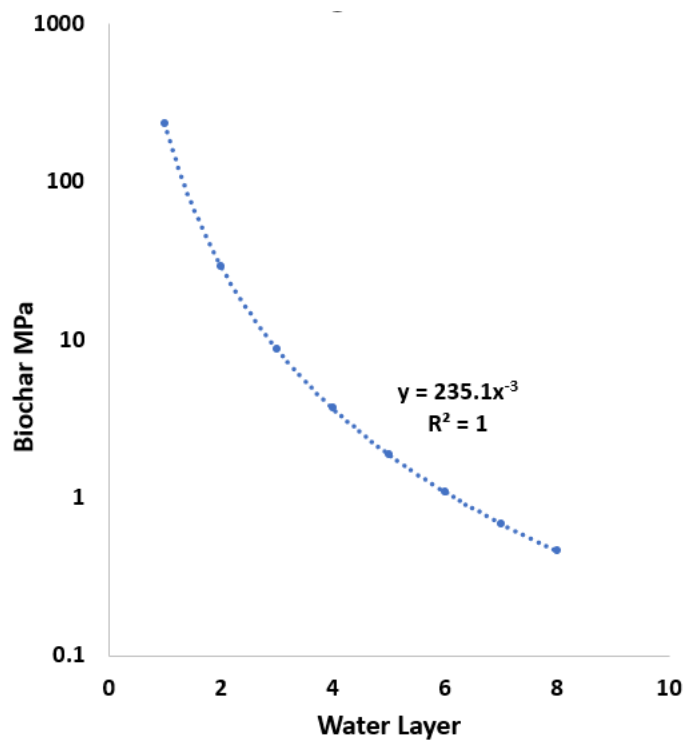


Figure 2-1 Film model used to determine materials specific surface area. Assuming a Hamaker constant of  $1.90E-19$  J and one monolayer of film water is  $3.50E-10$  m.

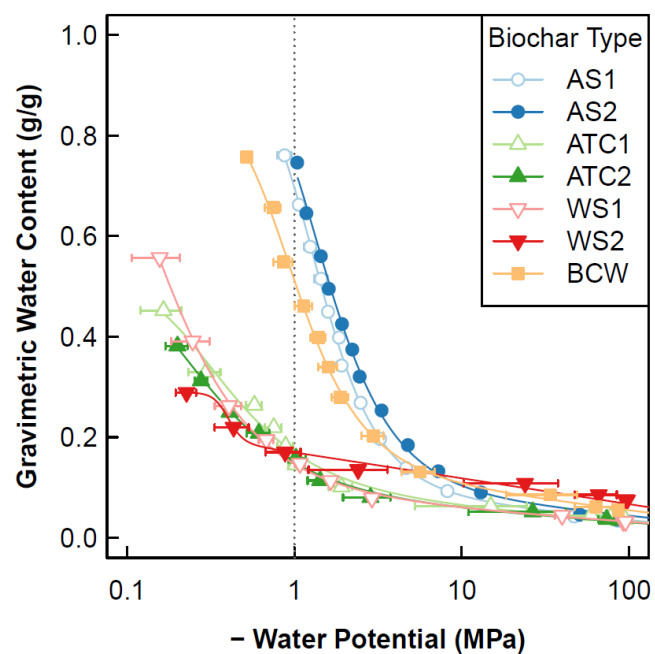


Figure 2-2 WRC for seven different biochar. Mean of three replications with standard error bar.

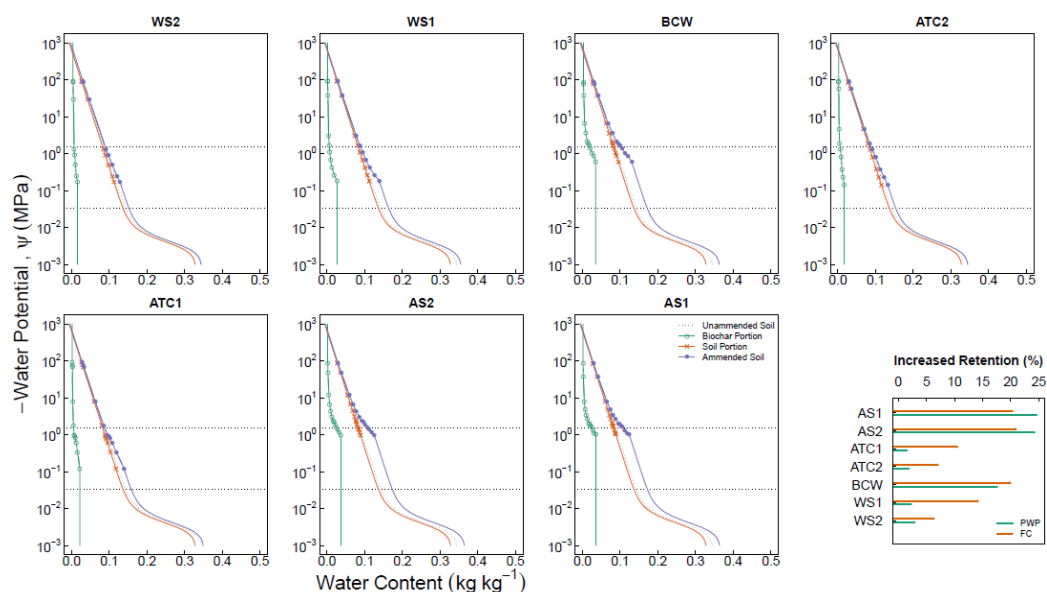


Figure 2-3 Modeled Atwater loamy-sand SWRC for 5% biochar application rate.

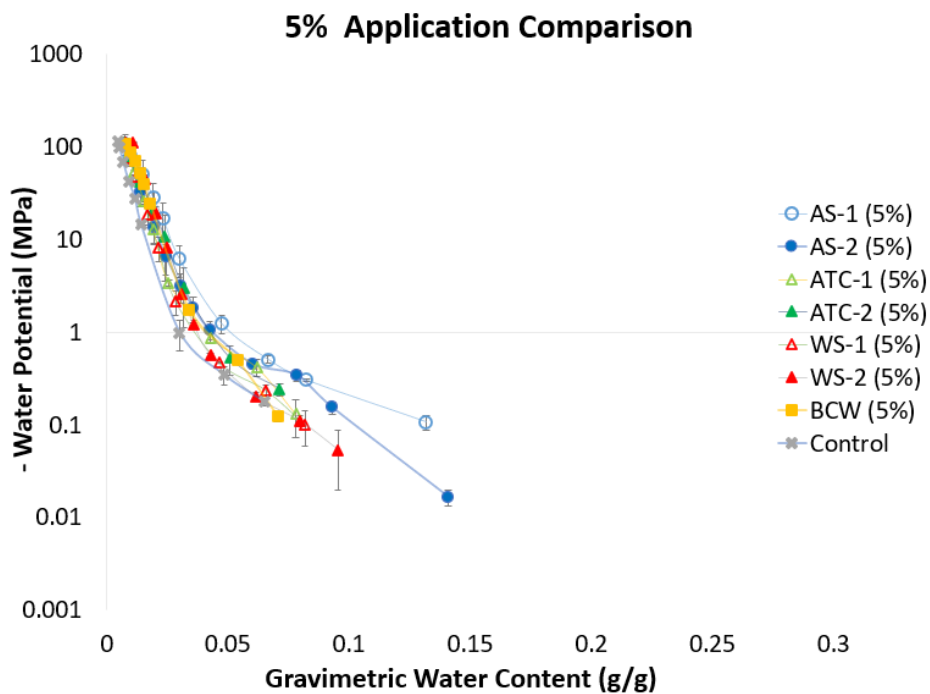


Figure 2-4 SWRC for 5% application rate, derived using WP4C. Mean of three replications with standard error bar.

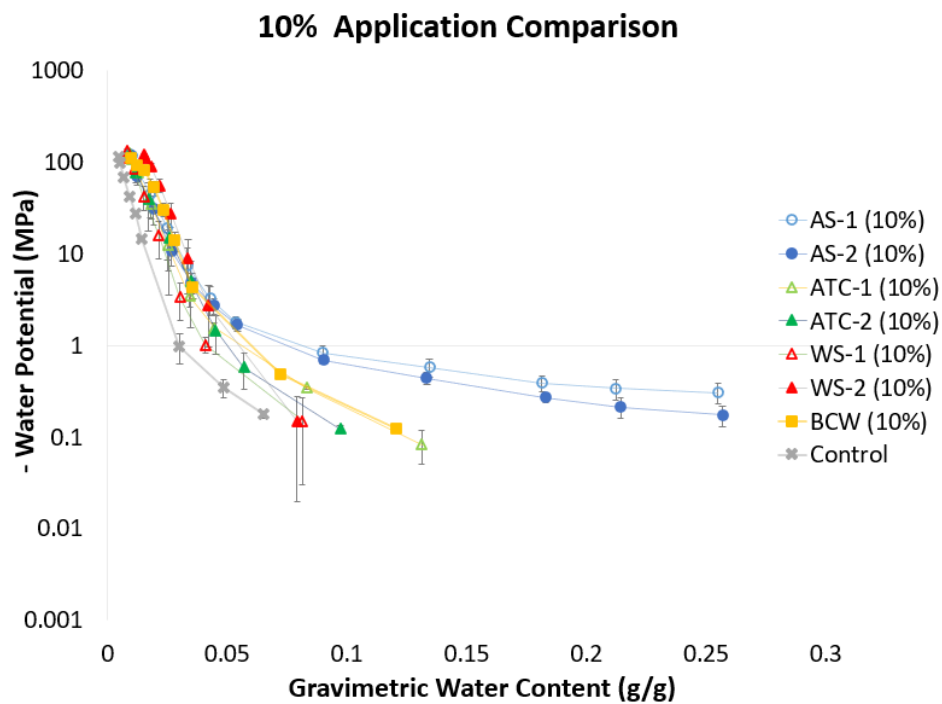


Figure 2-5 SWRC for 10% application rate, derived using WP4C. Mean of three replications with standard error bar.

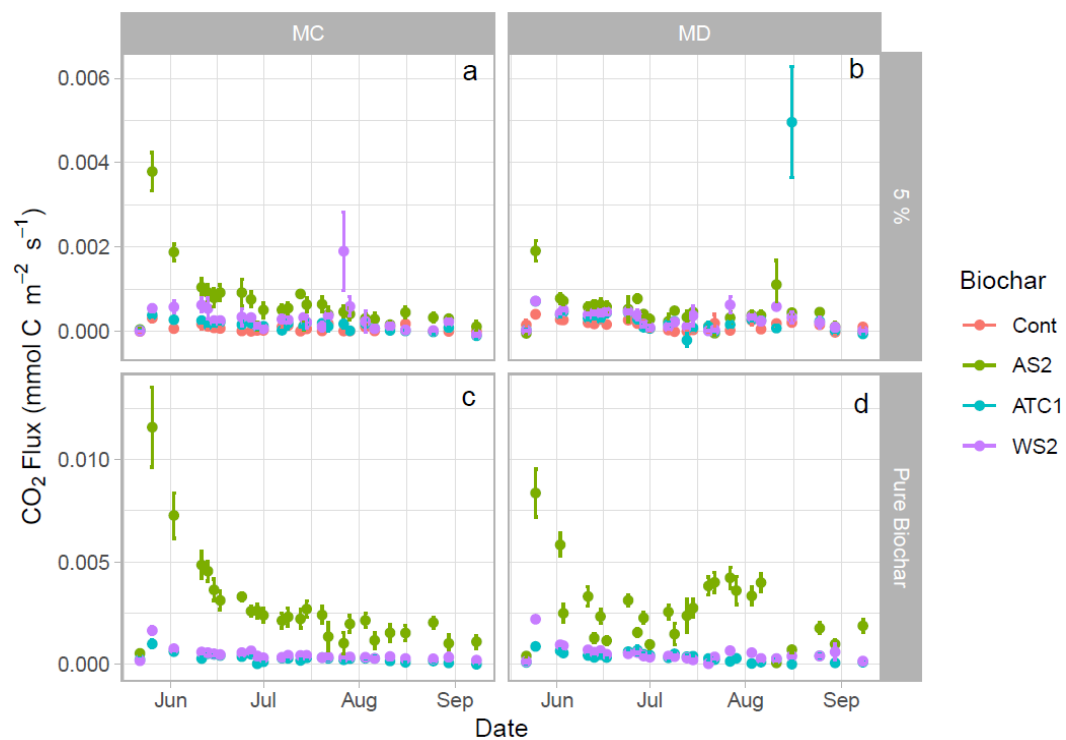


Figure 2-6 CO<sub>2</sub> flux for both MC and MD experiments taken throughout the incubation period. Mean of four replications with standard error bar.

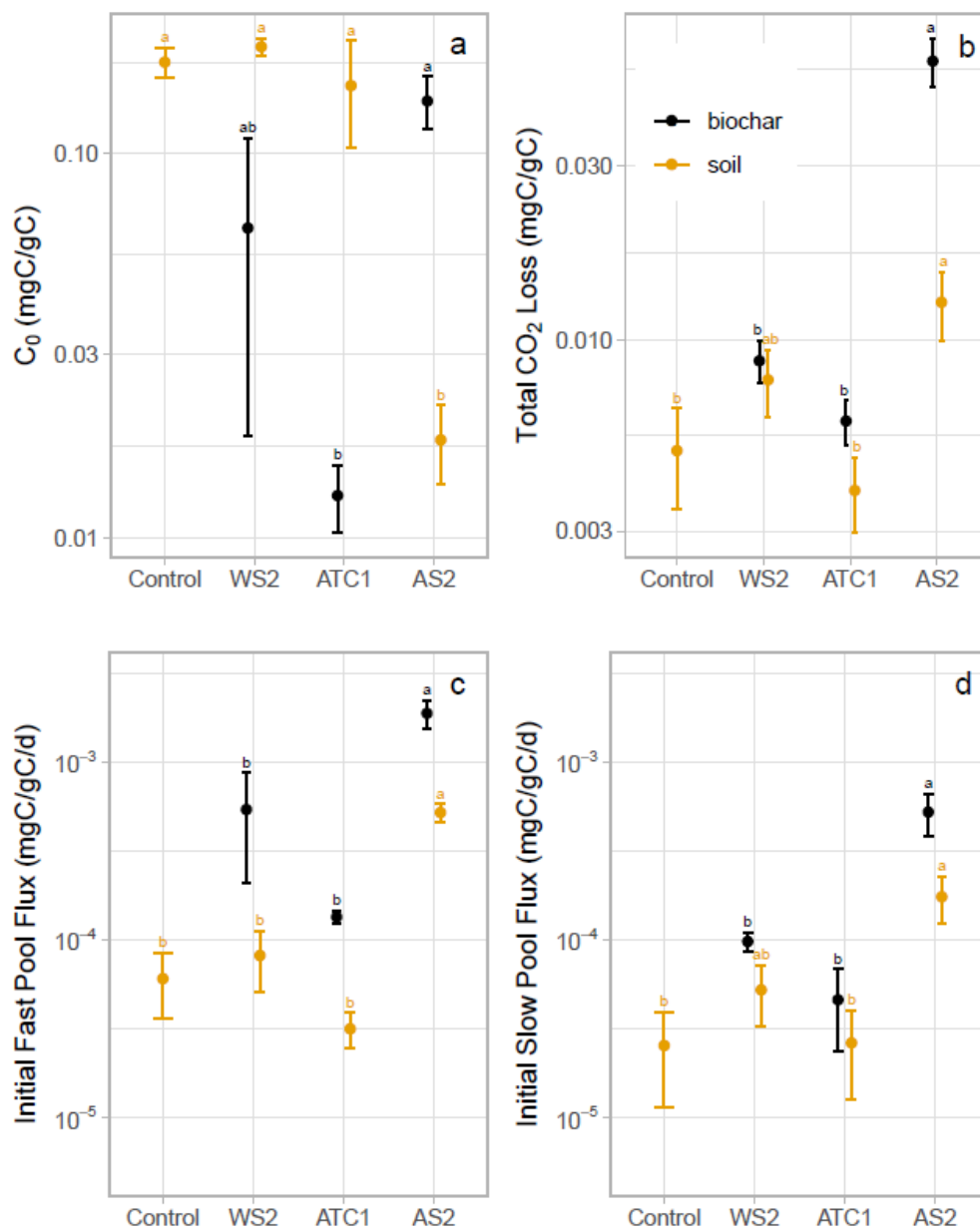


Figure 2-7 Labile carbon fraction (a), total  $CO_2$  loss (b), and initial rates (fast and slow pools, c and d) of carbon loss for Moisture Constant incubation.

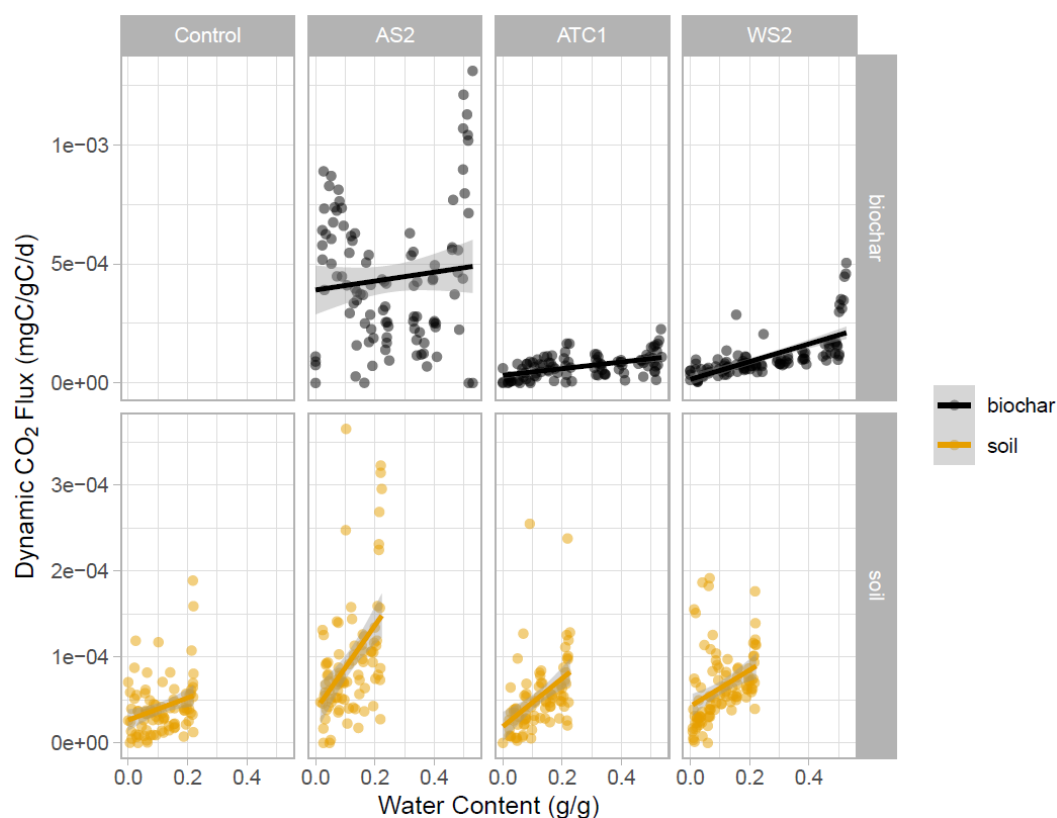


Figure 2-8 Rate of carbon loss for Moisture Dynamic incubation, y-axis is CO<sub>2</sub> flux in mgC/gC/d and x-axis is moisture content in g/g.

Table 2-1. R134a absorbance, bulk density, and hydrophobicity of biochar and mixtures.

Biochar	R134a (% wt/cm <sup>3</sup> )	Bulk Density (g/cm <sup>3</sup> )	*WDPT (s)	Class	*5% (s)	*10% (s)
AS-1	0.31	0.35	>3600	Extremely repellent	<1	2.1
AS-2	0.38	0.30	2.32	Slightly-repellent	<1	<1
WS-1	0.97	0.44	419.5	Strong repellent	<1	<1
WS-2	3.74	0.46	6.27	Slightly repellent	<1	<1
ATC-1	1.75	0.33	15.1	Slightly repellent	<1	<1
ATC-2	0.51	0.35	>3600	Extremely repellent	<1	1.5
BCW	0.57	0.26	166.46	Strong repellent	<1	<1
Control	N/A	1.48	<1	Non-repellent	<1	<1

\* Biochar R134a and bulk density provided by Dr. Hugh McLaughlin

\* Mean of nine measurements

Table 2-2. Initial Moisture for Incubation Experiments

Treatment	Moisture Dynamic ( $\theta_m$ at 20 g water)*	Moisture Constant ( $\theta_m$ at 1.01 MPa)*
AS-2	0.526	0.659
WS-2	0.522	0.152
ATC-1	0.529	0.140
5% AS-2	0.221	0.041
5% WS-2	0.220	0.041
5% ATC-1	0.218	0.040
Control	0.216	0.029

\* Mean of three replications

Table 2-3. Carbon and nitrogen content of soil and biochar.

Treatment	C (%)	N (%)	C:N (%)	pH	EC ( $\mu\text{S}/\text{cm}$ )
Control	0.78	0.06	13.00	6.70	350.3
AS-2	68.4	0.94	72.58	9.42	5773
WS-2	72.5	0.44	163.9	7.96	1083
ATC-1	72.3	0.66	110.1	9.42	431.9

Table 2-4. Specific surface area for biochar, 5%, and 10% rates

Biochar	SSA ( $\text{m}^2/\text{g}$ )	SSA 5% ( $\text{m}^2/\text{g}$ )	SSA 10% ( $\text{m}^2/\text{g}$ )
AS-1	69 <sup>c</sup>	16 <sup>b</sup>	23 <sup>b</sup>
AS-2	74 <sup>c</sup>	17 <sup>b</sup>	21 <sup>b</sup>
WS-1	68 <sup>c</sup>	17 <sup>b</sup>	19 <sup>b</sup>
WS-2	159 <sup>a</sup>	24 <sup>a</sup>	35 <sup>a</sup>
ATC-1	78 <sup>c</sup>	16 <sup>b</sup>	21 <sup>b</sup>
ATC-2	72 <sup>c</sup>	17 <sup>b</sup>	21 <sup>b</sup>
BCW	113 <sup>b</sup>	17 <sup>b</sup>	22 <sup>b</sup>
Control		11 <sup>c</sup>	11 <sup>c</sup>

\*SSA  $p < 0.001$

\*SSA 5%  $p < 0.001$

\*SSA 10%  $p < 0.001$

## Chapter 3.

# Impact of biochar amendments on soil water and plant uptake dynamics under different cropping systems

## Abstract

Application of biochar amendments in agricultural systems has received much attention in recent years. In this study, we assess the 5-year impacts of biochar application on soil water and plant interactions for an irrigated fresh market tomato and a rainfed pasture cropping system. In particular, we focus on three varieties of locally-produced biochar from agricultural waste materials – almond shell, walnut shell and almond pruning residues that are pyrolyzed using a mobile pyrolysis unit. We used the soil hydrological model HYDRUS-1D to explicitly track seasonal and annual soil water fluxes through changes in water retention, drainage, evaporation, and plant water uptake under biochar application. Modeling results show that the application of biochar at 5% increased soil water availability within the top 20 cm for a rainfed system, irrespective of biochar amendment type. This is clearly indicative of higher plant water uptake and greater water use efficiency (WUE) under biochar application. In contrast, a similar biochar amendment for the irrigated system did not affect WUE, instead reducing seasonal soil evaporation loss and thereby reducing irrigation demand. In both cropping systems, year-to-year variability in precipitation significantly impacted the total amount of water saved under biochar application with certain amendments retaining more water than others. Given that biochar application increased water retention irrespective of cropping systems, we further used a simple approach to determine yield trade-off, if any, between control and biochar treatments. Our economic balance clearly demonstrates that the water saved by amending soil with biochar does not offset the yield disparity if compensated with carbon credits and therefore, application of biochar should be actively considered for both its direct and indirect benefits to potential greenhouse gas mitigation (e.g. diverting orchard waste from open burning), water savings and soil health.

## 3.1 Introduction

The use of soil amendments in cropping systems has been well acknowledged as an agronomic practice that leads to improved soil health and other benefits. Among various materials, biochar is a substance that is increasingly gaining attention primarily due to its high sorption potential (Delwiche et al., 2014; Jones et al., 2011; Kameyama et al., 2012; Major et al., 2012). Biochar is a pyrolysis by-product and can be synthesized from waste materials such as animal manure, leftover plant biomass, and woody material (e.g., dead trees). The incorporation of biochar in soil has the potential to enhance soil carbon sequestration (Lehmann et al., 2006) and change soil water status (Horel et al., 2019; Kameyama et al., 2012; Novak et al., 2009; Villagra-Mendoza & Horns, 2018).

Soil water status is one of the most important abiotic factors controlling crop productivity, and one that is affected by climatic conditions and soil physico-chemical properties. A crucial aspect of biochar addition to soils is its potential to change the soil

water status by increasing water retention capacity. One of the mechanisms for biochar to do so is by providing a large wettable surface area that increases the affinity of biochar-treated soils to water. Over longer time scales, elevated moisture retention can promote biological activity that is expected to lead to biophysical aggregation of soil and subsequent development of soil structure that promotes both infiltration and water storage. However, the overall effects of biochar on soil physical and hydraulic properties have not been consistent in the literature, especially varying across different cropping systems. Studies have shown both beneficial (Abel et al., 2013; Ajayi et al., 2016; Arthur et al., 2015; Kameyama et al., 2012; Kroeger et al., 2021; Villagra-Mendoza & Horns, 2018; Zhou et al., 2018) and negligible (Jeffery et al., 2015; Pressler et al., 2017; Wiersma et al., 2020) effects of biochar on soil hydraulic and physical properties. Using both laboratory and field measurements, Abel et al. (2013) observed a decrease in soil bulk density, increase in pore volume, and increase in available water content near wilting point for soils amended with biochar. Conversely, Major et al. (2012) detected no significant changes in soil water content for biochar amended soil after multiple seasons of maize-soybean rotation in Colombia. Similarly, biochar produced at two temperatures (400 °C and 600 °C) was applied to two nature restoration grasslands (Jeffery et al., 2015). After the end of the growing season, the authors did not detect any noticeable change in moisture retention, aggregate stability, or saturated hydraulic conductivity ( $K_{sat}$ ) (Jeffery et al., 2015). Therefore, these field studies highlight the disparity in observed soil water status under biochar applications across cropping systems and since time of application. More importantly, even if more water is retained in biochar amended soil during the growing season, it does not necessarily equate to more water for crops or higher crop yields (Aller et al., 2017). Thus, the effects of long-term interactions between biochar addition, soil types, and cropping systems remain poorly understood.

Given the complex and multiple interactions governing the impacts of biochar addition, modeling studies have been used to study the impact of biochar amendment on crop yield and overall environmental effects (Aller et al., 2018; Archontoulis et al., 2016; Horel et al., 2019; Huang et al., 2020; Jellali et al., 2016; Kameyama et al., 2012; Lefebvre et al., 2020; Lychuk et al., 2015; Major et al., 2012; Stylianou et al., 2021). For example, Lefebvre et al. (2020) modified the RothC model to evaluate sugarcane biochar and its potential for carbon sequestration in Brazil. Similarly, Lychuk et al. (2015) used the Environmental Policy Integrated Climate (EPIC) model to simulate 20 years of biochar impacts on maize yield and soil properties. Archontoulis et al. (2016) developed a mechanistic model within Agricultural Production Systems sIMulator (APSIM) to investigate the long-term effects of biochar on maize and wheat under different soils and environmental conditions. Together, these studies have shown positive effects of amending soils with biochar through modeling although describing the complexity of these models is beyond the scope of the current study. However, a gap currently exists in quantifying the impact of locally-produced biochar from mobile pyrolysis units and connecting it to changes in soil hydraulic properties and crop yield under short- to mid-term applications. In this regard, HYDRUS (Arora et al., 2011; Karandish & Šimůnek, 2018; Šimůnek et al., 2016; Turkeltaub et al., 2018) has been successfully used to simulate biochar effects on soil hydraulic properties (Arabyarmohammadi et al., 2018; Filipović et al., 2020; Horel et al., 2019; Wu et al., 2019). However, the majority of these studies have focused entirely on short-term effects (e.g. 48 hours - 85 days) of biochar application (Altdorff et al., 2019; Filipović et al., 2020; Horel et al., 2019; Stylianou et al., 2021; Wu et al., 2019). For example, Wu et al. (2019) stimulated 48 hours of water flow in soil amended with maize biochar (450 °C) at five different rates to topsoil (25 cm) and observed higher saturated water content ( $\theta_s$ ) and lower residual water content

( $\theta_r$ ) with increasing application rates. Horel et al. (2019) assessed biochar (600 °C) influences on soil water and carbon dioxide (CO<sub>2</sub>) emission using four application rates (0-5% wt/wt) for 85 days. They observed that soil hydraulic conductivity increased with biochar application rates. In contrast to this study, Huang et al. (2020) observed lower hydraulic conductivity in biochar amended soil compared to control. However, their study was focused on evaluating the hydraulic performance of green roofs amended with biochar (750 °C) using 15 cm soil column subjected to five hours of precipitation. Therefore, even among these short-term focused studies, contradictory results pertaining to soil hydraulic properties and water status have been reported, and these contradictions have been primarily attributed to differences in biochar type, cropping system and climatic conditions. To the best of our knowledge, very few studies have used numerical models to simulate mid-term (2-5 years) impacts of biochar application on soil hydraulic properties that specifically account for year-to-year climatic variability. To fill this gap, this study was carefully designed to model the mid-term impacts of three different types of locally-produced biochar on soil water retention and crop yield potential for a representative field site located in Atwater, California. The field site typifies coarse-textured soils prevalent in the Central Valley of California, which is one of the most productive agricultural regions in the world. The primary goal of this study is thus to quantify the effects of locally-produced biochar on soil water retention and crop yield under two cropping systems with different irrigation schemes and across climatic years. Our hypothesis is that adding locally-produced biochar to coarse textured soils will enhance soil water retention and achieve greater crop productivity regardless of cropping system or irrigation schemes but will vary significantly across wet and dry climatic years.

## **3.2 Materials and Method**

### **3.2.1 Modeling Strategy**

Numerical models can be beneficial tools to elucidating impacts of biochar addition in agricultural field environments, especially when considering year-to-year climate variability and associated changes in soil water status. Herein, 1-D variably-saturated flow modeling was applied to improve our understanding of the application of biochar on coarse-textured soils representative of California's Central Valley. While using the same soil representation, we implemented several numerical scenarios to quantify the range of soil water retention and crop yield possible under different irrigation strategies and cropping systems. In particular, we used two different cropping systems that are common in California's agriculture: a natural rainfed grassland (perennial system) and an irrigated fresh-market tomato soil profile. Further, a control (soil profile without biochar) and three types of biochar amendments were used to quantify how inherent biochar properties may act to increase or decrease soil water retention and consequently crop yield in these vadose zone environments (Figure 3.2). As illustrated in Figure 3.1, Atwater loamy-sand was used to represent the top 0-50 cm and sandy loam soil was used to represent the bottom 51-100 cm across all soil columns (NRCS, Soil Web Survey). Apart from the control, biochar amendments were incorporated within the top 20 cm of the soil profile and were applied one time at the start of the simulation (January 1, 2016). More details on soil and biochar characteristics are described below. Overall, 8 model simulations (2 cropping systems x 4 soil columns) were run for a period of 20 years, with the first 15 years as spin up time and the last 5 years capturing drastically different climate years and consequences of wet-dry transitions on soil retention status under biochar application.

### 3.2.2 Model Setup

Hydrus-1D (Šimůnek et al., 2001, 2003) was used for all simulations. The model domain was set up as a one dimension 100 cm soil column divided into 100 layers or 1 cm uniform spatial discretization. As suggested above, three soil layers were defined as biochar application zone, Atwater loamy sand and sandy loam soil. Apart from the control, the first layer was set at 0-20 cm depth and classified as the zone of biochar application.

The model was run for a period of 20 years with maximum temporal discretization set at 0.125 day. The upper and lower boundary conditions were set as atmospheric conditions with surface runoff and free drainage, respectively.

In Hydrus-1D, variably-saturated flow along the soil profile is described using Richards' equation as follows:

$$\frac{\partial \theta}{\partial t} = \frac{\partial}{\partial z} \left[ K(h) \left( \frac{\partial h}{\partial z} + 1 \right) \right] \quad (3.1)$$

The hydraulic conductivity function  $K(h)$ , which is required to solve the Richards equation, is described using a set of closed-form equations (Mualem, 1976; van Genuchten, 1980):

$$K(h) = K_{sat} \left( \frac{\theta(h) - \theta_r}{\theta_s - \theta_r} \right) \left\{ 1 - \left[ 1 - \left( \frac{\theta(h) - \theta_r}{\theta_s - \theta_r} \right)^{\frac{1}{m}} \right]^m \right\}^2 \quad (3.2)$$

$$\theta(h) = \theta_r + \frac{\theta_s - \theta_r}{[1 + |\alpha h|^n]^m} \quad (3.3)$$

$$m = 1 - \frac{1}{n} \quad (3.4)$$

where  $\theta(h)$  is the measured volumetric water content [ $L^3L^{-3}$ ] at the suction  $h$  [ $L$ ] that is taken positive for increasing suctions. The parameters  $\theta_r$  and  $\theta_s$  are the residual and saturated water contents [ $L^3L^{-3}$ ], respectively,  $K_{sat}$  is the saturated hydraulic conductivity [ $LT^{-1}$ ],  $\alpha$  [ $L^{-1}$ ],  $n$  [-],  $m$  [-], and  $l$  [-] are empirical parameters determining the shape of the hydraulic conductivity functions. In particular,  $\alpha$  [ $L^{-1}$ ] is related to the inverse of the air entry suction,  $n$  [-] is a measure of the pore-size distribution, and  $l$  [-] reflects pore discontinuity and tortuosity of the flow path. Soil hydraulic parameters used for all model simulations are described in the next section.

Plant root distribution and water uptake were modeled in HYDRUS using the associated Feddes parameters for each respective crop, assuming no solute stress. Other relevant model parameterization including biochar characteristics and meteorological forcing in support of numerical analyses are described in detail below.

### 3.2.3 Biochar & Soil Water Retention Curves (SWRC)

Three biochar treatments applied in this study were derived from local waste materials corresponding to almond shell (AS-2), walnut shell (WS-2), and almond pruning (ATC-1) residues that underwent slow pyrolysis at 300-350 °C using a mobile pyrolysis unit (see Supplemental Figure S3.1). These biochar were selected from a patch of seven tested biochar produced by the mobile unit as a means to lessen the surplus of orchard waste in the Central Valley and potential enhancement to soil ecosystem services (Thao et al., in

preparation). To emphasize, California alone supplies roughly 80% of world almonds (100% of United States) (USDA-FSA, 2015) with an estimated 505,857 harvested hectares in 2020 (USDA-NASS, 2020). Yet to produce 1 kilogram (kg) of nut conveyed 0.6 kg of almond shell and 2.5 kg of husk by-products, generating 2.7 million dry metric tons of almond wastes annually (Aktas et al., 2015). In addition, by using locally derived biochar from mobile pyrolysis units, we aim to minimize the materials transportation cost, thus lowering farm capital expense.

Soils (topsoil from 0-15 cm) used in this study were collected from a grassland near the UC Merced Castle Facility (Lat: 37.3732° Long: -120.5775°) and classified as Atwater loamy-sand series. This well drained Alfisol soil originated from sandy alluvium created by erosion of granite from the Sierra Nevada (Arkley, 1962). The method used to develop moisture retention curve for soil organic treatments followed the vapor sorption analysis for porous media described in Tuller and Or (2005). Soil water retention curves (SWRC) from the mid to dry region were determined for the control and all biochar amended soils (5% wt/wt) using WP4C dew-point potentiometer (Thao et al., in preparation). More importantly, soil hydraulic parameters ( $\alpha$ ,  $n$ ,  $\theta_r$ ) were estimated using SWRC by minimizing the sum of squared errors between the model and measured volumetric water content data. Moisture retention from the wet region was extrapolated for each treatment using the above soil hydraulic parameters and average-weighted porosity (Figure 3.2).

Additionally, measured physical and chemical properties of the Atwater loamy-sand and retrieved NRCS soil properties for the sandy loam layers are provided in Tables 3.1 and 3.2. As noted in Table 3.1, bulk density ( $\rho_b$ ), and soil organic matter (SOM) decrease with depth. In contrast, cation exchange capacity (CEC) and plant available water (PAW) are greater in the lower soil layer, compared to the upper layer. Soil erodibility or K factor also increase with depth. These trends can be attributed to soil particle size distribution (sand, silt, and clay percentage) and plant residue differences in the top and bottom soil layer.

All model simulations were carried out using hydraulic properties fitted directly to measured SWRC data as described above, except for porosity and Ksat (Table 3.3). For the 5% biochar amended soils, an average-weighted porosity was calculated using the top soil layer porosity (0.44) and porosity assessments of 0.8, 0.53, and 0.55 for individual biochar comprised of AS-2, WS-2, and ATC-1, respectively (Brewer et al., 2014). In contrast, Ksat for individual soil layers was estimated using the pedotransfer function (Rosetta Lite and the class pedotransfer of Carsel and Parrish) on the basis of soil particle size distribution and bulk density (Schaap et al., 2001). Bulk density for 5% amended soils were weight-averaged similar to porosity calculations.

### 3.2.4 Cropping Systems

As suggested above, two different cropping systems that are common to California agriculture were assessed through numerical modeling. The first is a natural rainfed grassland (perennial system) that has an effective rooting depth of 50-cm (USDA-NRCS, 1997). Grassland or commonly referred to as pasture is essential for rangeland vegetation and livestock agriculture (Forero et al., 2003). The second system is an irrigated fresh-market tomato field (annual system) with an effective rooting depth of 60-cm (USDA-NRCS, 1997). This crop holds a major role in the California vegetable industry, with the majority of acreage harvested in the Central Valley (Le Strange et al., 2000).

In order to capture plant water root uptake and control irrigation trigger, four observation nodes were positioned at regularly-spaced depth intervals of 20, 40, 60 and 80 cm within the modeled domain. Through this approach, the top two sensors lie within the effective root zone and the rest, below (Figure 3.1). For the irrigated tomato, the irrigation threshold was set to trigger at -150 cm pressure head at the topmost observation node. This is considered to be a typical threshold for coarse textured soils (Lopez, 2014).

### **3.2.5 Meteorological Forcing**

Daily evapotranspiration (ET) and precipitation data to drive model simulations were retrieved from the Merced CIMIS station (#148). Of this, the first 15 years (2000-2015) were used in the spin-off simulation to achieve steady state soil moisture profiles. Following this, the model was run for another five years (2016-2020), which forms the basis of this study.

Mean potential  $ET_0$  and precipitation for the 15 years spin-off and five years simulation are shown in Table 3.4. As shown, annual  $ET_0$  were similar in both the spin-off and simulated period, averaging at about ~1390 mm. Annual precipitation on the other hand varied among simulated years, with 2016, 2017, and 2019 receiving 100 mm (~4 inches) more rain than the 15-years average, 2018 being a normal year, and 2020 being a dry year (100 mm less). Such precipitation variability provides a natural scenario to test the impact of biochar application across years.

### **3.2.6 Crop Yield and WUE**

To determine if changes in water retention properties in biochar-amended soils act to increase or decrease crop productivity, the cumulative plant root water uptake function was taken as a proxy for plant performance or crop yield at the 5<sup>th</sup> year. Other studies have used this function to estimate crop yield as well (e.g., Ben-Gal & Shani, 2003). The mean yield report for rainfed pasture (Forero et al., 2003) and fresh market tomato (Le Stranger et al., 2000) was used as the reference yield for the Control. Subsequently, the difference in cumulative root water uptake among treatments were converted accordingly, e.g. 5% increase in root water uptake equates to 5% increase in yield. Additionally, WUE was calculated by dividing the final yield against the sum of water applied, expressed as ton per hectare per meter of water applied.

## **3.3 Results**

### **3.3.1 Impact of Biochar Application to Rainfed Pasture**

Hydrus-1D simulation for the rainfed pasture shows that biochar treatment significantly changed moisture profiles especially within the top 20 cm, as compared to the control (Figures 3.3a & 3.3b) (also see Supplemental Figure S3.2). The difference ranged from 1 to 9% higher moisture content for AS-2 compared to Control (see Table S3.1). Figure 3.4a and b further demonstrate that the model predicted substantially higher soil moisture content for both top (20-cm & 40-cm) and bottom observation nodes (60-cm & 80-cm) for all biochar-amended soils (Figure 3.4b) than the control (Figure 3.4a) (also see Supplemental Figures S3.3 & S3.4). These differences were greatest during the first two and a half years but diminished in the following years. Across years, soil moisture differences between biochar and control were least during the peak of the rainy season when maximum soil moisture was observed and greatest during the summer season. In this regard, noted differences began to decline in 2018 (1000 day mark on Figure 3.4).

This could be because of the drastically lower precipitation amount (~100 mm) in 2018 that followed the previous wet years (2016 & 2017).

In order to explicitly track how year-to-year variability in precipitation impacts other hydrologic components, Figure 3.5 demonstrates the differences in cumulative soil evaporation and water fluxes for biochar-amended and control soil profiles under the rainfed system. As illustrated in Figure 3.5, cumulative soil evaporation was highest for the control and lowest for AS-2 and WS-2 derived biochar (Figure 3.5a). This difference between biochar-amended soil and control equates to roughly 17 cm (or 170 mm) of water lost due to soil evaporation. This loss to evaporation can be further confirmed by tracking the surface and bottom fluxes for all soil profiles, thereby accounting for any water lost from the bottom of the domain. Figure 3.5b demonstrates greatest surface and lowest bottom fluxes for the control implying that rainwater was mostly lost to evaporation, with a small amount of water percolating below the effective rootzone for this soil profile, as compared to biochar-amended soils (Figure 3.5b). Interestingly, both AS-2 and WS-2 show highest predicted surface and bottom fluxes, thereby indicating significant water retention in these biochar-amended soils with decreased evaporation rates. Comparatively, ATC-1 demonstrated an intermediate evaporation rate and modest water retention within the soil profile. Taken together, these findings suggest that biochar amendments in coarse-textured soils increase water retention by reducing soil evaporation loss, while allowing for more drainage for a rainfed pasture system. Similar findings have been observed in other studies (Abel et al., 2013; Altdorff et al., 2019; Arthur et al., 2015; Günal et al., 2018; Kroeger et al., 2021; Mollinedo et al., 2015; Stylianou et al., 2021), supporting the belief that even 5% biochar augmentation can increase water retention within coarse textured soils.

### 3.3.2 Pasture Yield and WUE

Since the pasture was a rainfed system, all treatments received the same amount of applied water by precipitation (~ 0.05 acre-inch or 1731 mm). Table 3.5 shows the pasture yield and WUE at the end of the 5-year simulation period for control and biochar-amended soils. Assuming that yield for the control is 12.9 ton/hectare (average yield for rainfed pasture in CA) (Forero et al., 2003), Table 3.5 shows that control has the lowest yield (12.9 ton/ha) and lowest WUE (7.452 ton/ha/m) at the end of the fifth year, followed by ATC-1 (13.64 ton/ha & 7.879 ton/ha/m). Comparatively, WS-2 (14.09 ton/ha & 8.139 ton/ha/m) and AS-2 (14.03 ton/ha & 8.105 ton/ha/m) have the highest yield and WUE. These results are not surprising since significant water retention was obtained from WS-2 and AS-2 that specifically diminished soil evaporation loss, which would leave more water for plant root uptake. This water retention led to an 5.75%, 8.75%, and 9.25% increase in pasture yield for ATC-1, AS-2, and WS-2, respectively (Table 3.5).

### 3.3.3 Impact of Biochar Application to Irrigated Fresh-market Tomato

For the irrigated fresh-market tomato, predicted soil water content for control and biochar amended soils are shown in Figure 3.6. For the irrigated system, moisture content in the top soil layer (Figure 3.6a) was predicted to be constantly higher than the bottom soil layer (Figure 3.6b) across control and biochar amendment types (see Supplemental Figures S3.5 & S3.6). Additionally, observation nodes at different soil depths showed similar moisture fluctuations; an expected outcome since the irrigation threshold is identical for all soil profiles. However, in contrast to the model prediction for the rainfed system, we detected much higher soil moisture content within the top 20-cm soil depth for the control (Figure 3.7a) than the biochar amended soils (Figures 3.7b) (also see

Supplemental Figure S3.7). The difference ranged from 1 to 32% higher moisture content for the Control as compared to AS-2 (see Table S3.2). One explanation for this behavior is that more irrigation was triggered for the control as compared to biochar amended soils. This can be further confirmed by comparing evaporation losses across soil profiles. Figure 3.8a demonstrates higher cumulative evaporation for the control (543 cm) and ATC-1 biochar (545 cm) as compared to WS-2 (511 cm) and AS-2 (500 cm), similar to the rainfed system (Figure 3.8a). In fact, the maximum difference in cumulative soil evaporation rates was obtained between control and AS-2 amended soils and equates to approximately 430 mm of water lost. This higher evaporation rate observed in the control causes the -150 cm pressure head threshold to be reached more frequently, which triggers more irrigation. Additionally, both cumulative bottom and surface fluxes were predicted to be highest for the control, followed by ATC-1 (Figure 3.8b). This implies that not only evaporation losses were greatest, but more water percolated down below the effective rootzone for the control than biochar amended soils. Quantifying these differences, control yielded 17.5%, 14.0%, and 7.4% more drainage than AS-2, WS-2, and ATC-1, respectively.

### 3.3.4 Tomato Yield and WUE

Similar to the rainfed system, we analyzed differences in crop yield and WUE due to application of biochar for irrigated tomatoes (Table 3.6). Here, total water applied was greatest for the control at 15670 mm (~37.4 acre-inch), followed by ATC-1 at 15080 mm (~33.4 acre-inch), WS-2 was 13,780 mm (~25.5 acre-inch), and lowest was AS-2 at 13380 mm (~23.3 acre-inch). As suggested above, more water applied to the control is linked to higher evaporation demand for this soil profile. Interestingly, the highest crop yield was also associated with the control as opposed to the rainfed system. In comparison, there is a significant difference between water applied to yield for the irrigated system (Table 3.6). When comparing control against AS-2, the model applied 14.6% more water in the control, and the yield return was 15.2%. In the case for control versus WS-2, the model applied 12.1% more water with a 13.9% increase in yield return. For control versus ATC-1, the model applied 3.8% more water, but the yield increase was only 2.6%. Therefore, a critical question to ask is if there is any economic tradeoff between yield gained to water saved under biochar application. In other words, does the increase in crop revenue for the control (due to higher yield) offset the cost of pumping more water? Likewise, does the water saved (reduced irrigation) by amending the soil with a 5% biochar offset the yield disparity? This economic tradeoff is discussed in the next section. Note that a discrepancy in WUE among control and biochar amendments was not observed; WUE was 2.916 ton/ha/m, 2.899 ton/ha/m, 2.852 ton/ha/m, and 2.951 ton/ha/m for the control, AS-2, WS-2, and ATC-1, respectively (Table 3.6).

### 3.3.5 Tomato Economic Trade-off

Given the price of fresh market tomatoes in California is \$39.4/CWT (USDA-NASS, 2020), the total revenue for each treatment is \$16070 for control, \$13638 for AS-2, \$13811 for WS-2, and \$15635 for ATC-1. As expected, the control holds the highest economic value since it produced the most yield under an irrigated system. When comparing the differences in revenue, control yielded \$2432, \$2259, and \$435 more returns than AS-2, WS-2, and ATC-1, respectively (Table 3.7). To further assess if the return on yield offsets the cost of pumping more water, we assume a conventional pump with a flowrate of 100 GPM. Given this background, the price of water per acre-foot is \$70 (for Merced County in 2017), and operation cost of \$7.17/hr. (\$0.14/KWH \* 48 KWH/hr. + \$0.45 maintenance), the total cost for running the pump is \$1213 for control,

\$756 for AS-2, \$827 for WS-2, and \$1084 for ATC-1 (see Supplemental). Consequently, the difference in pump cost for the control versus biochar amendments returns a saving of \$539, \$455, and \$153, for AS-2, WS-2, and ATC-1 (Table 3.7). Based on these calculations, our analysis indicates that the yield revenue gained by pumping more water is greater than the revenue gained from water saved with biochar amendment for the irrigated fresh-market tomato system. Under these circumstances, in order to capture the higher yield revenue a tomato grower will choose to apply more water, given water accessibility is not a constraint and the cost of water remains the same.

## 3.4 Discussion

### 3.4.1 Biochar Application under Rainfed versus Irrigated Systems

In this study, we found both similarities and differences in the impact of biochar application to cropping systems that have varying irrigation practices. In the rainfed system, biochar enhanced both pasture yield and WUE by reducing cumulative evaporation and increasing soil moisture retention, which led to greater plant water uptake. In these simulations, these outcomes are directly linked to changes in soil hydraulic properties of biochar amended soils. Interestingly, similar outcomes have been reported in other studies and attributed to soil retention properties, e.g. increase in surface area of biochar amended soils (Horel et al., 2019; Novak et al., 2009; Sarkhot et al., 2013) and hydraulic conductivity (Kameyama et al., 2012; Villagra-Mendoza & Horns, 2018).

Similar to the rainfed system, we also observed a reduced cumulative evaporation for biochar amended soils under an irrigated fresh tomato system. In this irrigated system, crop yield was considerably impacted by biochar application. While WUE for the irrigated system was similar for the control and biochar, the control yielded the highest crop yield. We suspect that the imputed soil hydraulic parameters from the SWRC and Ksat (Table 3.3) influenced plant root water uptake and drainage in the simulation. To test this speculation, we lowered the irrigation threshold for biochar amendment and observed higher yield but also more cumulative bottom flux (data not shown). It's also likely that the higher Ksat attributed to biochar treatment allowed more infiltration in both cropping systems, thus reduced soil evaporation loss. For the rainfed system, these factors positively influence crop productivity and ecosystem services. However these benefits are lessened for the tomato system since irrigation in the model is set to trigger at the same threshold across treatments. This could explain why WUE was similar across treatments for the irrigated tomato system (Table 3.6). In comparing WUE between the two cropping systems, yield per unit of water applied is substantially higher in the rainfed system as compared to the irrigated system across all treatments (Figure 3.9).

### 3.4.2 Comparison across Biochar Types

Of the three biochar that were tested, AS-2 and WS-2 bore superior effects on crop yield and WUE for the rainfed grassland. ATC-1 holds an intermediary effect on crop and soil productivity in the rainfed system, and showed behavior similar to the control for the irrigated system. In comparing across these biochar-amended soils, our numerical analysis highlighted that water retention characteristics were most sensitive to the  $\alpha$  parameter. Because ATC-1 biochar has a larger size in comparison to AS-2 and WS-2 (visual observation), and since  $\alpha$  is inversely correlated to particle size, a lower  $\alpha$  value was assigned to ATC-1. These differences in water retention properties were therefore

translated to differences in evaporation, other hydrologic fluxes and crop yield across control and biochar treatments.

### 3.4.3 Indirect Benefits of Biochar Application

Various biochar economic studies have concluded that the direct benefits of biochar itself may not offset the price of conventional practices (Bach et al., 2016; Galinato et al., 2011; Maroušek et al., 2019), especially if the positive effect is not observed immediately. We observed this in our irrigated tomato simulation where the yield returns by irrigating more frequently outweigh the revenues returned from water saved by adding biochar. Contemporarily, unless the addition of biochar breakeven or generates more revenues (e.g. Keske et al., 2020), farmers may view this approach as a precarious investment. As a response, many authors have suggested the need to include indirect benefits linked to adopting biochar practices. These indirect benefits include global warming potential, soil carbon sequestration, and carbon credits (Bach et al., 2016; Galinato et al., 2011; Roberts et al., 2010; Sahoo et al., 2019; Thengane et al., 2020). Given that a carbon market exists to incentivize carbon sequestration, the greenhouse gas emissions avoided by diverting and converting waste materials into biochar while accounting for the carbon sequestered can make this approach a profitable investment (Galinato et al., 2011; Sahoo et al., 2019; Thengane et al., 2020). For example, one ton of biochar produced can sequester ~2.5 ton of CO<sub>2</sub> (Puettmann et al., 2020; Roberts et al., 2010; Thengane et al., 2020), hence a grower that applied 10 ton/ha of biochar can potentially sequester 25 ton of CO<sub>2</sub> back into the ecosystem. Considering a mean carbon price of \$102 USD/ton CO<sub>2</sub> (Thengane et al., 2020), the grower can attain a carbon credit of \$2550. Based on this setting, applying biochar to our irrigated tomato system may compensate for the revenue difference if we account for the carbon credit. Other indirect benefits include higher nutrient use efficiency (Ghezzehei et al., 2014; Sarkhot et al., 2013), thereby reducing farm fertilization expenses, enhancing microbial health (Ali et al., 2017; Wang et al., 2020), and removing public health concerns, e.g. pesticide application (Delwiche et al., 2014; Jones et al., 2011; Li et al., 2018).

Furthermore, our numerical simulation clearly shows that the application of biochar resulted in positive gains for the non-irrigated pasture as compared to the irrigated tomato system. For agronomic implication, the uses of biochar may be extended to widespread practice such as non-irrigated cover crop to enhance yield and water storage, especially during the winter rain season. Thus, non-irrigated setting may be a lower hanging fruit for biochar application before it can be applied to irrigated agriculture.

### 3.4.4 Model Limitations

In our economic analysis, we assumed that water is not a limiting factor, and that the price of pumping water remains constant throughout the five-year simulation. Realistically this is not the case, especially for the California Central Valley where drought and groundwater overdraft are critical concerns (Medellín-Azuara et al., 2016; Waterhouse et al., 2021). Moreover, rules and regulations such as the Sustainable Groundwater Act make it harder for farmers to pump groundwater in the absence of surface water. In some cases, water may not be accessible for purchase or pumping at all. We also did not consider the costs associated with the production and application of biochar to each system. In the literature, the price of biochar varies greatly and is dependent on multiple factors, such as feedstock, transportation cost, technology, and pyrolysis methods (Robert et al., 2010; Sahoo et al., 2019; Thengane et al., 2020). Nevertheless, our biochar was derived from local agriculture waste materials and

specifically made using a mobile pyrolysis unit. Since transportation cost is a big portion of the overall material cost (Maroušek et al., 2019; Robert et al., 2010), this is expected to significantly reduce the biochar price. Our overall aim was to analyze the impact of biochar that is generated locally from waste residues available on the farm and directly used in the farm itself. In addition, our biochar was created using slow pyrolysis at temperatures around 300-350 °C. Biochar can be produced from various technologies, e.g. gasification, slow pyrolysis, fast pyrolysis, etc., and at a range of temperatures (300-900 °C). Each variation creates biochar with different characteristic and physicochemical properties. Also, biochar was only applied once at the start of the simulation period, hence we did not consider the effects of biochar aging on soil properties. In the literature, biochar aging can either positively (e.g. oxidation of biochar that open up pore space) or negatively (e.g. pore space clogged with clay particles) influence biochar physiochemical properties and retention potential (Wang et al., 2020). Similarly, we were not able to factor in the effects of field operation e.g. tillage, in the model; physical disturbance that can influence soil water accessibility. For the rainfed pasture (a perennial system), this effect may be negligible. However soil physicochemical properties and moisture retention may be greatly impacted for annual crops such as the irrigated tomato, which require field operation. Lastly, our datasets used in HYDRUS and the model itself have constraints and assumptions. The model setup is chosen to best represent our cropping systems, available datasets, and to answer our research questions. HYDRUS limitations are not discussed here, and readers are encouraged to see Šimůnek et al. (2016) for more information.

### 3.5 Conclusion

In this study, we used HYDRUS-1D model to evaluate the mid-term effects of three different types of locally-produced biochar on soil water and plant interactions for a coarse textured soil. Our results demonstrated that biochar amendments increased moisture retention and reduced cumulative evaporation under a rainfed system. These changes in water components allowed for more plant water uptake to occur, over a longer time period, thereby increasing crop yield. For an irrigated fresh-market tomato, biochar amendments reduced soil evaporative loss and reduced irrigation application but resulted in a lower crop yield. Across cropping systems, positive WUE was observed in the rainfed system but not in the irrigated system with biochar application. WUE was substantially greater for the non-irrigated grassland, supporting the assertion that biochar may be more beneficial under natural rainfed cropping systems. Among the different types of biochar, ATC-1 was found to be inferior to AS-2 and WS-2 due to differences in soil hydraulic parameters, especially those related to the particle size (i.e.  $\alpha$ ). Overall, our findings indicate that biochar has the potential to enhance farm water usage by reducing soil water losses and can be a profitable investment, although indirect benefits such as carbon credit and cost reduction from mobile pyrolyzer must be considered.

### 3.6 Reference

- Abel, S., Peters, A., Trinks, S., Schonsky, H., Facklam, M., & Wessolek, G. (2013). Impact of biochar and hydrochar addition on water retention and water repellency of sandy soil. *Geoderma*, 202, 183-191. <https://doi.org/10.1016/j.geoderma.2013.03.003>

- Ajayi, A.E., Holthusen, D., & Horn, R. (2016). Changes in microstructural behaviour and hydraulic functions of biochar amended soils. *Soil and Tillage Research*, 155, 166-175. <https://doi.org/10.1016/j.still.2015.08.007>
- Aktas, T., Thy, P., Williams, R.B., McCaffrey, Z., Khatami, R. and Jenkins, B.M. (2015). Characterization of almond processing residues from the Central Valley of California for thermal conversion. *Fuel Processing Technology*, 140, pp.132-147. <https://doi.org/10.1016/j.fuproc.2015.08.030>
- Ali, S., Rizwan, M., Qayyum, M.F., Ok, Y.S., Ibrahim, M., Riaz, M., Arif, M.S., Hafeez, F., Al-Wabel, M.I., & Shahzad, A.N. (2017). Biochar soil amendment on alleviation of drought and salt stress in plants: a critical review. *Environmental Science and Pollution Research*, 24(14), 12700-12712. DOI 10.1007/s11356-017-8904-x
- Aller, D., Rathke, S., Laird, D., Cruse, R., & Hatfield, J. (2017). Impacts of fresh and aged biochars on plant available water and water use efficiency. *Geoderma*, 307, 114-121. <https://doi.org/10.1016/j.geoderma.2017.08.007>
- Aller, D.M., Archontoulis, S.V., Zhang, W., Sawadgo, W., Laird, D.A., & Moore, K. (2018). Long term biochar effects on corn yield, soil quality and profitability in the US Midwest. *Field Crops Research*, 227, 30-40. <https://doi.org/10.1016/j.fcr.2018.07.012>
- Altdorff, D., Galagedara, L., Abedin, J., & Unc, A. (2019). Effect of biochar application rates on the hydraulic properties of an agricultural-use boreal podzol. *Soil Systems*, 3(3), 53. <https://doi.org/10.3390/soilsystems3030053>
- Arabyarmohammadi, H., Darban, A.K., van der Zee, S.E., Abdollahy, M., & Ayati, B. (2018). Fractionation and leaching of heavy metals in soils amended with a new biochar nanocomposite. *Environmental Science and Pollution Research*, 25(7), 6826-6837. <https://doi.org/10.1007/s11356-017-0976-0>
- Archontoulis, S.V., Huber, I., Miguez, F.E., Thorburn, P.J., Rogovska, N., & Laird, D.A. (2016). A model for mechanistic and system assessments of biochar effects on soils and crops and trade-offs. *Global Change Biology: Bioenergy*, 8(6), 1028-1045. <https://doi.org/10.1111/gcbb.12314>
- Arkley, R.J. (1962). *Soil Survey, Merced Area, California* (No. 7). The Service.
- Arora, B., Mohanty, B.P., & McGuire, J.T. (2011). Inverse estimation of parameters for multidomain flow models in soil columns with different macropore densities. *Water Resources Research*, 47(4). <https://doi.org/10.1029/2010WR009451>
- Arthur, E., Tuller, M., Moldrup, P., & de Jonge, L.W. (2015). Effects of biochar and manure amendments on water vapor sorption in a sandy loam soil. *Geoderma*, 243, 175-182. <https://doi.org/10.1016/j.geoderma.2015.01.001>
- Bach, M., Wilske, B., & Breuer, L. (2016). Current economic obstacles to biochar use in agriculture and climate change mitigation. *Carbon Management*, 7(3-4), 183-190. <https://doi.org/10.1080/17583004.2016.1213608>

- Ben-Gal, A. & Shani, U. (2003). Water use and yield of tomatoes under limited water and excess boron. *Plant and Soil*, 256(1), 179-186.  
<https://doi.org/10.1023/A:1026229612263>
- Brewer, C.E., Chuang, V.J., Masiello, C.A., Gonnermann, H., Gao, X., Dugan, B., Driver, L.E., Panzacchi, P., Zygourakis, K., & Davies, C.A. (2014). New approaches to measuring biochar density and porosity. *Biomass and Bioenergy*, 66, 176-185.  
<https://doi.org/10.1016/j.biombioe.2014.03.059>
- Delwiche, K.B., Lehmann, J., & Walter, M.T. (2014). Atrazine leaching from biochar-amended soils. *Chemosphere*, 95, 346-352.  
<https://doi.org/10.1016/j.chemosphere.2013.09.043>
- Filipović, V., Černe, M., Šimůnek, J., Filipović, L., Romić, M., Ondrašek, G., Bogunović, I., Mustać, I., Krevh, V., Ferencević, A., & Robinson, D. (2020). Modeling water flow and phosphorus sorption in a soil amended with sewage sludge and olive pomace as compost or biochar. *Agronomy*, 10(8), 1163.  
<https://doi.org/10.3390/agronomy10081163>
- Forero, L., Reed, B., Klonsky, K., & DeMoura, R., (2003). Sample Costs To Establish And Produce Pasture Sacramento Valley-Flood Irrigation. University Of California, Cooperative Extension, Pa-Sv-03.
- Galinato, S.P., Yoder, J.K., & Granatstein, D. (2011). The economic value of biochar in crop production and carbon sequestration. *Energy Policy*, 39(10), 6344-6350.  
<https://doi.org/10.1016/j.enpol.2011.07.035>
- Ghezzehei, T.A., Sarkhot, D.V., & Berhe, A.A. (2014). Biochar can be used to capture essential nutrients from dairy wastewater and improve soil physico-chemical properties. *Solid Earth*, 5(2): 953-962. <https://doi.org/10.5194/se-5-953-2014>
- Günel, E., Erdem, H., & Çelik, İ. (2018). Effects of three different biochars amendment on water retention of silty loam and loamy soils. *Agricultural Water Management*, 208, 232-244. <https://doi.org/10.1016/j.agwat.2018.06.004>
- Horel, Á., Tóth, E., Gelybó, G., Dencső, M., & Farkas, C. (2019). Biochar Amendment Affects Soil Water and CO<sub>2</sub> Regime during Capsicum Annuum Plant Growth. *Agronomy*, 9(2), 58. <https://doi.org/10.3390/agronomy9020058>
- Huang, S., Huang, D., Garg, A., Jiang, M., Mei, G., & Pekkat, S. (2020). Stormwater management of biochar-amended green roofs: peak flow and hydraulic parameters using combined experimental and numerical investigation. *Biomass Conversion and Biorefinery*, 1-12. <https://doi.org/10.1007/s13399-020-01109-x>
- Jeffery, S., Meinders, M.B., Stoof, C.R., Bezemer, T.M., van de Voorde, T.F., Mommer, L., & van Groenigen, J.W. (2015). Biochar application does not improve the soil hydrological function of a sandy soil. *Geoderma*, 251, 47-54.  
<https://doi.org/10.1016/j.geoderma.2015.03.022>
- Jellali, S., Diamantopoulos, E., Haddad, K., Anane, M., Durner, W., & Mlayah, A. (2016). Lead removal from aqueous solutions by raw sawdust and magnesium

pretreated biochar: experimental investigations and numerical modelling. *Journal of Environmental Management*, 180, 439-449.  
<https://doi.org/10.1016/j.jenvman.2016.05.055>

Jones, D.L., Edwards-Jones, G., & Murphy, D.V. (2011). Biochar mediated alterations in herbicide breakdown and leaching in soil. *Soil Biology and Biochemistry*, 43(4), 804-813. <https://doi.org/10.1016/j.soilbio.2010.12.015>

Kameyama, K., Miyamoto, T., Shiono, T., & Shinogi, Y. (2012). Influence of sugarcane bagasse-derived biochar application on nitrate leaching in calcareous dark red soil. *Journal of Environmental Quality*, 41(4), 1131-1137. doi:10.2134/jeq2010.0453

Karandish, F. & Šimůnek, J. (2018). An application of the water footprint assessment to optimize production of crops irrigated with saline water: A scenario assessment with HYDRUS. *Agricultural Water Management*, 208, 67-82.  
<https://doi.org/10.1016/j.agwat.2018.06.010>

Keske, C., Godfrey, T., Hoag, D.L., & Abedin, J. (2020). Economic feasibility of biochar and agriculture coproduction from Canadian black spruce forest. *Food and Energy Security*, 9(1), e188. <https://doi.org/10.1002/fes3.188>

Kroeger, J.E., Pourhashem, G., Medlock, K.B., & Masiello, C.A. (2021). Water cost savings from soil biochar amendment: A spatial analysis. *Global Change Biology Bioenergy*, 13(1), 133-142. <https://doi.org/10.1111/gcbb.12765>

Lefebvre, D., Williams, A., Meersmans, J., Kirk, G.J., Sohi, S., Goglio, P., & Smith, P. (2020). Modelling the potential for soil carbon sequestration using biochar from sugarcane residues in Brazil. *Scientific Reports*, 10(1), 1-11.  
<https://doi.org/10.1038/s41598-020-76470-y>

Lehmann, J., Gaunt, J., & Rondon, M. (2006). Bio-char sequestration in terrestrial ecosystems - A review. *Mitigation and Adaptation Strategies for Global Change*, 11(2): 403-427.

Le Strange, M., Schrader, W., & Hartz, T. (2000). Fresh-market tomato production in California. UCANR Publications.

Li, X., Luo, J., Deng, H., Huang, P., Ge, C., Yu, H., & Xu, W. (2018). Effect of cassava waste biochar on sorption and release behavior of atrazine in soil. *Science of The Total Environment*, 644, 1617-1624. <https://doi.org/10.1016/j.scitotenv.2018.07.239>

Lopez, V.D. (2014). Biochar as a soil amendment: Impact on hydraulic and physical properties of an arable loamy sand soil. University of California, Merced.

Lychuk, T.E., Izaurralde, R.C., Hill, R.L., McGill, W.B., & Williams, J.R. (2015). Biochar as a global change adaptation: predicting biochar impacts on crop productivity and soil quality for a tropical soil with the Environmental Policy Integrated Climate (EPIC) model. *Mitigation and Adaptation Strategies for Global Change*, 20(8), 1437-1458. <https://doi.org/10.1007/s11027-014-9554-7>

- Major, J., Rondon, M., Molina, D., Riha, S.J., & Lehmann, J. (2012). Nutrient leaching in a Colombian savanna Oxisol amended with biochar. *Journal of Environmental Quality*, 41(4), 1076-1086. doi:10.2134/jeq2011.0128
- Maroušek, J., Strunecký, O., & Stehel, V. (2019). Biochar farming: Defining economically perspective applications. *Clean Technologies and Environmental Policy*, 21(7), 1389-1395. <https://doi.org/10.1007/s10098-019-01728-7>
- Medellín-Azuara, J., MacEwan, D., Howitt, R.E., Sumner, D.A., Lund, J.R., Scheer, J., Gailey, R., Hart, Q., Alexander, N.D., Arnold, B., & Kwon, A. (2016). Economic analysis of the 2016 California drought on agriculture. Center for Watershed Sciences. Davis, CA: UC Davis.
- Mo'allim, A., Kamal, M., Muhammed, H., Mohd Soom, M., Mohamed Zawawi, M., Wayayok, A., & Che Man, H. (2018). Assessment of Nutrient Leaching in Flooded Paddy Rice Field Experiment Using Hydrus-1D. *Water*, 10(6), 785. <https://doi.org/10.3390/w10060785>
- Mollinedo, J., Schumacher, T.E., & Chintala, R. (2015). Influence of feedstocks and pyrolysis on biochar's capacity to modify soil water retention characteristics. *Journal of Analytical and Applied Pyrolysis*, 114, 100-108. <https://doi.org/10.1016/j.jaap.2015.05.006>
- Mualem, Y. (1976). A new model for predicting the hydraulic conductivity of unsaturated porous media. *Water Resources Research*, 12(3), 513-522. <https://doi.org/10.1029/WR012i003p00513>
- Novak, J.M., Lima, I., Xing, B., Gaskin, J.W., Steiner, C., Das, K.C., Ahmedna, M., Rehrah, D., Watts, D.W., Busscher, W.J., & Schomberg, H. (2009). Characterization of designer biochar produced at different temperatures and their effects on a loamy sand. *Annals of Environmental Science*, 3(1), 195-206.
- Pressler, Y., Foster, E.J., Moore, J.C., & Cotrufo, M.F. (2017). Coupled biochar amendment and limited irrigation strategies do not affect a degraded soil food web in a maize agroecosystem, compared to the native grassland. *Global Change Biology Bioenergy*, 9(8), 1344-1355. <https://doi.org/10.1111/gcbb.12429>
- Puettmann, M., Sahoo, K., Wilson, K., & Oneil, E. (2020). Life cycle assessment of biochar produced from forest residues using portable systems. *Journal of Cleaner Production*, 250, 119564. <https://doi.org/10.1016/j.jclepro.2019.119564>
- Roberts, K.G., Gloy, B.A., Joseph, S., Scott, N.R., & Lehmann, J. (2010). Life cycle assessment of biochar systems: estimating the energetic, economic, and climate change potential. *Environmental Science & Technology*, 44(2), 827-833. <https://doi.org/10.1021/es902266r>
- Sahoo, K., Bilek, E., Bergman, R., & Mani, S. (2019). Techno-economic analysis of producing solid biofuels and biochar from forest residues using portable systems. *Applied Energy*, 235, 578-590. <https://doi.org/10.1016/j.apenergy.2018.10.076>

- Sarkhot, D.V., Ghezzehei, T.A., & Berhe, A.A. (2013). Biochar for nutrient recapture from dairy wastewater: recovery of major nutrients. *Journal of Environment Quality*, 42(5): 1545-1554
- Schaap, M.G., Leij, F.J. and Van Genuchten, M.T., 2001. Rosetta: A computer program for estimating soil hydraulic parameters with hierarchical pedotransfer functions. *Journal of Hydrology*, 251(3-4), 163-176. [https://doi.org/10.1016/S0022-1694\(01\)00466-8](https://doi.org/10.1016/S0022-1694(01)00466-8)
- Šimůnek, J., Jarvis, N.J., Van Genuchten, M.T., & Gärdenäs, A. (2003). Review and comparison of models for describing non-equilibrium and preferential flow and transport in the vadose zone. *Journal of Hydrology*, 272(1-4), 14-35. [https://doi.org/10.1016/S0022-1694\(02\)00252-4](https://doi.org/10.1016/S0022-1694(02)00252-4)
- Šimůnek, J., Van Genuchten, M.T., & Šejna, M. (2016). Recent developments and applications of the HYDRUS computer software packages. *Vadose Zone Journal*, 15(7). <https://doi.org/10.2136/vzj2016.04.0033>
- Šimůnek, J., Wendroth, O., Wypler, N., & Van Genuchten, M.T. (2001). Non-equilibrium water flow characterized by means of upward infiltration experiments. *European Journal of Soil Science*, 52(1), 13-24. <https://doi.org/10.1046/j.1365-2389.2001.00361.x>
- Stylianou, M., Panagiotou, C.F., Andreou, E., Frixou, F., Christou, A., & Papanastasiou, P. (2021). Assessing the influence of biochars on the hydraulic properties of a loamy sand soil. *Biomass Conversion and Biorefinery*, 11(2), 315-323. <https://doi.org/10.1007/s13399-020-01114-0>
- Thengane, S.K., Kung, K., York, R., Sokhansanj, S., Lim, C.J., & Sanchez, D.L. (2020). Technoeconomic and emissions evaluation of mobile in-woods biochar production. *Energy Conversion and Management*, 223, 113305. <https://doi.org/10.1016/j.enconman.2020.113305>
- Tuller, M. and Or, D. (2005). Water films and scaling of soil characteristic curves at low water contents. *Water Resources Research*, 41(9). <https://doi.org/10.1029/2005WR004142>
- Turkeltaub, T., Jia, X., Zhu, Y., Shao, M.A., & Binley, A. (2018). Recharge and Nitrate Transport Through the Deep Vadose Zone of the Loess Plateau: A Regional-Scale Model Investigation. *Water Resources Research*, 54(7), 4332-4346. <https://doi.org/10.1029/2017WR022190>
- USDA– Foreign Agricultural Service (USDA-FAS), 2015. *Tree Nuts: World Markets and Trade*. Published October 2015.
- USDA-National Agricultural Statistics Service. (2020). *State agriculture overview for California*. [https://www.nass.usda.gov/Quick\\_Stats/Ag\\_Overview/stateOverview.php?state=CALIFORNIA](https://www.nass.usda.gov/Quick_Stats/Ag_Overview/stateOverview.php?state=CALIFORNIA) (accessed February 20, 2021).

- USDA-Natural Resources Conservation Service. (1997). NRCS Irrigation Guide. Natural Resources Conservation Service, Washington, DC. 702 pages.  
[https://www.nrcs.usda.gov/Internet/FSE\\_DOCUMENTS/nrcs144p2\\_033068.pdf](https://www.nrcs.usda.gov/Internet/FSE_DOCUMENTS/nrcs144p2_033068.pdf)
- USDA-Natural Resources Conservation Service. (2021). United States Department of Agriculture - Natural Resources Conservation Service. Web Soil Survey.  
<https://websoilsurvey.sc.egov.usda.gov/> (accessed February 20, 2021).
- Van Genuchten, M.T. (1980). A closed-form equation for predicting the hydraulic conductivity of unsaturated soils. *Soil Science Society of America Journal*, 44(5), 892-898. <https://doi.org/10.2136/sssaj1980.03615995004400050002x>
- Villagra-Mendoza, K. & Horn, R. (2018). Effect of biochar on the unsaturated hydraulic conductivity of two amended soils. *International Agrophysics*, 32(3), 373-378.  
<https://doi.org/10.1515/intag-2017-0025>
- Wang, D., Felice, M.L., & Scow, K.M. (2020). Impacts and interactions of biochar and biosolids on agricultural soil microbial communities during dry and wet-dry cycles. *Applied Soil Ecology*, 152, 103570. <https://doi.org/10.1016/j.apsoil.2020.103570>
- Wang, L., O'Connor, D., Rinklebe, J., Ok, Y.S., Tsang, D.C., Shen, Z. and Hou, D. (2020). Biochar aging: mechanisms, physicochemical changes, assessment, and implications for field applications. *Environmental Science & Technology*, 54(23), pp.14797-14814. <https://doi.org/10.1021/acs.est.0c04033>
- Waterhouse, H., Arora, B., Spycher, N.F., Nico, P.S., Ulrich, C., Dahlke, H.E., & Horwath, W.R. (2021). Influence of agricultural managed aquifer recharge (AgMAR) and stratigraphic heterogeneities on nitrate reduction in the deep subsurface. *Water Resources Research*, 57(5), e2020WR029148.  
<https://doi.org/10.1029/2020WR029148>
- Wiersma, W., van der Ploeg, M.J., Sauren, I.J., & Stoof, C.R. (2020). No effect of pyrolysis temperature and feedstock type on hydraulic properties of biochar and amended sandy soil. *Geoderma*, 364, 114209.  
<https://doi.org/10.1016/j.geoderma.2020.114209>
- Wu, Y., Yang, A., Zhao, Y., & Liu, Z. (2019). Simulation of soil water movement under biochar application based on the hydrus-1d in the black soil region of china. *Applied Ecology and Environmental Research*, 17(2), 4183-4192.  
[http://dx.doi.org/10.15666/aer/1702\\_41834192](http://dx.doi.org/10.15666/aer/1702_41834192)
- Zhou, H., Yu, X., Chen, C., Zeng, L., Lu, S., & Wu, L. (2018). Evaluating hydraulic properties of biochar-amended soil aggregates by high-performance pore-scale simulations. *Soil Science Society of America Journal*, 82(1), 1-9.  
doi:10.2136/sssaj2017.02.0053



Figure 3-1 Conceptual diagram of HYDRUS 1-D simulation domain demonstrating control and biochar amendment scenarios for two cropping systems.

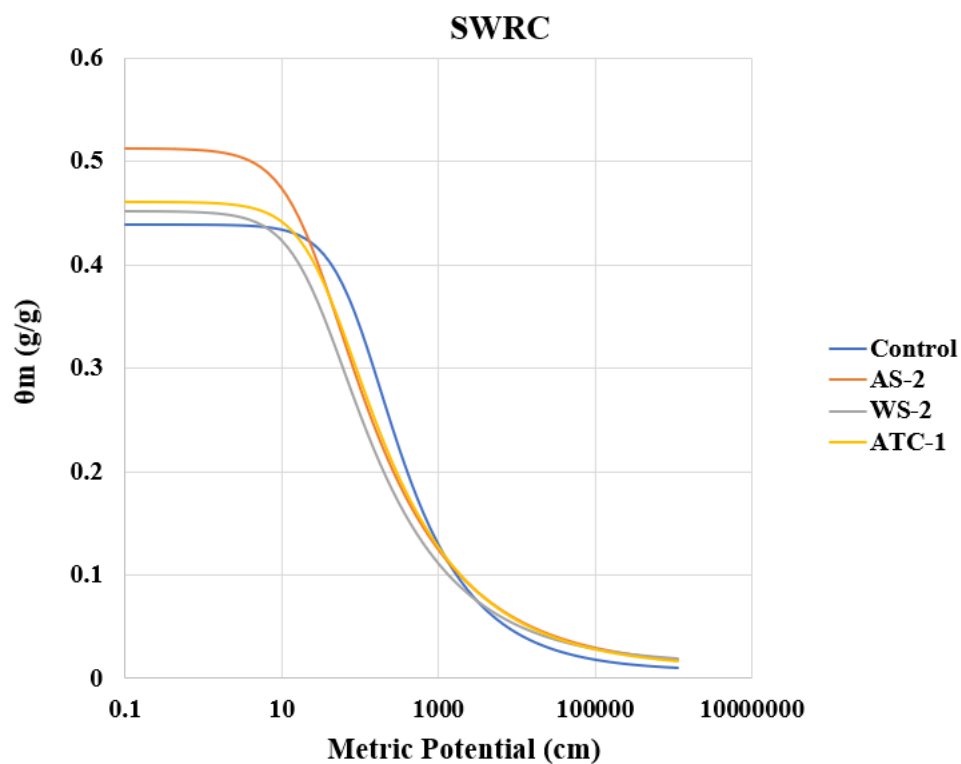


Figure 3-2 Soil Water Retention Curves for control and individual biochars, AS-2, WS-2, and ATC-1.

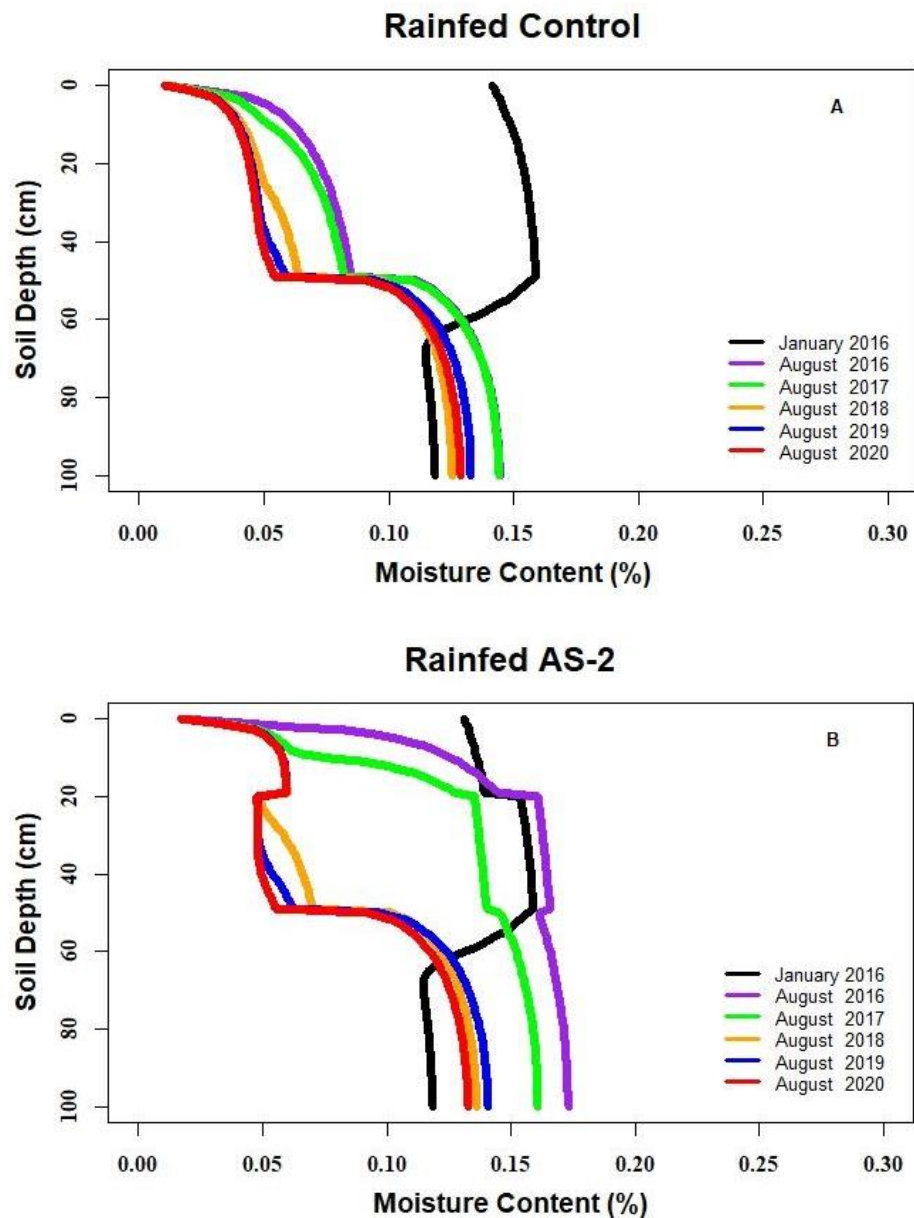


Figure 3-3 Moisture profile over time for rainfed control (A) and rainfed AS-2 (B). Solid black line represents the initial soil moisture content (day zero), and solid red line is moisture content in August for the 5th year. All other curves represent yearly moisture content for the month of August.

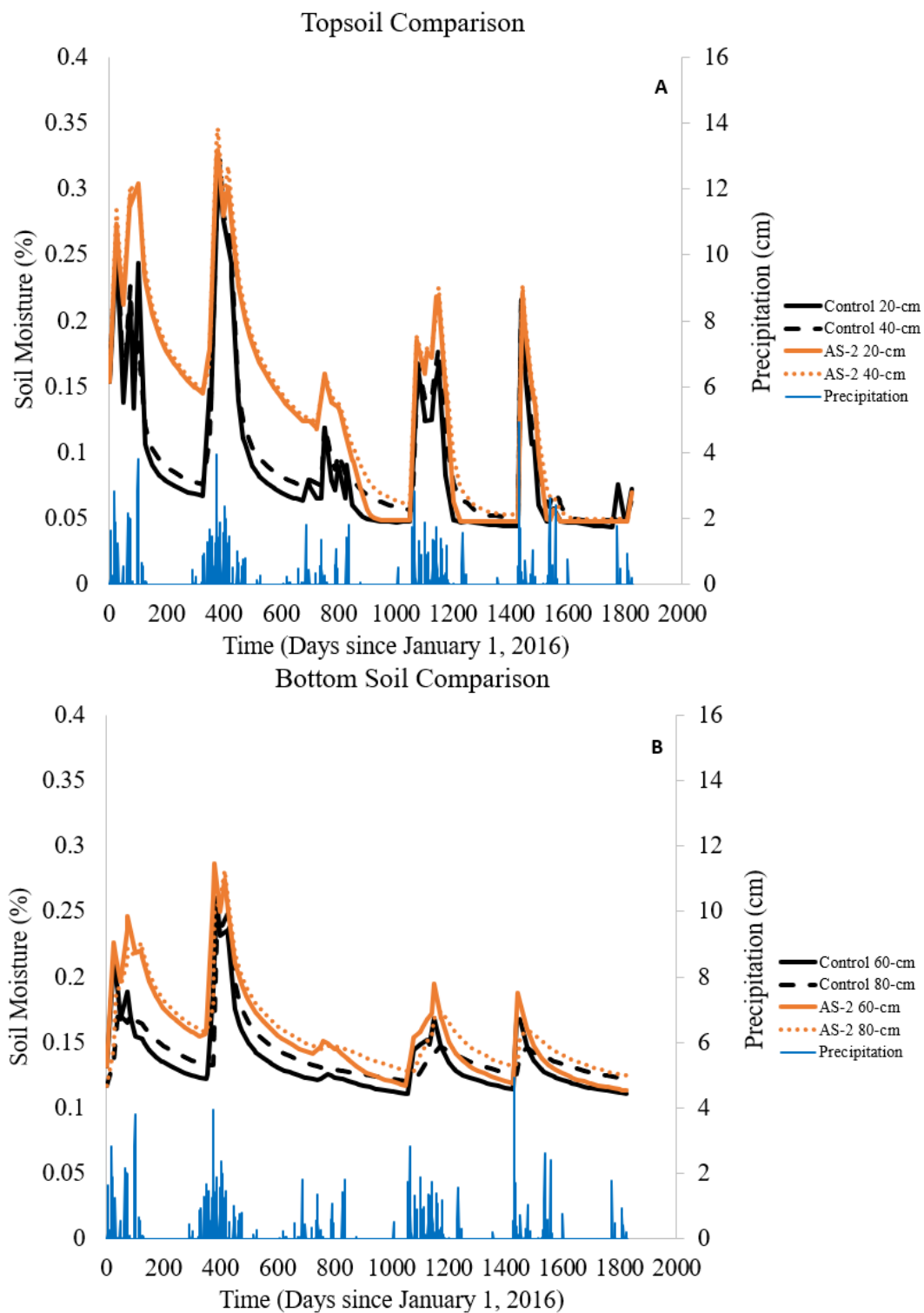


Figure 3-4 Seasonal moisture comparison between rainfed control and rainfed AS-2 biochar for the topsoil (A) and bottom soil layer (B).

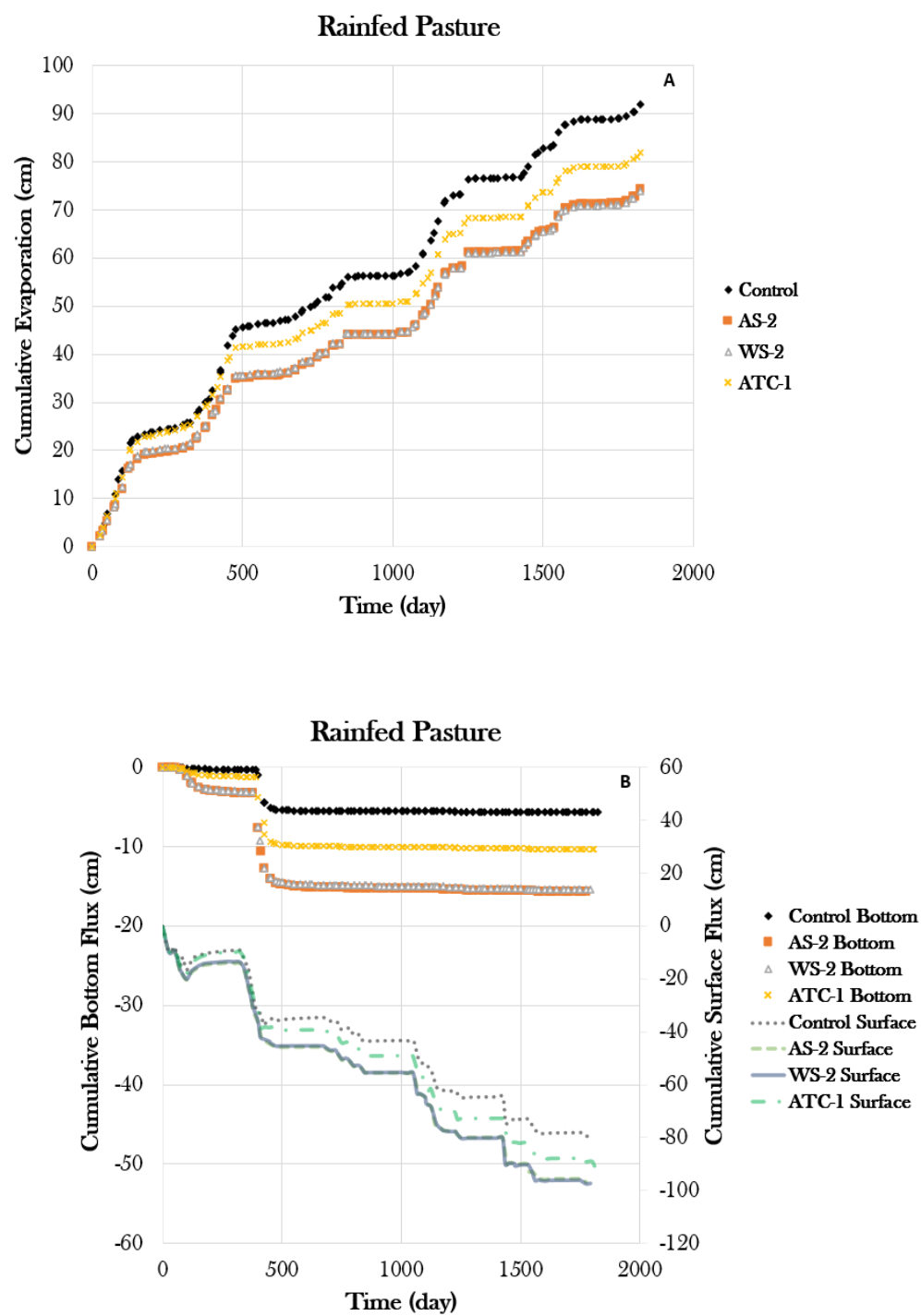


Figure 3-5 Cumulative evaporation (A) and Cumulative surface and drainage fluxes (B).

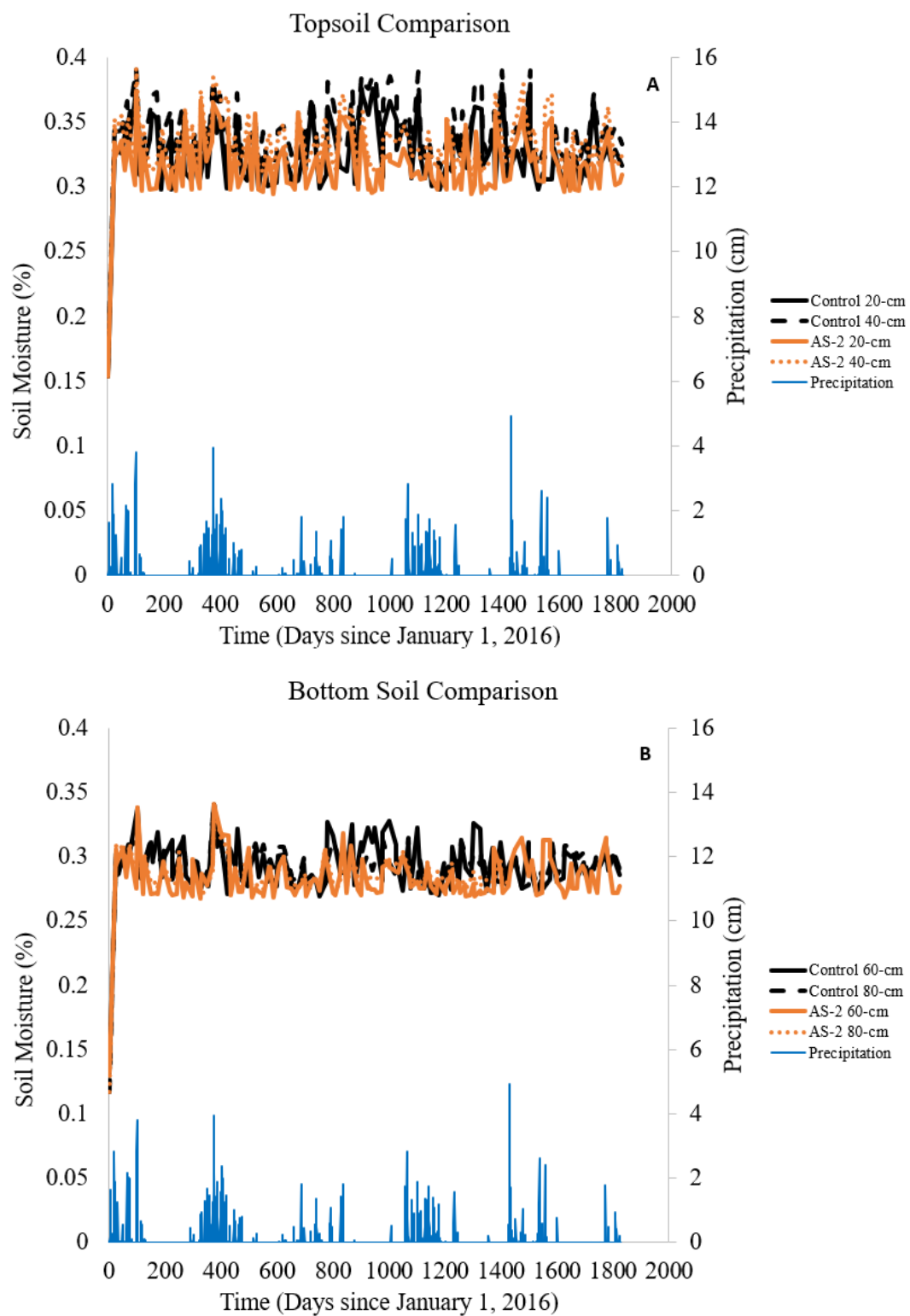


Figure 3-6 Seasonal moisture comparison between irrigated control and irrigated AS-2 biochar for the topsoil (A) and bottom soil layer (B).

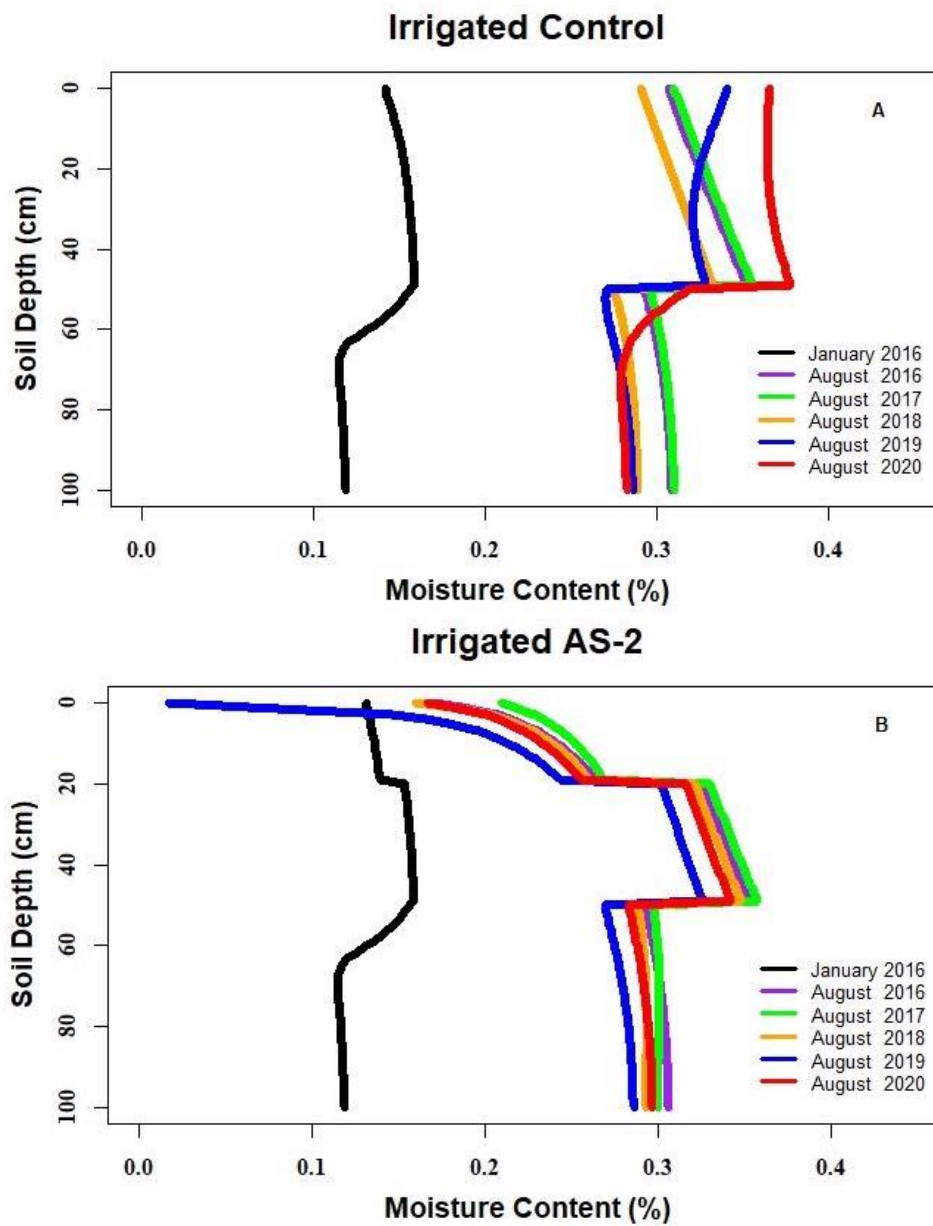


Figure 3-7 Moisture profile over time for irrigated control (A) and irrigated AS-2 (B). Solid blue line represents the initial soil moisture content (day zero), and solid red line is post-season soil moisture content (August) for the 5th year. All other curves represent yearly post-season (August) moisture content.

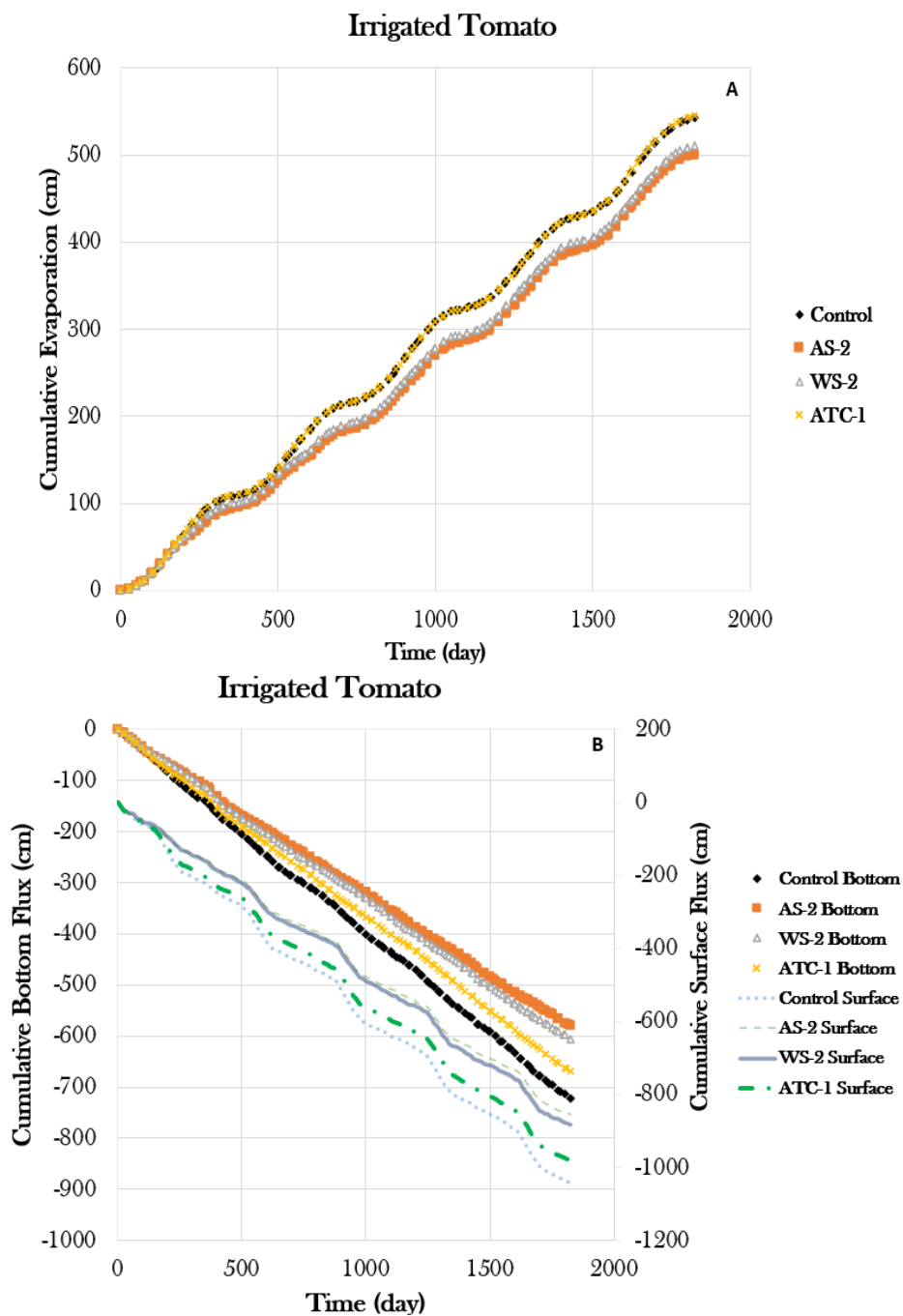


Figure 3-8 Moisture profile over time for irrigated control (A) and irrigated AS-2 (B). Solid blue line represents the initial soil moisture content (day zero), and solid red line is post-season soil moisture content (August) for the 5th year. All other curves represent yearly post-season (August) moisture content.

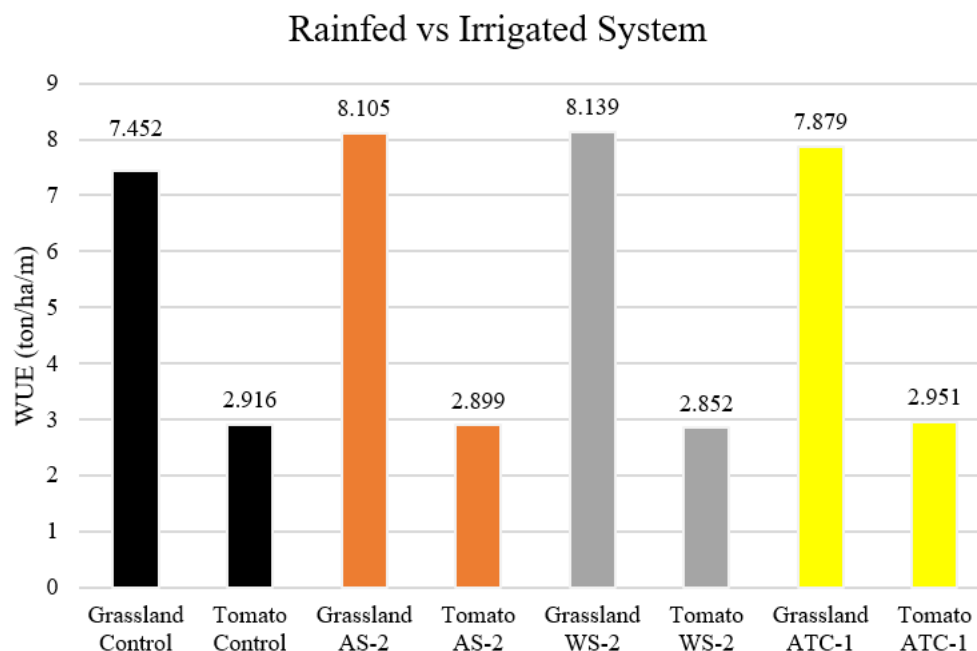


Figure 3-9 WUE Comparison in ton/hectare/mm of water, for rainfed grassland and irrigated tomato system.

Table 3-1. Physical Characteristics of soil layers used in model simulations

Soil layer	Bulk Density ( $g/cm^3$ )	Sand (%)	Silt (%)	Clay (%)	PAW ( $cm/cm$ )	*Soil Erosion
Atwater loamy sand	1.48	82.9	8.61	8.46	0.08	0.15
Sandy loam	1.38	66.0	19.0	15.0	0.12	0.24

\* *K* factor for soil erosion

Table 3-2. Chemical Characteristics of soil layers used in model simulations

Soil layer	SOM (%)	C (%)	N (%)	C:N	CEC ( $cmol$ - $c/kg$ )	Ca ( $cmol$ - $c/kg$ )	K ( $cmol$ - $c/kg$ )	Mg ( $cmol$ - $c/kg$ )	pH
Atwater loamy sand	1.70	0.78	0.06	13.0	4.87	3.97	0.51	0.17	6.70
Sandy loam	0.50	N/A	N/A	N/A	7.50	N/A	N/A	N/A	6.70

N/A = not available

Table 3-3 van Genuchten Parameters used in model simulations

Treatment	$\theta_r$	$\theta_s$	$\alpha$	$n$	$\rho_b$ (g/cm <sup>3</sup> )	$K_{sat}$ (cm/days)*
Control	0.007	0.44	0.011	1.526	1.48	144.3
5% AS-2	0.009	0.51	0.045	1.389	1.24	242.1
5% WS-2	0.014	0.45	0.039	1.418	1.34	202.8
5% ATC-1	0.009	0.46	0.029	1.431	1.26	234.9
Sandy-Loam	0.054	0.42	0.024	1.460	1.38	54.90

Table 3-4 Annual ET<sub>o</sub> and precipitation

Year	ET <sub>o</sub> (mm)	Precipitation <sup>a</sup> (mm)
2000-2015*	1397	298
2016	1419	449
2017	1375	407
2018	1393	271
2019	1360	412
2020	1424	191

<sup>a</sup> Day 0 for the simulation start at January 1<sup>st</sup>, 2016

\* 15 years average

Table 3-5 Non-Irrigated Pasture Water Applied &amp; Yield

Treatment	Total Water (m)	Root Water Uptake (mm)	Yield <sup>a</sup> (ton/ha)	WUE (ton/ha/m)	Yield Comparison* (%)
Control	1.731	800	12.90	7.452	
5% AS-2	1.731	870	14.03	8.105	8.75
5% WS-2	1.731	874	14.09	8.139	9.25
5% ATC-1	1.731	846	13.64	7.879	5.75

<sup>a</sup> 12.9 ton/hectare is average pasture yield (May-October) in California (Forero et al., 2003).

\* 1 - Biochar/Control = % Difference compared to Control.

Table 3-6 Irrigated Tomato Water Applied &amp;. Yield Comparison

Treatment	Total Water (m)	Root Water Uptake (mm)	Yield <sup>a</sup> (ton/ha)	WUE (ton/ha/m)	Difference Water (%)*	Difference Yield (%)*
Control	15.7	3030	45.7	2.916		
5% AS-2	13.4	2570	38.8	2.899	-14.6	-15.2
5% WS-2	13.8	2610	39.3	2.852	-12.2	-14.0
5% ATC-1	15.1	2950	44.5	2.951	-3.80	-2.60

<sup>a</sup> 45.7 ton/hectare is average fresh-market tomato yield in California (Le Stranger et al., 2000).

\* 1 - Biochar/Control = % Difference compared to Control.

Table 3-7 Irrigated Tomato Economic Comparison

Comparison	\$ Yield	\$ Water
Control vs AS-2	-2,432	539
Control vs. WS-2	-2259	455
Control vs ATC-1	-435	153

## **Chapter 4.**

# **The effects of different biochar-dairy manure co-composts on soil hydraulic properties, nutrients retention, greenhouse gas emissions, and tomato productivity; observations from a soil column experiment**

## **Abstract**

Finding feasible solutions for sustainable food production is challenging. Here we try to understand the balance between crop productivity and ecological stewardship using agroecological based soil management strategies. More specifically, we evaluated the potential of different organic materials such as dairy manure compost and different biochar manure co-composts, derived locally from agricultural wastes, to enhance soil ecosystem services. We assessed their impact on soil hydrological properties, nutrient retention, greenhouse gas emissions, and crop productivity using data collected from an outdoor tomato column study. Results from the experiment showed biochar co-composts yielded substantial improvement to soil health by minimizing loss of essential nutrients such as  $\text{NO}_3^-$ -N and  $\text{NH}_4^+$ -N, sustained tomato yield, and improved crop water use efficiency. However, yield response to soil organic amendment is constrained by external factors such as irrigation strategies, with treatments under deficit irrigation greatly impacted. Overall, we observed a positive effect of adding biochar manure co-composts to soil, although best management practices are needed to optimize crop productivity and avoid unintentional consequences.

## **4.1 Introduction**

Maintaining a balance between food production and ecological stewardship is crucial for the sustainability of agriculture and human welfare. Still, farming systems like crop and animal production are known to be associated with several environmental issues, directly linked to soil and nutrient management such as non-point source contamination caused by leaching and field runoff. Common farming operations (e.g. irrigation scheduling and soil compaction caused by farm machinery) can also lead to unintended consequences and loss in farm revenue. Equally, the annual surplus of wastes generated from agriculture production also convey a high degree of ecological risks, particularly linked to climate change with modern practices like open burning and stockpiling of animal waste (e.g. dairy manure). These practices emit substantial greenhouse gas (GHGs), such as methane ( $\text{CH}_4$ ), carbon dioxide ( $\text{CO}_2$ ), and nitrous oxide ( $\text{N}_2\text{O}$ ) back into the atmosphere (Crippa et al., 2021).

Alternatively, diverting and converting these wastes into material like biochar and compost to be used as a nutrient-rich organic soil amendment for crop production has been viewed as an ecological technique to enhance soil ecosystem services (Wang et al., 2019; Xiao et al., 2017; Yin et al., 2021). Many studies have investigated and observed a positive effect of incorporating biochar and compost on soil health (Abideen et al., 2020;

Chen et al., 2020; Cooper et al., 2020; Shin et al., 2018) and plant growth (Bashir et al., 2020; Obadi et al., 2020; Teodoro et al., 2020). However, the process of creating organic materials such as compost also releases considerable GHGs (Nordahl et al., 2023; Sánchez et al., 2015; Yin et al., 2021). By contrast, composting with biochar has been shown to significantly reduce GHG emission during the composting process (Harrison et al., 2022; Xiao et al., 2017) and may yield a superior organic soil amendment (Sanchez et al., 2018; Wang et al., 2019). An extensive literature review conducted by Agegnehu et al. (2017) highlights the greater potential of biochar co-compost to positively impact soil ecosystem services, as compared to biochar or compost alone. Similarly, a more recent meta-analysis conducted by Wang et al. (2019) also reveals a substantial gain in yield (39.7%) for cereal crops grown with biochar co-compost, though much remains unknown about how agroecosystems respond to biochar co-compost application (Gao et al., 2023). Furthermore, balancing ecological stewardship and high levels of crop production remains a difficult task to resolve (Tully & Ryals, 2017). Few controlled studies have examined the agronomic and environmental effects of soil organic amendment like biochar manure co-compost on soil health, GHGs emission, and crop productivity.

#### **4.1.1 Research Objectives**

The overall research objective in this study is to understand the balance between agroecological based soil management and crop productivity. We assessed different soil organic amendments (e.g. manure compost and biochar manure co-compost) that are derived locally from agricultural waste materials (e.g. dairy manure and different orchard wastes). We hypothesized that the application of all soil organic amendments will have positive effects on soil health, more specifically soil hydraulic properties and nutrient retention, and enhance crop productivity, while also reducing environmental impacts on typical agricultural soils in the Central Valley of California. To test this hypothesis, we conducted and discussed here findings from an outdoor tomato column study.

## **4.2 Materials and Methods**

### **4.2.1 Tomato Column Experiment**

The soil column experiment was conducted outside at University of California, Merced, next to the greenhouse facility (37.364 °N, -120.422 °W) during the summer (July) of 2022 and lasted until early winter (November) 2022. The experiment was conducted outside rather than in the greenhouse to expose the plant to actual, fluctuating climatic conditions. The soil used in the column study was collected from an experimental field site and classified as a loamy, thermic Natric Durixeralf USDA Soil Taxonomic family (soil order: Alfisols) (Gao et al., 2023). The experimental design was a complete randomized block design with three blocks (Figure S4.1). The main factor was the soil organic amendments, which consisted of five different treatments, a no amendment (Control), dairy manure compost (Compost), almond shell biochar manure co-compost (ASB), walnut shell biochar manure co-compost (WSB), and almond clipping biochar manure co-compost (ACB). Each soil organic amendment was applied at a 5% (w/w) application rate and was thoroughly mixed, then backfilled into the top 15-cm. The biochars used for the co-composting process were products derived from local agricultural wastes using a rotational mobile pyrolyzer at temperature around 350°C - 400°C (Figure S4.2). Each biochar was then added to fresh dairy manure using a 5% mixture rate (w/w) and composted for 42 days using lab compost reactors (Harrison et al.,

unpublished data). The sub-factor was irrigation schemes, where half of the treatments within each block were irrigated at full crop water demand or crop evapotranspiration (ET<sub>c</sub>) while the other half were irrigated at 75% ET<sub>c</sub>, a practice known as deficit irrigation. The deficit irrigation served as a means to evaluate the influence of these soil organic amendments on plant productivity given that water is a constraining variable in drought prone agricultural regions such as California. A total of 30 columns (5 treatments x 2 irrigation x 3 replication) were established. The soil column was made from a polyvinyl chloride (PVC) tube with a 15 cm diameter top, a circumference of 53 cm, and a height of 70 cm. The bottom of each column was capped, and a drainage line attached to a 12 oz plastic bottle was installed at the bottom to capture leachate.

#### 4.2.2 Column Measurement

Organic beefsteak tomato (*Solanum lycopersicum*) was chosen as the crop for the column study. The rationale for selecting this crop is because it followed the wheat-tomato crop rotation at the field site (Gao et al., 2023). In addition, tomato holds a major role in the California vegetable industry, with the majority of acreage harvested in the Central Valley (USDA-NASS, 2020). This tomato variety is generally planted from March through July in the region. The column was spaced 30.5 cm apart from each other on a wooden stand, similar to standard field spacing. Tomato was transplanted on July 13, 2022 and harvested by November 23, 2022, a total of 133 growing days. Measurements used as proxy for plant productivity as influenced by soil treatments and irrigation regimes were fractional green canopy and leaf chlorophyll content. Plant canopies (n = 3) were estimated using the Canopeo apps developed by Patrignani & Ochsner (2015) and images were taken at a height of 50 cm above the plant canopy near solar noon. Leaf chlorophyll content was measured using the SPAD 502 meter (Spectrum Technologies, Plainfield, IL, USA) on three youngest mature leaves in each plot (n = 9). The SPAD 502 is a portable and nondestructive technique used to estimate leaf chlorophyll concentrations (Xiong et al., 2015) and has been shown to greatly enhance nitrogen fertilization management (Ghosh et al., 2020). In addition, we also monitored fruit set in each plot throughout the season and used the observation as an indicator of plant stress.

Daily tomato ET<sub>c</sub> was calculated by multiplying the reference ET generated by the nearby CIMIS station (#148) by a specific crop coefficient (k<sub>c</sub>) for tomatoes grown in the Central Valley region (Hanson & May, 2006). Excluding the water used to bring the initial soil condition to field capacity and plant establishment, a total of 558 mm and 432 mm of water was applied to the 100% and 75% ET<sub>c</sub> plot, respectively. Furthermore, a total of 168 kg N/ha was applied to all plots; separated into three equal applications (56 kg N/ha, applied in August, September, and October 2022). At harvest, tomato fruits were picked from each plot and weighted. Fruit juice was then extracted from all fruit and used for sugar content determination. Sugar concentration (%) was measured using a handheld Brix Refractometer with the capacity to measure sugar density in solution from 0-90%. This specific unit also includes automatic temperature compensation (between 10°C to 30 °C) with an accuracy of ± 0.2%. A total of three sugar measurements were conducted for each plot (n = 3). Plant biomass was determined by oven drying the aboveground biomass at 100°C for 48 hours. Water use efficiency (WUE) and nitrogen use efficiency (NUE) was calculated by dividing the respective yield in each plot with total water and nitrogen applied.

### 4.2.3 Soil Hydrological Properties

Since soil hydrological properties as influenced by different soil organic amendments is a main interest, moisture retention curves ( $n = 3$ ) were established for all soil organic treatments and control using the WP4C Dewpoint Potentiometer (METER Group, Pullman, WA). The method used to develop moisture retention curve followed the vapor sorption analysis described in Tuller & Or (2005) and reported in Thao et al. (unpublished data). The moisture retention curve of a substance describes its potential to hold onto water in the presence of different suctions. For field application, understanding the retention curve is extremely critical as moisture is directly linked to many factors such as plant available water, nutrient leaching, biota activity, and GHGs emission. Measurement of hydrophobicity, or the repulsive nature of a material to water, was also performed for all experimental treatments ( $n = 9$ ) using the water droplet penetration test (WDPT).

Similarly, soil moisture sensors were also essential tools in the column experiment. Ten soil moisture sensors connected to two EM50 data loggers (METER Group, Pullman, WA) were installed in the deficit irrigation plots in Block 2 (randomly selected). Of this, five Decagon 5EM sensors with the capacity to measure soil moisture and temperature were installed at 20 cm depth, or right below the zone of application, to monitor moisture retention near the active rootzone (referred to as surface moisture from hereafter). Five Decagon 5TE sensors, with the capacity to measure soil moisture, temperature, and bulk electrical conductivity (EC) were also installed in the same plot at 50 cm soil depth to monitor moisture movement within the profile (referred to as subsurface moisture from hereafter). Moisture sensors were installed one month before transplant to allow for environmental acclimation. The two data loggers were set to take readings every hour and soil moisture data were collected on a weekly basis.

### 4.2.4 Greenhouse Gas Emissions

GHG ( $\text{CO}_2$ ,  $\text{CH}_4$ , and  $\text{N}_2\text{O}$ ) sampling was conducted using a cavity ring-down laser spectrometer Picarro Gas Analyzer (Picarro G2508, Picarro Inc., Santa Clara, CA) with a five minute continuous flux reading. The unit is connected to a closed system static chamber (26 cm in diameter and 13 cm tall). Gas fluxes ( $\text{nmol m}^{-2} \text{s}^{-1}$ ) were calculated in the Picarro Soil Flux Processor program using the exponential model developed by Hutchinson & Mosier (1981) to account for nonlinear changes in headspace concentration (Gao et al., 2023; Harrison et al., 2022). GHG emissions were measured five different times throughout the season: at preplant or after soil treatment incorporation, after the first, second, and third fertilizer applications, and post-harvest. A PVC chamber (26 cm in diameter fitted down to 15 cm and 30 cm in height) was attached to the tomato column for gas sampling. As the plant canopy developed and expanded, the canopy was carefully packed inside the chamber to avoid physical damage. After each sampling, gas concentrations were given time to return to ambient concentration before the next measurement.

### 4.2.5 Nutrient Retention and Soil Analysis

We evaluated the soil organic treatments' potential to retain essential nutrients, such as nitrate nitrogen ( $\text{NO}_3^- \text{-N}$ ) and ammonium nitrogen ( $\text{NH}_4^+ \text{-N}$ ), by collecting and analyzing leachate and soil samples. We are particularly interested in these two forms of inorganic nitrogen since they are the primary nitrogen sources for plant uptake but are also highly susceptible to leaching, and are a major environmental and public health concern in the

state (Harter et al., 2002). After the post-harvest GHG sampling, we conducted a flush on the soil column. Hence, each column was given a total of 102 mm (~ 4 inch) water to flush out any residual nutrients within the soil profile. Leachate samples were then collected from all plots twice, the day after the flushing event and five days afterward, following a large precipitation event. Leachate samples collected in both respective dates were thoroughly mixed, and a subsample from each was taken for inorganic nitrogen analysis. After the flushing event, soil samples were taken from each column at five depths intervals (0-15, 20-30, 30-40, 40-50, and 50-60 cm) by cutting the entire column into different sections. Moisture content for each sample was determined by oven drying a subsample at 100 °C for 48 hours. For soil analysis, 6 g of soil were mixed with 30 mL of 2M KCl and shaken for one hour. Samples were then filtered using Whatman #1 filter papers into a 50 mL centrifuge tube and frozen at -4 °C degree prior to inorganic nitrogen analysis.  $\text{NO}_3^-$ -N and  $\text{NH}_4^+$ -N concentration ( $\text{mg L}^{-1}$ ) and amount ( $\text{mg kg Dry Soil}$ ) was determined for leachate and soil samples by the microplate colorimetric techniques using the vanadium-chloride method and salicylate-nitroprusside method, respectively (Mulvaney et al., 1996).

#### 4.2.6 Statistical Analysis

Statistical analyses were done using the R package (R Core Team, 2020). All datasets were subjected to the Normality (Shapiro-Wilk) and Homogeneity of Variance (Levene's) tests. When necessary, datasets that failed to meet the assumptions of ANOVA were log-transformed prior to analyses. A two-way Analysis of Variance (ANOVA) was performed to determine statistical differences among treatments for measured parameters for the tomato column experiment, with statistical significance established at the 90% confidence interval or  $p < 0.1$ . Tukey-HSD tests were used to distinguish significance among treatments. In addition, linear regression was also performed on tomato yield datasets with leaf chlorophyll content and canopy coverage.

### 4.3 Results

#### 4.3.1 Crop Productivity

##### 4.3.1.1 Crop Yield

No statistical difference was detected for aboveground biomass of tomato plants as influenced by soil organic amendments ( $p = 0.465$ ) or irrigation regime ( $p = 0.396$ ). For tomato fruit, although we observed greater yield in the amended treatments compared to the control, the difference was also not significant ( $p = 0.653$ ). Significant treatment difference however was detected for irrigation regime ( $p = 0.065$ ) with fruit yield in the 100%  $\text{ET}_c$  greater than the 75%  $\text{ET}_c$  (Figure 4.1a). As for sugar content, significant differences were observed for treatment ( $p = 0.013$ ), irrigation ( $p = 0.074$ ), and interaction between treatments and irrigation levels ( $p = 0.001$ ). Since interaction was observed, the sugar dataset was separated by soil organic treatment and reanalyzed as a one-way ANOVA. For treatments irrigated at deficit rate, sugar concentration in WSB (5.89%), Compost (5.89%), and Control (5.50%) were significantly lower than ASB (8.33%) (Table S4.1). ACB had intermediate sugar concentration (7.11%) and was not significantly different from the other treatments. For treatments irrigated at 100%  $\text{ET}_c$ , WSB (6.50%) and Compost (7.11%) again has significantly lower sugar content compared to ASB (8.22%), ACB (10%), and Control (9.56%) (Table S4.1). When

comparing fruit sugar content with irrigation regimes, we see much higher concentration in the 75%  $ET_c$  treatments, compared to its 100%  $ET_c$  counterpart (Figure 4.1b).

#### 4.3.1.2 Water Use Efficiency and Nitrogen Use Efficiency

We did not see any statistical differences in WUE, expressed as ton/hectare of tomato yield per meter of water applied, for soil organic treatments ( $p = 0.722$ ). A significant difference was detected for irrigation regimes ( $p = 0.078$ ), again with WUE in 100%  $ET_c$  greater than 75%  $ET_c$  (Figure 4.2). NUE, expressed as ton/hectare of tomato yield per kg of N applied, in the column study followed WUE, with no difference detected for soil treatments ( $p = 0.653$ ) but was present for irrigation regimes ( $p = 0.065$ ), with greater NUE observed in 100%  $ET_c$  plots (Figure S4.3).

### 4.3.2 Soil Hydrological Properties

#### 4.3.2.1 Moisture Retention Curves & Hydrophobicity

Moisture retention curves for treatments in the tomato column study ( $n = 3$ ) are shown in Figure 4.3. Here we clearly see that moisture retention in the control is substantially lower than moisture retention from the soil organic amendments (Figure 4.3). In other words, at the same gravimetric water content, water in the organic treatments is held at a much greater force than the control. When assessing the hydrophobicity of each material, other than the Control all other soil organic amendments were found to be extremely hydrophobic (Table S4.2). Note that hydrophobicity was observed only on the pure materials and not on the mixed soil (data not shown).

#### 4.3.2.2 Surface and Subsurface Moisture

Moisture at the 20 cm surface level shows that deficit WSB and deficit Control had much higher moisture content throughout the entire growing season, compared to surface moisture observed in the deficit Compost and deficit ASB treatments (Figure S4.4a). At the 50 cm subsurface, moisture content in the deficit WSB and Compost treatments is much higher than the Control, ACB, and ASB (Figure S4.4b). This same pattern is also reflected in the bulk EC detected by the subsurface sensors (Figure S4.4c).

### 4.3.3 Nutrient Retention

#### 4.3.3.1 Soil and Leachate $NO_3^-$ -N and $NH_4^+$ -N

Post flushed soil  $NO_3^-$ -N and  $NH_4^+$ -N with depth for the column experiment is shown in Figure 4.4. For treatment in the 100%  $ET_c$ , we see relatively similar  $NO_3^-$ -N ( $< 0.5$  mg  $NO_3^-$ -N/ kg Dry Soil) throughout the soil profile for WSB, Compost, and ACB (Figure 4.4a). Control was similar to the organic amendments up until 50 cm and 60 cm. At these depths we observed a spike in soil  $NO_3^-$ -N for the Control. For 75%  $ET_c$ , except for ASB, soil  $NO_3^-$ -N increased with depth for all treatments (Figure 4.4b). After 30 cm, soil  $NO_3^-$ -N was greater for the ACB treatment compared to the others. Figure 4.4c reveals soil  $NH_4^+$ -N with depths for the 100%  $ET_c$ . Soil  $NH_4^+$ -N was similar for all treatments up until 30 cm. After this depth, Compost and WSB have a decline in soil  $NH_4^+$ -N, whereas ASB, ACB, and Control have a spike in soil  $NH_4^+$ -N. Soil  $NH_4^+$ -N in the deficit irrigation plots was generally lower compared to the fully irrigated plots. We also observed a similar soil  $NH_4^+$ -N pattern for all treatments with depth in the deficit plots (Figure 4.4d).

Leachate  $\text{NO}_3^-$ -N and  $\text{NH}_4^+$ -N concentration ( $\text{mg L}^{-1}$ ) for the tomato column study is displayed in Figure 4.5. For  $\text{NO}_3^-$ -N, no statistical significance was detected for soil treatments ( $p = 0.658$ ); though the Control was much higher in concentration (Figure 4.5a). We did however observe a significant difference with irrigation regimes ( $p = 0.094$ ), with leachate  $\text{NO}_3^-$ -N statistically greater in the 75%  $\text{ET}_c$  plots compared to concentration in the 100%  $\text{ET}_c$ . No statistical difference was detected for leachate  $\text{NH}_4^+$ -N across soil treatments ( $p = 0.994$ ) or irrigation level ( $p = 0.477$ ) (Figure 4.5b).

#### 4.3.3.2 GHG Emissions

Table 4.1 shows soil GHG emissions at different periods in the column study. At preplant, a significant difference was detected for  $\text{CO}_2$  emission among treatments ( $p = 0.095$ ), with emission from WSA ( $16.95 \text{ mg CO}_2 \text{ m}^{-2} \text{ s}^{-1}$ ) greater than Control ( $7.24 \text{ mg CO}_2 \text{ m}^{-2} \text{ s}^{-1}$ ). Emissions from ASB, ACB, and Compost were not statistically different from each other or from WSA and Control. No statistical difference was observed for  $\text{CH}_4$  and  $\text{N}_2\text{O}$  emission at preplant. Differences in  $\text{CO}_2$  emissions measured after the first fertilization event were not significant among soil treatments but were statistically greater in the 75%  $\text{ET}_c$  plots compared to 100%  $\text{ET}_c$  ( $p = 0.027$ ). No statistical difference was observed for  $\text{CH}_4$  and  $\text{N}_2\text{O}$  across soil treatments and irrigation regimes. GHG emissions measured after the second fertilization were not significantly different across soil treatments and irrigation level. Similarly, gas measurement taken after the third fertilization was not statistically different across treatments and irrigation for  $\text{CO}_2$  and  $\text{CH}_4$ . After the third fertilization event, a significant difference was detected for  $\text{N}_2\text{O}$  emission as influenced by soil treatments ( $p = 0.03$ ). As shown in Table 4.1, deficit ACB has the highest  $\text{N}_2\text{O}$  emission ( $3621 \text{ ng N}_2\text{O m}^{-2} \text{ s}^{-1}$ ), followed by 100%  $\text{ET}_c$  ACB ( $2655 \text{ ng N}_2\text{O m}^{-2} \text{ s}^{-1}$ ), whereas  $\text{N}_2\text{O}$  was lowest in the deficit WSB ( $-2897 \text{ ng N}_2\text{O m}^{-2} \text{ s}^{-1}$ ), followed by deficit Compost ( $-1859 \text{ ng N}_2\text{O m}^{-2} \text{ s}^{-1}$ ). In general, there was a positive  $\text{N}_2\text{O}$  flux in the fully irrigated treatments and a negative flux (uptake) in the deficit plots on this particular day. GHGs emissions taken at post-harvest were not significantly different across soil treatments and irrigation level.

## 4.4 Discussion

### 4.4.1 Influence on Crop Productivity

The application of organic amendments to soil is a means to restore soil carbon stocks, mitigate GHG emissions, enhance soil ecosystem services, and sustain crop productivity (Lehmann & Kleber, 2015; Longbottom et al., 2022). However, in this study we observed that the response of crop yield to soil organic amendments varied with irrigation strategies. Although we observed greater yield with soil treatments (Figure 4.1a), this effect was not statistically different. It appears that yield was more constrained by environmental factors such as water availability. As indicated, most of the statistical differences were detected for irrigation schemes (e.g. fruit, sugar content, leachate  $\text{NO}_3^-$ -N, WUE, and NUE).

### 4.4.2 Crop Productivity under Irrigation Schemes

Plant measurements such as leaf chlorophyll content and fractional green canopy may help us understand why no significant difference was observed in yield across soil organic treatments, but differences were observed for irrigation schemes. Fractional green canopy was not significantly different for soil treatments, except for canopy taken in

September where ambient temperature was high (Table S4.3). During this date, plant canopy in the deficit irrigation plots was statistically smaller than the fully irrigated plots ( $p = 0.0123$ ). This may be an indicator of plant water stress. After this period, seasonal temperature dropped and plant canopy in the deficit plots was able to recover and was comparable to the 100%  $ET_c$  (Table S4.3). This may be the reason why we did not see statistical differences in plant biomass. On the other hand, SPAD meter reveals that in most cases leaf chlorophyll content in ACB, Compost, and Control were significantly lower compared to WSB and ASB (Table S4.4). This observation was true across treatments and irrigation regimes (Table S4.4). Leaf chlorophylls are essential for photosynthesis and can be used as a proxy for photosynthetic potential (Suplito et al., 2020; Xiong et al., 2015). In general, plants will expand their canopy in order to intercept as much photosynthetic available radiation as possible for consumption. Therefore, in theory we should see a difference in plant productivity given that a positive relationship for tomato biomass to mean leaf chlorophyll content was observed ( $r^2 = 0.288$ ,  $p = 0.0022$ ) (Table 4.2). Yet a superior relationship was also detected for biomass to fractional green canopy ( $r^2 = 0.594$ ,  $p < 0.0001$ ) (Table 4.2), and since plant canopy was not statistically different across soil treatments or irrigation regimes, the effects leaf chlorophyll imposed onto biomass may have been overshadowed.

Fruit yield was significantly affected by irrigation regimes with yield in the deficit plots much lower compared to the full irrigation. This could be linked to the observation stated above where the plant may have been water stressed. Possibly, there could be negative chronic effects on fruit development even after the plant canopy recovered, e.g. canopy development at the cost of fruit yet. Studies have shown reduced yield for tomatoes that were exposed to water stress conditions (Cui et al., 2019; Medyouni et al., 2021; Patanè et al., 2010). Another assumption is stress induced premature fruit in the 75%  $ET_c$ , which is supported by fruit-set count taken throughout the season. Figure 4.6 shows the fruit-set count at different dates with the y-axis being treatment replications. Hence, a treatment reaching three implies that all replications for that treatment set fruit on that particular date. As observed, treatments receiving the deficit rate set fruit earlier in the season compared to the fully irrigated plots. Furthermore, both deficit ASB and ACB had only two replications that produced fruit, while deficit Compost did not set fruit until later in the season. Since the fruit was developed prematurely, fruit may be smaller in size but higher in sugar content at harvest due to longer maturity. Deficit Compost has the lowest yield among the 75%  $ET_c$  treatments, whereas Control has the lowest yield among the 100%  $ET_c$ . Similar to deficit ASB and ACB, Control in the 100%  $ET_c$  also has only two replications that set fruit. It is possible that the low yield in the 100%  $ET_c$  Control was caused by nutrient stress. This is revealed in both soil and leachate samples where Control has much higher soil  $NO_3^-$ -N and  $NH_4^+$ -N residuals with depths and concentration (Figures 4.4 & 4.5). Since Control was irrigated at full  $ET_c$ , the water may have pushed available nitrogen below the rootzone.

#### 4.4.3 Influence on Soil Hydrological Properties

In this column study, moisture retention curves developed for all soil treatments show higher water retention potential for the different organic amendments (Figures 4.3), although actual soil moisture retention under climatic conditions varied. Moisture sensors installed below the zone of application in deficit treatments exhibit similar moisture patterns for WSB and Control, both were relatively higher than ASB, ACB, and Compost. All organic amendments displayed higher moisture at the 50 cm subsurface

region compared to Control (Figure S4.4b). This indicates that more water is percolating down in the profile for soil with co-composts amendments, which can be a positive effect for groundwater recharge but a concern for nutrient leaching. However, both yield and leachate  $\text{NO}_3^-$ -N and  $\text{NH}_4^+$ -N in the deficit plots were not statistically different across soil treatments (discussed more in Section 4.4). This observation may be linked to augmented soil structure stemmed by more microbial activity from the added organic materials (Anderson et al., 2011). The increase in microbial activity in conjunction with organic matter decomposition may strengthen soil pore connectivity and allow for better water flow (Baiamonte et al., 2019; Bohara et al., 2019). Several studies have detected improvement in soil aggregate stability from soil amended with biochar and manure co-compost (Chen et al., 2020) and attributed the findings to enhanced microbial growth (Cooper et al., 2020; Sanchez-Monedero et al., 2018).

#### 4.4.4 Influence on Soil Nutrient Retention

Nutrient retention is critical for crop production and is a major factor for understanding the balance between soil management and crop productivity (Tully & Ryals, 2017; Wu & Ma, 2015). Improvement in nutrient retention can lead to increased yield potential, decrease environmental impacts, while raising farm revenue by reducing fertilizer expenses. In our study, we observed greater potential of biochar co-composts to retain more inorganic nitrogen ( $\text{NO}_3^-$ -N and  $\text{NH}_4^+$ -N) while also maintaining crop yield. Inorganic nitrogen in both soil and leachate were generally lower in co-compost treatments as compared to Control. This is visibly shown in plots that were irrigated at full crop water demand (Figure 4.4a, 4.4c). Since fruit yield in the 100%  $\text{ET}_c$  was not affected, this is evident of greater retention at high irrigation rate. When comparing nitrogen loss across irrigation regimes, we observed higher soil  $\text{NO}_3^-$ -N with depth (Figure 4.4a, 4.4b) and leachate  $\text{NO}_3^-$ -N (Figure 4.5a) in the deficit plots as compared to the 100%  $\text{ET}_c$ . This result is expected as more nitrogen should be retained with less water percolation (Di & Cameron, 2002). The irrigation flush after harvest then leached out the preserved nitrogen in the deficit plots. Results from our experiments are aligned with numerous leaching studies that shown high potential of biochar to adsorb  $\text{NO}_3^-$ -N and  $\text{NH}_4^+$ -N (Bohara et al., 2019; Knowles et al., 2011; Kuo et al., 2020; Shin et al., 2018; Zheng et al., 2013).

#### 4.4.5 Influence on GHGs

No major differences were detected for  $\text{CH}_4$  and  $\text{N}_2\text{O}$  emissions taken at different dates across soil treatments and irrigation schemes.  $\text{CO}_2$  however was higher for the WSB co-compost treatments at the preplant period compared to Control. This could be due to rapid mineralization of the organic material after soil incorporation (Baiamonte et al., 2019; Bohara et al., 2019). Following this, the higher  $\text{CO}_2$  emission detected in the deficit plots after the second fertilization may be associated with more available oxygen. Oxygen limitation conditions, e.g. moisture content greater than field capacity, is known to have a negative effect on soil respiration (Ghezzehei et al., 2019; Manzoni et al., 2012). Note that average  $\text{CO}_2$  emission was generally higher in deficit plots compared to fully irrigated plots (data not shown).

#### 4.4.6 Offset between Agroecological based Soil Management vs Crop Productivity

Figure 4.7 presents the main findings from our column experiment, divided into three major sections as influenced by soil organic treatments: 1) soil hydrological properties, 2)

soil nutrient retention and greenhouse gas emissions, and 3) crop productivity. As illustrated, all sections are interconnected so changes in one section, either negatively or positively, yield responses from the other two. For instance the increase in soil  $\text{NO}_3^-$ -N and  $\text{NH}_4^+$ -N retention from co-composts treatments (Figure 4.4a, 4.4c) was triggered by higher moisture retention (Figure 4.3), however crop yield was only sustained and not enhanced. Here soil hydrological properties here were not only affected by organic treatments but also by irrigation inputs. It is possible that yield was not affected by soil treatments because available nutrients were leached below the active rootzone with irrigation (Gao et al., 2020). The nutrients that were retained may be bound to the organic materials making it not available for plant uptake (Yao et al., 2012). This could explain why we observed higher soil  $\text{NO}_3^-$ -N with depth (Figure 4.4b) and leachate  $\text{NO}_3^-$ -N concentration (Figure 4.5a) in the deficit plots while yield across soil treatments was not impacted.

The response of plants to soil organic amendments and irrigation strategies further complicates the system. For instance, no difference in tomato biomass was detected across soil treatments and irrigation regimes (Table S4.1), yet fruit yield was significantly impacted in the deficit rate (Figure 4.1a). Likewise, tomato canopy was similar in size throughout the season for all plots (Table S4.3), but leaf chlorophyll content in WSB and ASB were constantly higher than ACB, Compost, and Control (Table S4.4) across irrigation schemes. In particular, the higher leaf chlorophyll content in WSB co-compost may be an indicator of greater nutrient uptake, as revealed in the yield for 100%  $\text{ET}_c$ . These observations demonstrate plant natural resiliency to adverse conditions but do convey a yield tradeoff (Dutta et al., 2020; Husen, 2021). Here the positive effects from organic treatments as reflected in higher leaf chlorophyll content and greater soil nutrient retention may be overshadowed by plant physiological response to water stress. Across soil organic treatments, manure compost under deficit rate underperforms in both yield and WUE compared to co-compost treatments.

Ultimately, by adding organic amendment to agricultural soil our goal is to increase crop yield by improving moisture and nutrient uptake (Lehmann & Kleber, 2015). But nutrient retention from organic amendment is less effective under common irrigation practices (Gao et al., 2020). In a 3 year field study, Gao et al. (2020) observed highest N leaching in biochar treated plots subjected to high irrigation frequency. Yet we also risk stressing the plant and reducing yield potential if we lower the amount of water applied (Medyouni et al., 2021). This shows the intricate nature when trying to couple crop production with ecological management. Moreover, handling such tasks requires a personnel (e.g. farmer or farm manager) to have extensive knowledge in soil, crop, irrigation, and environmental science. This may be a reason why such practices have not been adopted by farmers (Swinton et al., 2015). Similar to the 4R Nutrient Stewardship (Johnston & Bruulsema, 2014) there may be a need to develop best management practices guidelines for soil organic amendments.

## 4.5 Conclusion

Overall, we observed positive effects of adding organic amendment such as biochar manure co-compost to soil. We observed greater nutrient retention and crop water use efficiency, but yield response varied and is constrained by irrigation strategies. Our results also show that using biochar manure co-composts as a soil organic amendment has greater potential to positively affect soil ecosystem services, as compared to using organic amendment such as compost alone. Most critically, the transferability of excess

wastes from the agriculture sector into a product with potential to sustain crop productivity, lessen ecological concerns, and alleviate climate change may open a holistic route toward sustainable food production.

## 4.6 Reference

- Abideen, Z., Koyro, H.W., Huchzermeyer, B., Bilquees, G.U.L. and Khan, M.A. (2020). Impact of a biochar or a biochar-compost mixture on water relation, nutrient uptake and photosynthesis of *Phragmites karka*. *Pedosphere*, 30(4), 466-477. [https://doi.org/10.1016/S1002-0160\(17\)60362-X](https://doi.org/10.1016/S1002-0160(17)60362-X)
- Agegnehu, G., Srivastava, A.K. and Bird, M.I. (2017). The role of biochar and biochar-compost in improving soil quality and crop performance: A review. *Applied Soil Ecology*, 119, 156-170. <https://doi.org/10.1016/j.apsoil.2017.06.008>
- Anderson, C.R., Condrón, L.M., Clough, T.J., Fiers, M., Stewart, A., Hill, R.A. and Sherlock, R.R. (2011). Biochar induced soil microbial community change: implications for biogeochemical cycling of carbon, nitrogen and phosphorus. *Pedobiologia*, 54(5-6), 309-320. <https://doi.org/10.1016/j.pedobi.2011.07.005>
- Baiamonte, G., Crescimanno, G., Parrino, F. and De Pasquale, C. (2019). Effect of biochar on the physical and structural properties of a sandy soil. *Catena*, 175, 294-303. <https://doi.org/10.1016/j.catena.2018.12.019>
- Bashir, A., Rizwan, M., ur Rehman, M.Z., Zubair, M., Riaz, M., Qayyum, M.F., Alharby, H.F., Bamagoos, A.A. and Ali, S. (2020). Application of co-composted farm manure and biochar increased the wheat growth and decreased cadmium accumulation in plants under different water regimes. *Chemosphere*, 246, 125809. <https://doi.org/10.1016/j.chemosphere.2019.125809>
- Bohara, H., Dodla, S., Wang, J.J., Darapuneni, M., Acharya, B.S., Magdi, S. and Pavuluri, K. (2019). Influence of poultry litter and biochar on soil water dynamics and nutrient leaching from a very fine sandy loam soil. *Soil and Tillage Research*, 189, 44-51. <https://doi.org/10.1016/j.still.2019.01.001>
- Chen, K., Peng, J., Li, J., Yang, Q., Zhan, X., Liu, N. and Han, X. (2020). Stabilization of soil aggregate and organic matter under the application of three organic resources and biochar-based compound fertilizer. *Journal of Soils and Sediments*, 1-11. <https://doi.org/10.1007/s11368-020-02693-1>
- Cooper, J., Greenberg, I., Ludwig, B., Hippich, L., Fischer, D., Glaser, B. and Kaiser, M. (2020). Effect of biochar and compost on soil properties and organic matter in aggregate size fractions under field conditions. *Agriculture, Ecosystems & Environment*, 295, 106882. <https://doi.org/10.1016/j.agee.2020.106882>
- Crippa, M., Solazzo, E., Guizzardi, D., Monforti-Ferrario, F., Tubiello, F. N., & Leip, A. (2021). Food systems are responsible for a third of global anthropogenic GHG emissions. *Nature Food*, 2(3), 198–209. <https://doi.org/10.1038/s43016-021-00225-9>

- Cui, J., Shao, G., Lu, J., Keabetswe, L. and Hoogenboom, G. (2019). Yield, quality and drought sensitivity of tomato to water deficit during different growth stages. *Scientia agricola*, 77. <https://doi.org/10.1590/1678-992X-2018-0390>
- Di, H.J. & Cameron, K.C. (2002). Nitrate leaching in temperate agroecosystems: sources, factors and mitigating strategies. *Nutrient Cycling in Agroecosystems*, 64, 237-256. <https://doi.org/10.1023/A:1021471531188>
- Dutta, P., Chakraborti, S., Chaudhuri, K.M. and Mondal, S. (2020). Physiological responses and resilience of plants to climate change. *New Frontiers in Stress Management for Durable Agriculture*, 3-20. DOI: 10.1007/978-981-15-1322-0\_1
- Gao, S., Harrison, B.P., Thao, T., Gonzales, M.L., An, D., Ghezzehei, T.A., Diaz, G. and Ryals, R.A. (2023). Biochar co-compost improves nitrogen retention and reduces carbon emissions in a winter wheat cropping system. *Global Change Biology, Bioenergy*. <https://doi.org/10.1111/gcbb.13028>
- Gao, S., Wang, D., Dangi, S.R., Duan, Y., Pflaum, T., Gartung, J., Qin, R. and Turini, T. (2020). Nitrogen dynamics affected by biochar and irrigation level in an onion field. *Science of The Total Environment*, 714, 136432. <https://doi.org/10.1016/j.scitotenv.2019.136432>
- Ghezzehei, T.A., Sulman, B., Arnold, C.L., Bogie, N.A. and Berhe, A.A. (2019). On the role of soil water retention characteristic on aerobic microbial respiration. *Biogeosciences*, 16(6). doi:10.5194/bg-16-1187-2019.
- Ghosh, M., Swain, D.K., Jha, M.K., Tewari, V.K. and Bohra, A. (2020). Optimizing chlorophyll meter (SPAD) reading to allow efficient nitrogen use in rice and wheat under rice-wheat cropping system in eastern India. *Plant Production Science*, 23(3), 270-285. <https://doi.org/10.1080/1343943X.2020.1717970>
- Hanson, B. & May, D. (2006). New crop coefficients developed for high-yield processing tomatoes. *California Agriculture*, 60(2), 95-99. <https://doi.org/10.3733/ca.v060n02p95>
- Harrison, B.P., Gao, S., Gonzales, M., Thao, T., Bischak, E., Ghezzehei, T.A., Berhe, A.A., Diaz, G. and Ryals, R.A. (2022). Dairy Manure Co-composting with Wood Biochar Plays a Critical Role in Meeting Global Methane Goals. *Environmental Science & Technology*, 56(15), 10987-10996. <https://doi.org/10.1021/acs.est.2c03467>
- Harter, T., Davis, H., Mathews, M.C., Meyer, R.D. (2002) Shallow groundwater quality on dairy farms with irrigated forage crops. *Journal of Contaminant Hydrology*, 55(3), 287-315 [https://doi.org/10.1016/S0169-7722\(01\)00189-9](https://doi.org/10.1016/S0169-7722(01)00189-9)
- Husen, A. (2021). The Harsh environment and resilient plants: an overview. *Harsh Environment and Plant Resilience: Molecular and Functional Aspects*, pp.1-23. DOI: 10.1007/978-3-030-65912-7\_1

- Hutchinson, G. L., & Mosier, A. R. (1981). Improved soil cover method for Field measurement of nitrous oxide fluxes. *Soil Science Society of America Journal*, 45(2), 311–316. <https://doi.org/10.2136/sssaj1981.03615995004500020017x>
- Johnston, A.M. & Bruulsema, T.W. (2014). 4R nutrient stewardship for improved nutrient use efficiency. *Procedia Engineering*, 83, 365-370. <https://doi.org/10.1016/j.proeng.2014.09.029>
- Knowles, O.A., Robinson, B.H., Contangelo, A. and Clucas, L. (2011). Biochar for the mitigation of nitrate leaching from soil amended with biosolids. *Science of the total Environment*, 409(17), 3206-3210. <https://doi.org/10.1016/j.scitotenv.2011.05.011>
- Kuo, Y.L., Lee, C.H. and Jien, S.H. (2020). Reduction of Nutrient Leaching Potential in Coarse-Textured Soil by Using Biochar. *Water*, 12(7), 2012. <https://doi.org/10.3390/w12072012>
- Lehmann, J. & Kleber, M. (2015). The contentious nature of soil organic matter. *Nature*, 528(7580), 60-68. doi:10.1038/nature16069
- Longbottom, T., Wahab, L., Min, K., Jurusik, A., Moreland, K., Dolui, M., Thao, T., Gonzales, M., Perez Rojas, Y. and Alvarez, J. (2022). What's Soil Got to Do with Climate Change. *GSA Today*, 32, 4-10. <https://doi.org/10.1130/GSATG519A.1>
- Manzoni, S., Schimel, J.P. and Porporato, A. (2012). Responses of soil microbial communities to water stress: results from a meta-analysis. *Ecology*, 93(4), 930-938. <https://doi.org/10.1890/11-0026.1>
- Medyouni, I., Zouaoui, R., Rubio, E., Serino, S., Ahmed, H.B. and Bertin, N. (2021). Effects of water deficit on leaves and fruit quality during the development period in tomato plant. *Food Science & Nutrition*, 9(4), 1949-1960. <https://doi.org/10.1002/fsn3.2160>
- Mulvaney, R.L. (1996). Nitrogen—inorganic forms. *Methods of soil analysis: Part 3 Chemical Methods*, 5, 1123-1184. <https://doi.org/10.2136/sssabookser5.3.c38>
- Nordahl, S.L., Preble, C.V., Kirchstetter, T.W. and Scown, C.D. (2023). Greenhouse Gas and Air Pollutant Emissions from Composting. *Environmental Science & Technology*. <https://doi.org/10.1021/acs.est.2c05846>
- Obadi, A., AlHarbi, A., Abdel-Razzak, H. and Al-Omran, A. (2020). Biochar and compost as soil amendments: effect on sweet pepper (*Capsicum annuum* L.) growth under partial root zone drying irrigation. *Arabian Journal of Geosciences*, 13(13), 1-12. <https://doi.org/10.1007/s12517-020-05529-x>
- Patanè, C. & Cosentino, S.L. (2010). Effects of soil water deficit on yield and quality of processing tomato under a Mediterranean climate. *Agricultural Water Management*, 97(1), 131-138. <https://doi.org/10.1016/j.agwat.2009.08.021>
- Patrignani, A. & Ochsner, T.E. (2015). Canopeo: A powerful new tool for measuring fractional green canopy cover. *Agronomy Journal*, 107(6), 2312-2320. <https://doi.org/10.2134/agronj15.0150>

- R Core Team. (2020). R: A language and environment for statistical computing. R Foundation for Statistical Computing. [www.R-project.org](http://www.R-project.org)
- Sánchez, A., Artola, A., Font, X., Gea, T., Barrena, R., Gabriel, D., Sánchez-Monedero, M.Á., Roig, A., Cayuela, M.L. and Mondini, C. (2015). Greenhouse gas emissions from organic waste composting. *Environmental Chemistry Letters*, 13, 223-238. <https://doi.org/10.1007/s10311-015-0507-5>
- Sanchez-Monedero, M.A., Cayuela, M.L., Roig, A., Jindo, K., Mondini, C. and Bolan, N. (2018). Role of biochar as an additive in organic waste composting. *Bioresource Technology*, 247, 1155-1164. <https://doi.org/10.1016/j.biortech.2017.09.193>
- Shin, J., Choi, E., Jang, E., Hong, S.G., Lee, S. and Ravindran, B. (2018). Adsorption characteristics of ammonium nitrogen and plant responses to biochar pellet. *Sustainability*, 10(5), 1331. <https://doi.org/10.3390/su10051331>
- Suplito, M.R., David, F.B. and Olalia, L.C. (2020). Relationship of vegetation indices and SPAD meter readings with sugarcane leaf nitrogen under Pampanga Mill District, Philippines condition. In *IOP Conference Series: Earth and Environmental Science* (Vol. 540, No. 1, 012016). IOP Publishing. DOI 10.1088/1755-1315/540/1/012016
- Swinton, S.M., Rector, N., Robertson, G.P., Jolejole-Foreman, C.B. and Lupi, F. (2015). Farmer decisions about adopting environmentally beneficial practices. *The Ecology of Agricultural Landscapes: Long-term Research on the Path to Sustainability*, 340-359.
- Teodoro, M., Trakal, L., Gallagher, B.N., Šimek, P., Soudek, P., Pohořelý, M., Beesley, L., Jačka, L., Kovář, M., Seyedsadr, S. and Mohan, D. (2020). Application of co-composted biochar significantly improved plant-growth relevant physical/chemical properties of a metal contaminated soil. *Chemosphere*, 242, 125255. <https://doi.org/10.1016/j.chemosphere.2019.125255>
- Tuller, M. & Or, D. (2005). Water films and scaling of soil characteristic curves at low water contents. *Water Resources Research*, 41(9). <https://doi.org/10.1029/2005WR004142>
- Tully, K. & Ryals, R. (2017). Nutrient cycling in agroecosystems: Balancing food and environmental objectives. *Agroecology and Sustainable Food Systems*, 41(7), 761-798. <https://doi.org/10.1080/21683565.2017.1336149>
- USDA-National Agricultural Statistics Service. (2020). State agriculture overview for California. [https://www.nass.usda.gov/Quick\\_Stats/Ag\\_Overview/stateOverview.php?state=CALIFORNIA](https://www.nass.usda.gov/Quick_Stats/Ag_Overview/stateOverview.php?state=CALIFORNIA) (accessed February 1, 2023).
- Wang, Y., Villamil, M.B., Davidson, P.C. and Akdeniz, N. (2019). A quantitative understanding of the role of co-composted biochar in plant growth using meta-analysis. *Science of the Total Environment*, 685, 741-752. <https://doi.org/10.1016/j.scitotenv.2019.06.244>

- Wu, W. & Ma, B. (2015). Integrated nutrient management (INM) for sustaining crop productivity and reducing environmental impact: A review. *Science of the Total Environment*, 512, 415-427. <https://doi.org/10.1016/j.scitotenv.2014.12.101>
- Xiao, R., Awasthi, M.K., Li, R., Park, J., Pensky, S.M., Wang, Q., Wang, J.J. and Zhang, Z. (2017). Recent developments in biochar utilization as an additive in organic solid waste composting: A review. *Bioresource Technology*, 246, 203-213. <https://doi.org/10.1016/j.biortech.2017.07.090>
- Xiong, D., Chen, J., Yu, T., Gao, W., Ling, X., Li, Y., Peng, S. and Huang, J. (2015). SPAD-based leaf nitrogen estimation is impacted by environmental factors and crop leaf characteristics. *Scientific Reports*, 5(1), 13389. <https://doi.org/10.1038/srep13389>
- Yao, Y., Gao, B., Zhang, M., Inyang, M. and Zimmerman, A.R. (2012). Effect of biochar amendment on sorption and leaching of nitrate, ammonium, and phosphate in a sandy soil. *Chemosphere*, 89(11), 1467-1471. <https://doi.org/10.1016/j.chemosphere.2012.06.002>
- Yin, Y., Yang, C., Li, M., Zheng, Y., Ge, C., Gu, J., Li, H., Duan, M., Wang, X. and Chen, R. (2021). Research progress and prospects for using biochar to mitigate greenhouse gas emissions during composting: a review. *Science of The Total Environment*, 798, 149294. <https://doi.org/10.1016/j.scitotenv.2021.149294>
- Zheng, H., Wang, Z., Deng, X., Herbert, S. and Xing, B. (2013). Impacts of adding biochar on nitrogen retention and bioavailability in agricultural soil. *Geoderma*, 206, 32-39. <https://doi.org/10.1016/j.geoderma.2013.04.018>

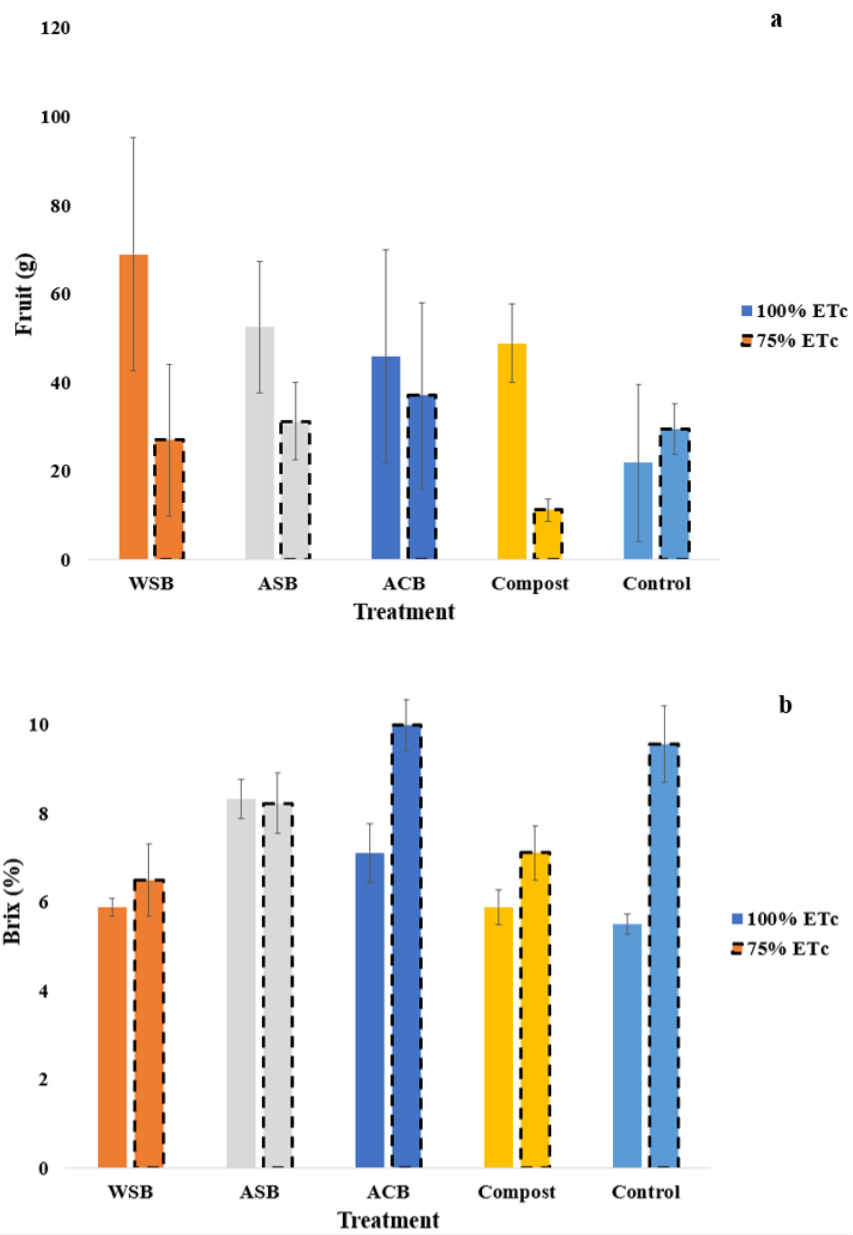


Figure 4-1 Tomato fruit yield (a) and sugar content (b). Mean of three replications with standard error bar.

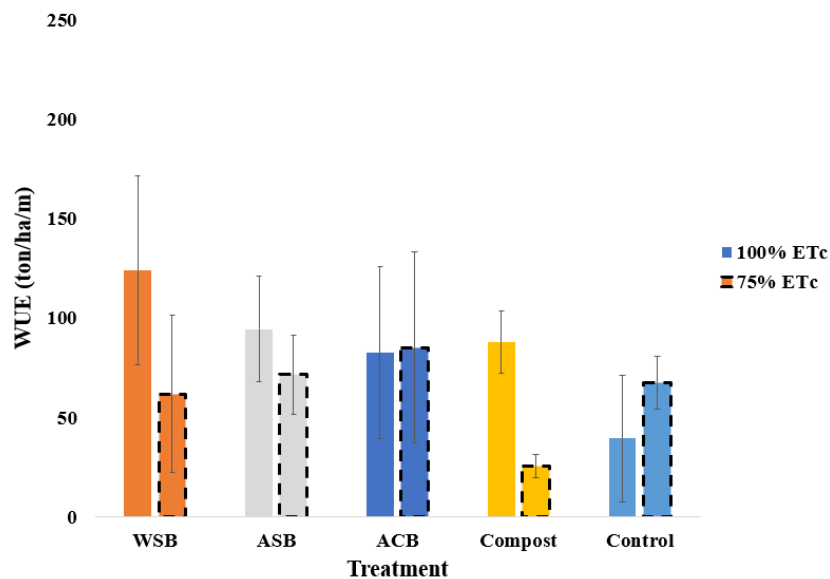


Figure 4-2 Tomato water use efficiency (WUE). Unit is expressed as ton/hectare/m. Mean of three replications with standard error bar

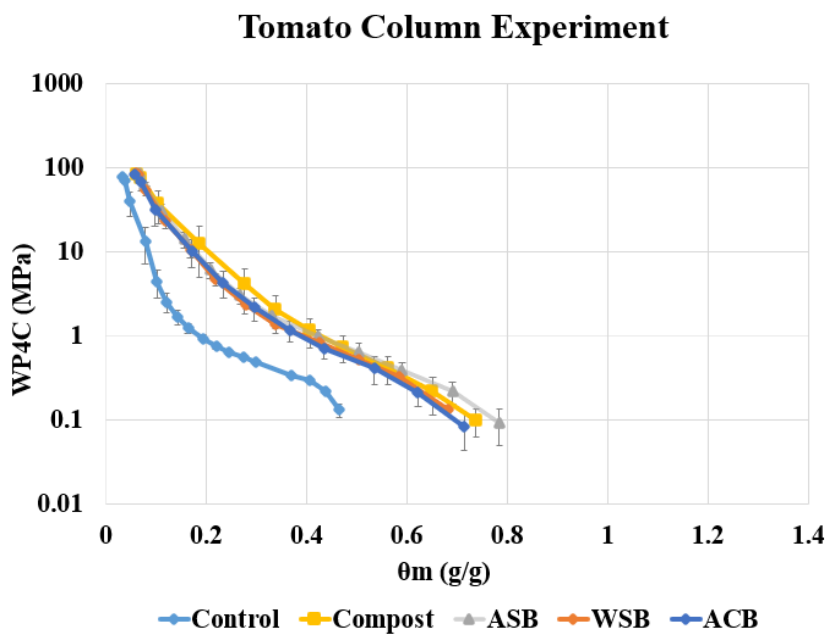


Figure 4-3 Moisture retention curves for soil treatments in the tomato column, where x-axis is gravimetric water content and y-axis is suction potential. Mean of three replications with standard error bar.

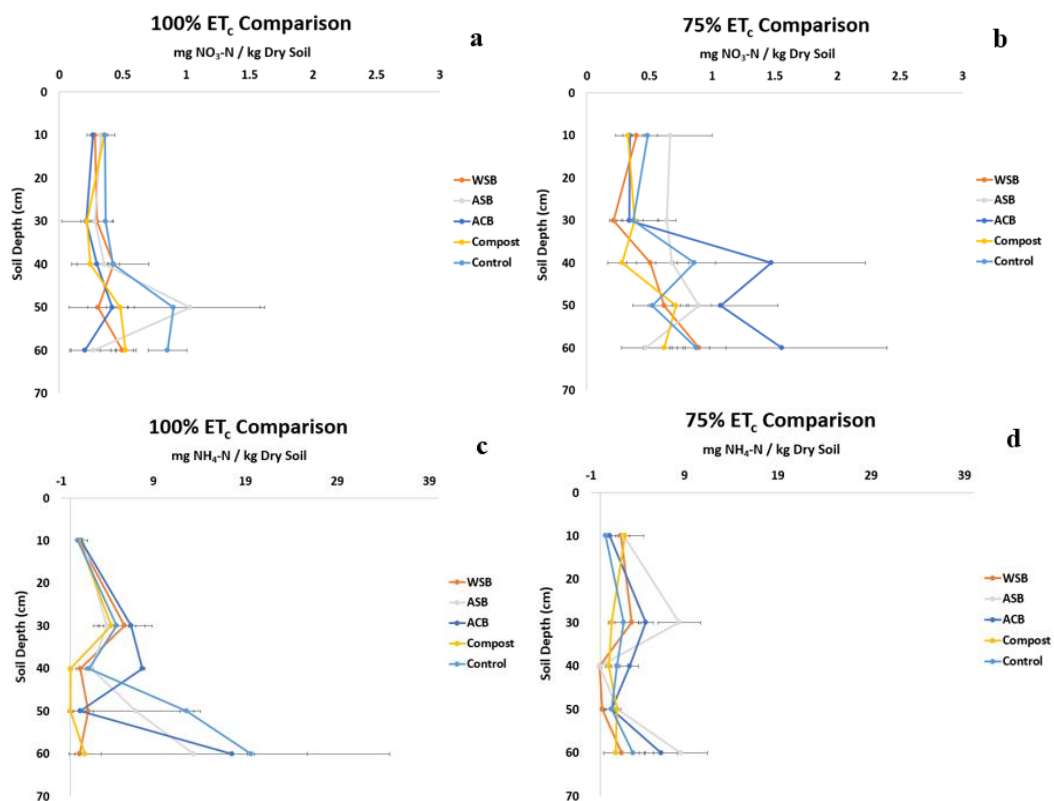


Figure 4-4 Post flushed soil  $\text{NO}_3^-$ -N and  $\text{NH}_4^+$ -N with depth for 100%  $\text{ET}_c$  (a, c) and 75%  $\text{ET}_c$  (b, d). Mean of three replications with standard error bar.

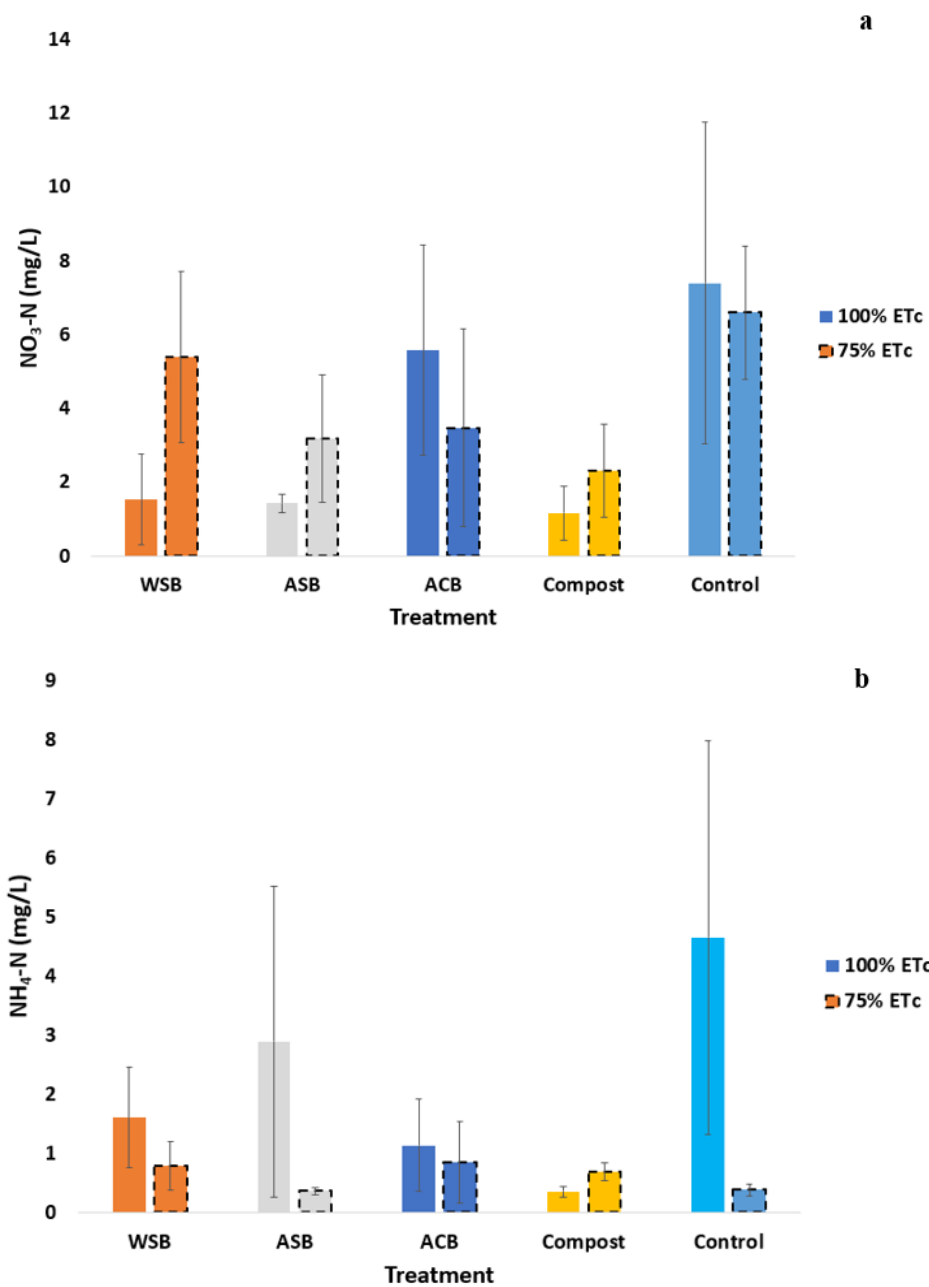


Figure 4-5 NO<sub>3</sub><sup>-</sup>-N (a) and NH<sub>4</sub><sup>+</sup>-N (b) concentration in leachate collected at the end of tomato study. Mean of three replications with standard error bar.

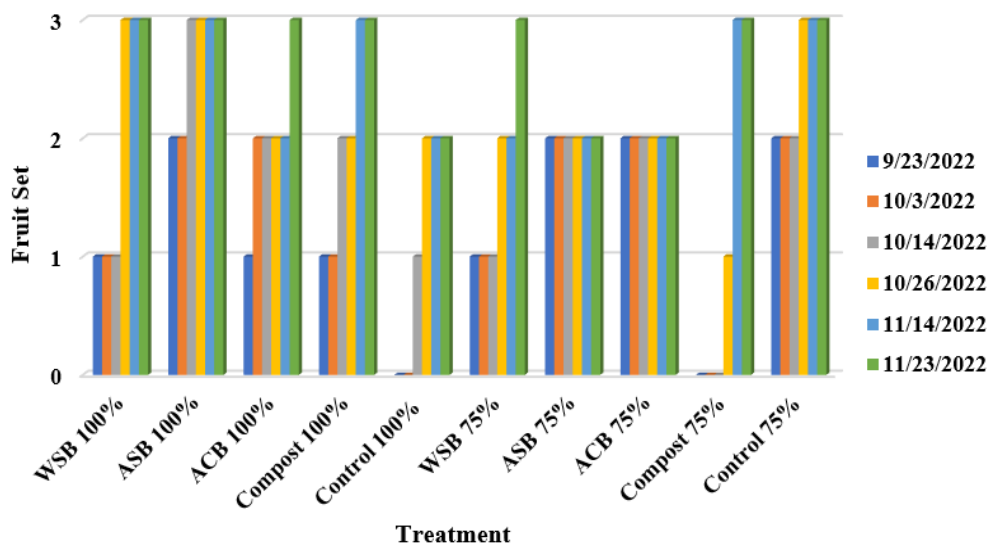


Figure 4-6 Fruit-set count taken throughout the season, x-axis is soil organic treatments and y-axis is replications.

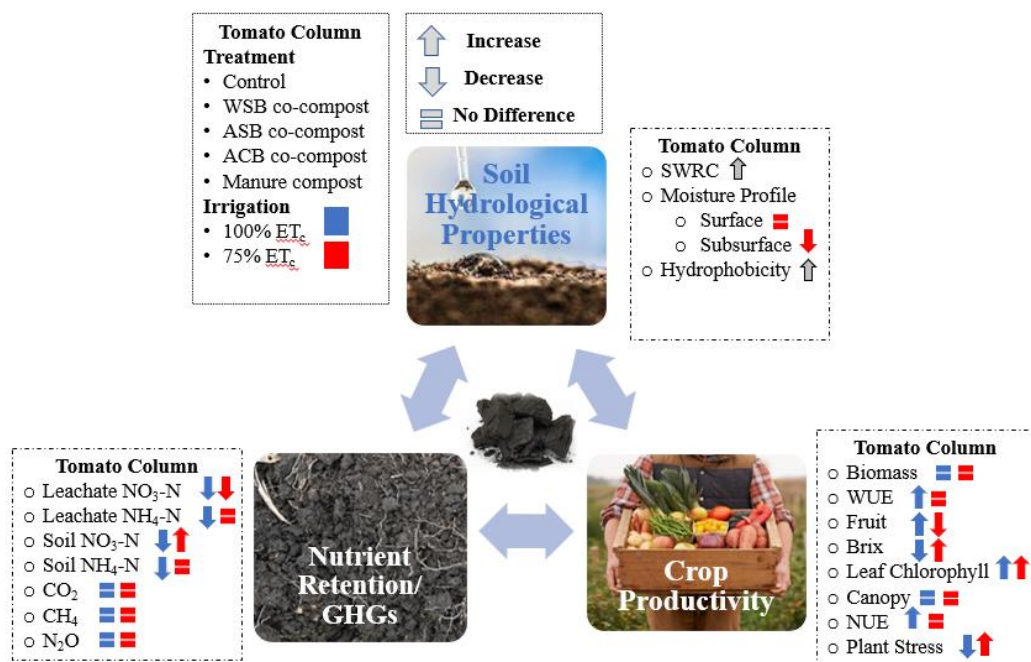


Figure 4-7 Summary of tomato column experiment. An increase, decrease, or equal is in response to soil organic amendments.

Table 4-1 Mean greenhouse gas emissions (n = 3), measured with Picarro Gas Analyzer. Data analyzed using a two-way ANOVA, followed by Tukey-HSD test given statistical significance detected. Value with letters indicate statistically significant ( $p < 0.10$ ) among soil treatments, whereas value with the \* asterisk indicates statistical significance across irrigation level.

Preplant	WSA	ASB	ACB	Compost	Control
CO <sub>2</sub> (mg CO <sub>2</sub> m <sup>-2</sup> s <sup>-1</sup> )	16.95 <b>a</b>	13.47 <b>ab</b>	11.71 <b>ab</b>	12.67 <b>ab</b>	7.24 <b>b</b>
CH <sub>4</sub> (ng CH <sub>4</sub> m <sup>-2</sup> s <sup>-1</sup> )	24.46	19.79	112.6	85.51	15.84
N <sub>2</sub> O (ng N <sub>2</sub> O m <sup>-2</sup> s <sup>-1</sup> )	897.9	888.3	922.1	615.5	526.2
<b>1<sup>st</sup> Fertilization</b>					
CO <sub>2</sub> -100% ET <sub>c</sub> (mg CO <sub>2</sub> m <sup>-2</sup> s <sup>-1</sup> )	30.41	26.55	24.38	29.69	31.62
CH <sub>4</sub> -100% ET <sub>c</sub> (ng CH <sub>4</sub> m <sup>-2</sup> s <sup>-1</sup> )	131.9	422.3	395.9	-642.2	228.7
N <sub>2</sub> O-100% ET <sub>c</sub> (ng N <sub>2</sub> O m <sup>-2</sup> s <sup>-1</sup> )	13517	2655	7724	17138	4827
CO <sub>2</sub> -75% ET <sub>c</sub> (mg CO <sub>2</sub> m <sup>-2</sup> s <sup>-1</sup> )	32.59	36.69 *	35.48 *	35.97 *	33.79
CH <sub>4</sub> -75% ET <sub>c</sub> (ng CH <sub>4</sub> m <sup>-2</sup> s <sup>-1</sup> )	167.2	184.8	281.5	281.5	369.5
N <sub>2</sub> O-75% ET <sub>c</sub> (ng N <sub>2</sub> O m <sup>-2</sup> s <sup>-1</sup> )	4586	3621	5069	2896	-241.4
<b>2<sup>nd</sup> Fertilization</b>					
CO <sub>2</sub> -100% ET <sub>c</sub> (mg CO <sub>2</sub> m <sup>-2</sup> s <sup>-1</sup> )	14.92	22.86	18.39	11.01	21.72
CH <sub>4</sub> -100% ET <sub>c</sub> (ng CH <sub>4</sub> m <sup>-2</sup> s <sup>-1</sup> )	0.00	51.91	193.55	52.79	105.57
N <sub>2</sub> O-100% ET <sub>c</sub> (ng N <sub>2</sub> O m <sup>-2</sup> s <sup>-1</sup> )	-1521	2341	-1279	3621	-555.2
CO <sub>2</sub> -75% ET <sub>c</sub> (mg CO <sub>2</sub> m <sup>-2</sup> s <sup>-1</sup> )	16.03	14.43	17.67	15.11	19.36
CH <sub>4</sub> -75% ET <sub>c</sub> (ng CH <sub>4</sub> m <sup>-2</sup> s <sup>-1</sup> )	-20.23	193.6	131.9	140.8	-5.890
N <sub>2</sub> O-75% ET <sub>c</sub> (ng N <sub>2</sub> O m <sup>-2</sup> s <sup>-1</sup> )	482.8	796.6	1448	965.5	4104
<b>3<sup>rd</sup> Fertilization</b>					
CO <sub>2</sub> -100% ET <sub>c</sub> (mg CO <sub>2</sub> m <sup>-2</sup> s <sup>-1</sup> )	23.03	25.56	23.51	11.97	35.77
CH <sub>4</sub> -100% ET <sub>c</sub> (ng CH <sub>4</sub> m <sup>-2</sup> s <sup>-1</sup> )	-167.2	67.74	-404.7	87.98	58.94
N <sub>2</sub> O-100% ET <sub>c</sub> (ng N <sub>2</sub> O m <sup>-2</sup> s <sup>-1</sup> )	-161.7 <b>bcd</b>	313.8 <b>bc</b>	2655 <b>ab</b>	362.1 <b>bc</b>	1859 <b>ab</b>
CO <sub>2</sub> -75% ET <sub>c</sub> (mg CO <sub>2</sub> m <sup>-2</sup> s <sup>-1</sup> )	31.62	22.30	30.15	30.34	31.89
CH <sub>4</sub> -75% ET <sub>c</sub> (ng CH <sub>4</sub> m <sup>-2</sup> s <sup>-1</sup> )	343.1	-281.5	87.98	-290.3	219.9
N <sub>2</sub> O-75% ET <sub>c</sub> (ng N <sub>2</sub> O m <sup>-2</sup> s <sup>-1</sup> )	-2897 <b>d</b>	-941.4 <b>bc</b>	3621 <b>a</b>	-1859 <b>c</b>	-627.6 <b>bc</b>
<b>Post-harvest</b>					
CO <sub>2</sub> -100% ET <sub>c</sub> (mg CO <sub>2</sub> m <sup>-2</sup> s <sup>-1</sup> )	1.230	1.470	0.600	1.690	1.570
CH <sub>4</sub> -100% ET <sub>c</sub> (ng CH <sub>4</sub> m <sup>-2</sup> s <sup>-1</sup> )	-11.44	7.650	-64.22	52.79	11.44
N <sub>2</sub> O-100% ET <sub>c</sub> (ng N <sub>2</sub> O m <sup>-2</sup> s <sup>-1</sup> )	161.7	1448	79.66	-917.3	482.8
CO <sub>2</sub> -75% ET <sub>c</sub> (mg CO <sub>2</sub> m <sup>-2</sup> s <sup>-1</sup> )	1.09-	1.450	1.300	1.010	1.330
CH <sub>4</sub> -75% ET <sub>c</sub> (ng CH <sub>4</sub> m <sup>-2</sup> s <sup>-1</sup> )	19.35	87.98	64.22	11.44	32.55
N <sub>2</sub> O-75% ET <sub>c</sub> (ng N <sub>2</sub> O m <sup>-2</sup> s <sup>-1</sup> )	482.8	-7483	-1159	1279	989.7

\*Preplant CO<sub>2</sub> Treatment  $p = 0.095$

\*1<sup>st</sup> Fertilization CO<sub>2</sub> 75% ET<sub>c</sub> Irrigation  $p = 0.0271$

\*3<sup>rd</sup> Fertilization N<sub>2</sub>O ET<sub>c</sub> Treatment  $p = 0.03$

Table 4-2 Relationship between yield vs mean chlorophyll content and fractional green canopy.

Variables	Slope	Intercept	R <sup>2</sup>	p-value	Significance	Std Error
Biomass vs SPAD	3.677	- 160.9	0.288	0.0022	***	1.094
Biomass vs F <sub>c</sub>	2.542	- 0.970	0.594	6.2E-07	****	0.397
Fruit vs SPAD	0.363	+ 21.56	0.002	0.8141	ns	1.530
Fruit vs F <sub>c</sub>	0.242	+ 37.50	0.004	0.7439	ns	0.735
Brix vs SPAD	0.297	- 9.110	0.220	0.0088	***	0.105
Brix vs F <sub>c</sub>	-0.029	+ 7.916	0.008	0.6196	ns	0.057

\*Level of significance: \*  $p < 0.1$ , \*\*  $p < 0.05$ , \*\*\*  $p < 0.01$ , \*\*\*\*  $p < 0.001$ , ns indicates  $p > 0.1$

## **Chapter 5.**

### **Conclusion**

Using a variety of research approaches, e.g. laboratory measurement, numerical modeling, lab incubation experiments, and outdoor soil column study, we investigated the ecological and agronomic effects of different biochar and also biochar dairy manure co-composts, derived from local wasted organic materials, on soil ecosystem services. In Chapter 2, findings from our study reveal an increase in soil moisture retention with biochar application rates (5% and 10% w/w), particularly noticeable at the wilting point region. Biochar derived from almond shells had the most influence on soil moisture regime and soil respiration. Although specific surface area varies among the tested biochars, with walnut shell biochar yielding the highest SSA. In Chapter 3, our numerical simulation shows that the application of biochar at 5% (w/w) increased soil water availability within the topsoil for a rainfed pasture system, irrespective of biochar amendment type. In contrast, a similar biochar amendment for the irrigated fresh market tomato system did not affect water use efficiency, instead reducing seasonal soil evaporation loss and thereby reducing irrigation demand. In both cropping systems, year-to-year variability in precipitation significantly impacted the total amount of water saved under biochar application with certain amendments retaining more water than others. In Chapter 4, findings from our tomato column study revealed positive effects of adding biochar manure co-composts to soil. We observed greater nitrogen retention and crop water use efficiency, but yield response varied and is constrained by irrigation strategies. Our results further show that using biochar manure co-composts as a soil organic amendment has greater potential to positively affect soil ecosystem services, as compared to compost alone. Overall, results from all three chapters support the notions that converting wasted organic materials into nutrient-rich organic soil amendment can have a positive effect on soil hydrological properties and ecosystem services and may open a holistic route toward sustainable food production.

## Appendices

### Appendix A: Supplemental for Chapter 2

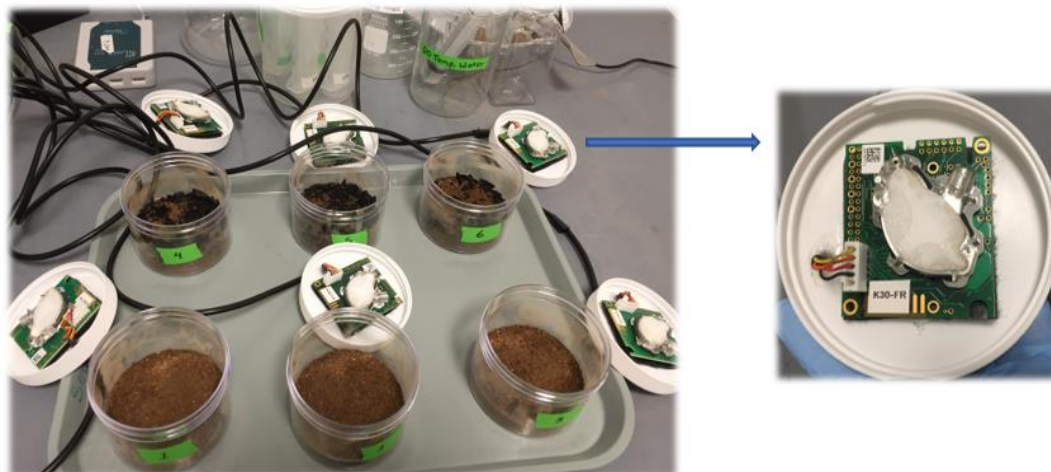


Figure S2.1. Incubation samples and K30 FR 10000 PPM CO<sub>2</sub> sensors.

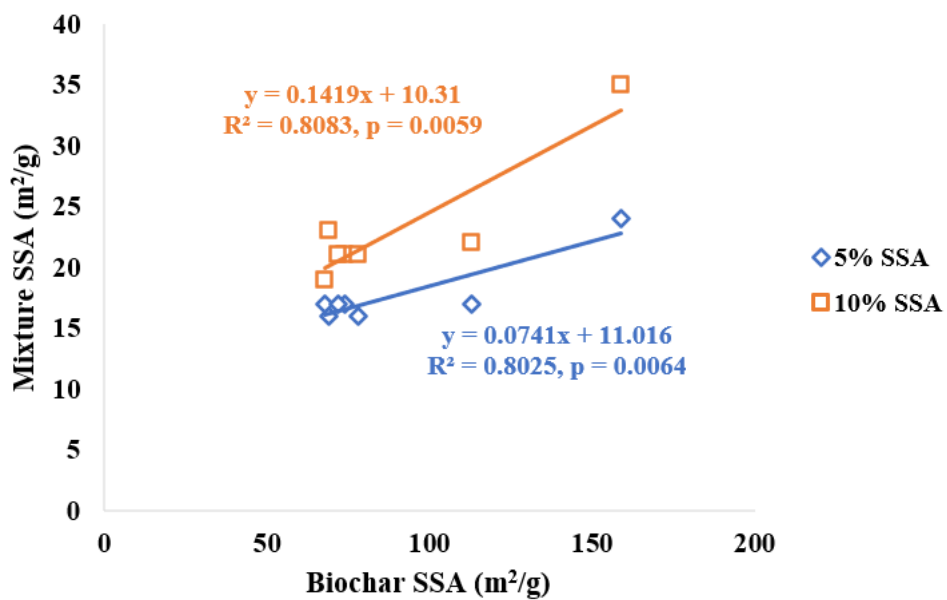


Figure S2.2. Relationships between biochar SSA to biochar mixtures SSA.

## Appendix B: Supplemental for Chapter 3



Figure S3.1

Figure S3.1. 1X-Mobile Pyrolysis Unit used to create biochar at 300-350 C.

Table S3.1. Moisture difference for rainfed Control and AS-2 at the top 20 cm.

Soil Depth (cm)	August 2016 (%)	August 2017 (%)	August 2018 (%)	August 2019 (%)	August 2020 (%)
0	0.01	0.01	0.01	0.01	0.01
1	0.02	0.01	0.01	0.01	0.01
2	0.03	0.01	0.01	0.02	0.02
3	0.04	0.01	0.02	0.02	0.02
4	0.05	0.01	0.02	0.02	0.02
5	0.05	0.01	0.02	0.02	0.02
6	0.06	0.01	0.02	0.02	0.02
7	0.06	0.01	0.02	0.02	0.02
8	0.06	0.01	0.02	0.02	0.02
9	0.06	0.02	0.02	0.02	0.02
10	0.06	0.03	0.02	0.02	0.02
11	0.07	0.04	0.02	0.02	0.02
12	0.07	0.04	0.02	0.02	0.02
13	0.07	0.05	0.02	0.02	0.02
14	0.07	0.05	0.01	0.02	0.02
15	0.07	0.05	0.01	0.02	0.02
16	0.07	0.06	0.01	0.02	0.02
17	0.07	0.06	0.01	0.02	0.02
18	0.07	0.06	0.01	0.02	0.02
19	0.07	0.06	0.01	0.02	0.02
20	0.09	0.07	0.00	0.00	0.00

\* AS-2 - Control = Moisture Difference

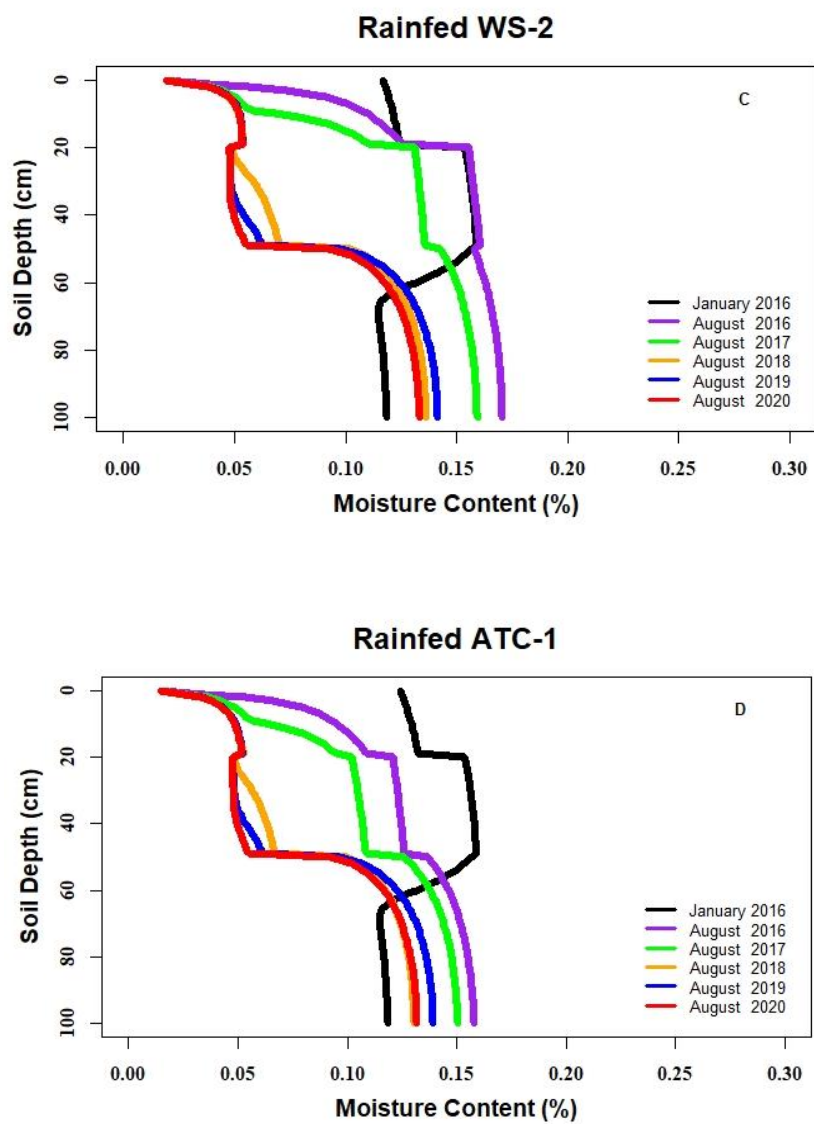


Figure S3.2. Moisture profile over time for rainfed WS-2 (C) and rainfed ATC-1 (D).

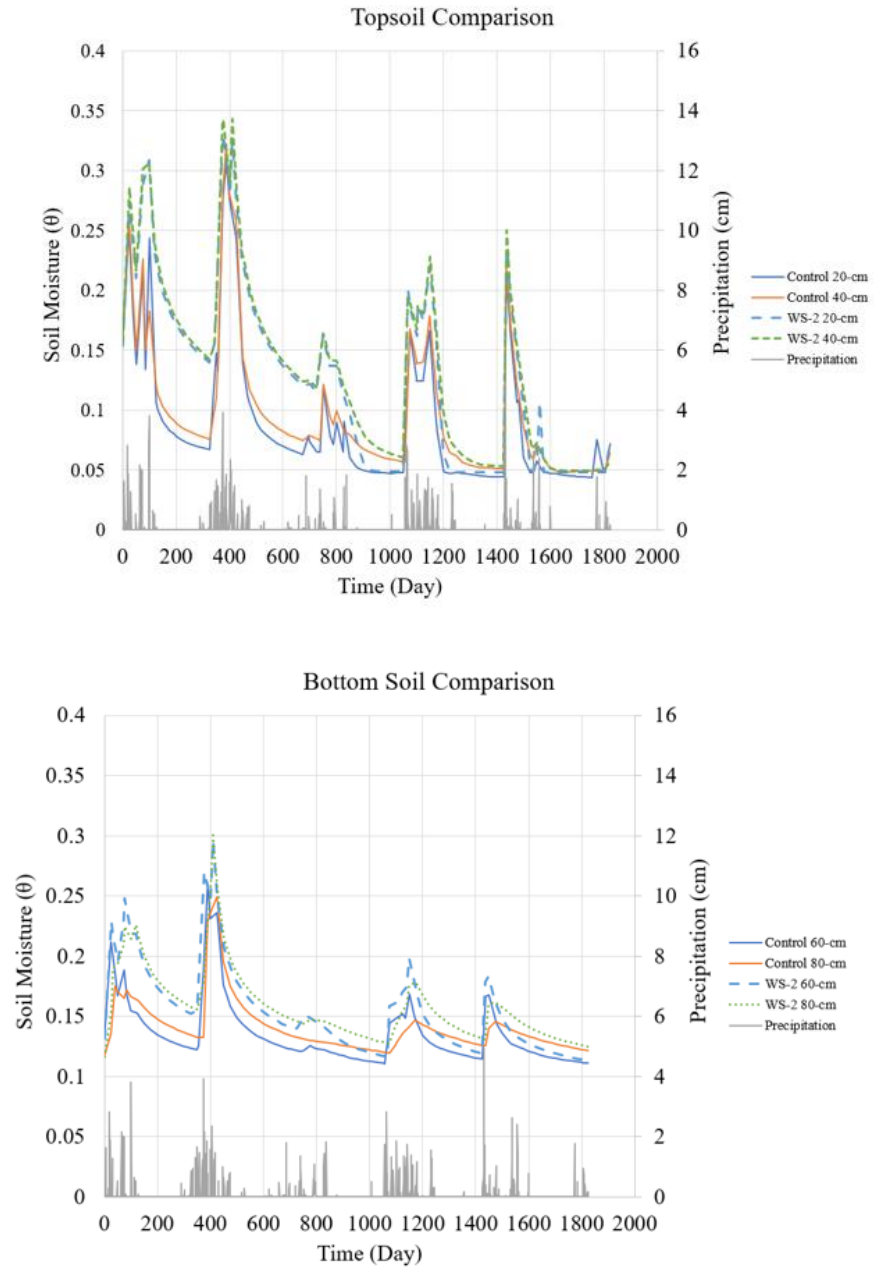


Figure S3.3. Rainfed Control vs WS-2 Topsoil (top) and Bottom soil layer (bottom).

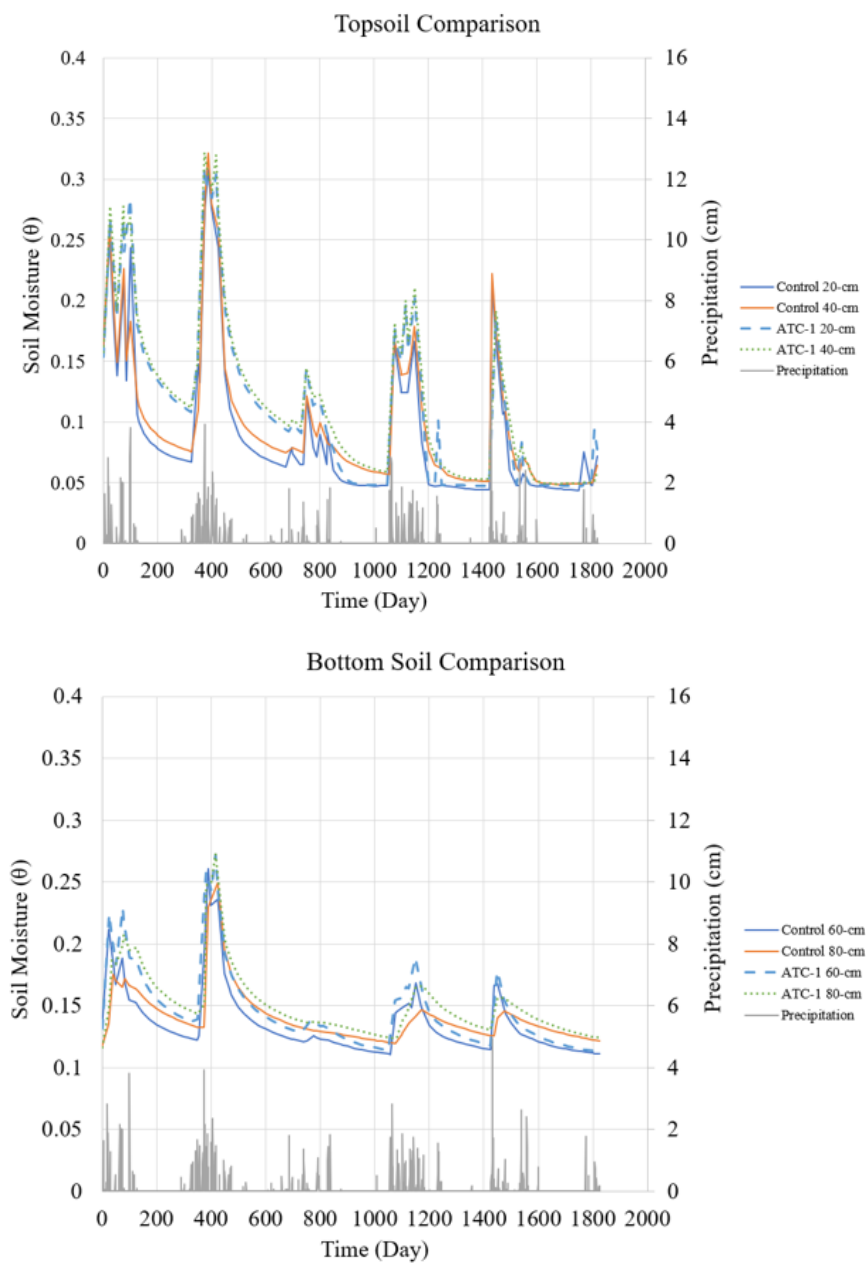


Figure S3.4. Rainfed Control vs ATC-1 Topsoil (top) and Bottom soil layer (bottom).

Table S3.2. Moisture difference for irrigated Control and AS-2 at the top 20 cm.

Soil Depth (cm)	August 2016 (%)	August 2017 (%)	August 2018 (%)	August 2019 (%)	August 2020 (%)
0	-0.1374	-0.1003	-0.1301	-0.3245	-0.1996
1	-0.1212	-0.0936	-0.1107	-0.278	-0.1845
2	-0.1103	-0.0883	-0.0984	-0.226	-0.1737
3	-0.1021	-0.0836	-0.0894	-0.1926	-0.1651
4	-0.0958	-0.08	-0.0826	-0.1723	-0.158
5	-0.0906	-0.0767	-0.077	-0.1581	-0.1523
6	-0.0862	-0.074	-0.0727	-0.1474	-0.1469
7	-0.0824	-0.0717	-0.0687	-0.1386	-0.1425
8	-0.0794	-0.0697	-0.0654	-0.1312	-0.1384
9	-0.0763	-0.0678	-0.0627	-0.1243	-0.1346
10	-0.0738	-0.0662	-0.06	-0.1186	-0.1313
11	-0.0716	-0.0649	-0.0578	-0.1131	-0.1282
12	-0.0696	-0.0639	-0.0558	-0.1084	-0.1252
13	-0.0677	-0.063	-0.0541	-0.1038	-0.1224
14	-0.066	-0.062	-0.0523	-0.0994	-0.1199
15	-0.0647	-0.0611	-0.0508	-0.0955	-0.1177
16	-0.0634	-0.0604	-0.0494	-0.0918	-0.1153
17	-0.0622	-0.0598	-0.0483	-0.0881	-0.113
18	-0.061	-0.0594	-0.0474	-0.0847	-0.111
19	-0.0599	-0.0589	-0.0463	-0.0816	-0.1091
20	0.0006	0.002	0.014	-0.0229	-0.0488

\* AS-2 - Control = Moisture Difference

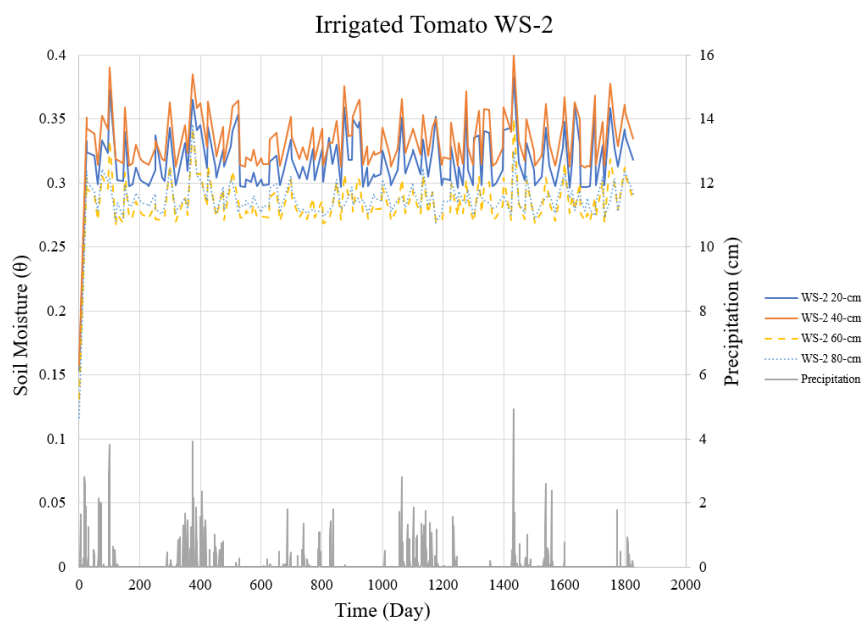


Figure S3.5. Seasonal moisture content for irrigated WS-2 biochar.

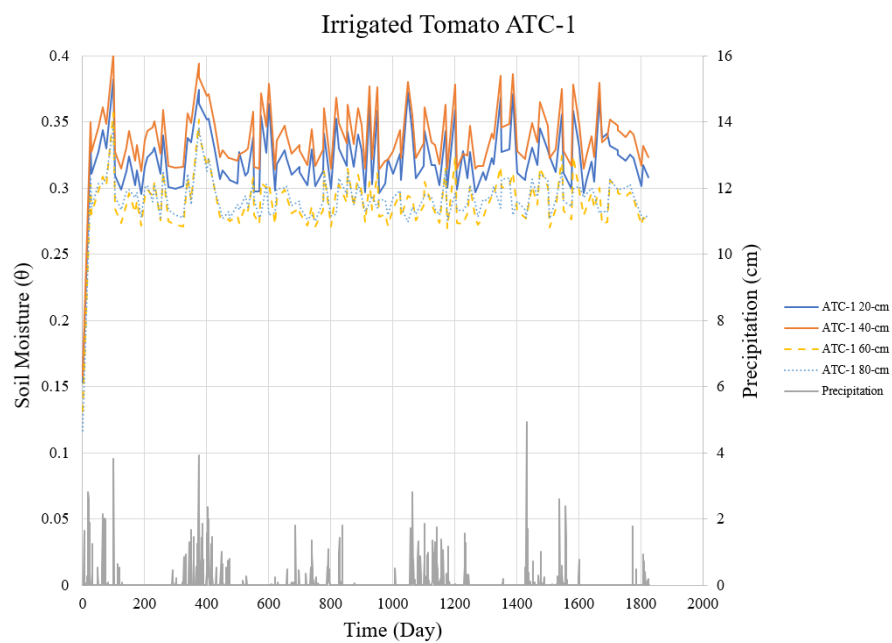
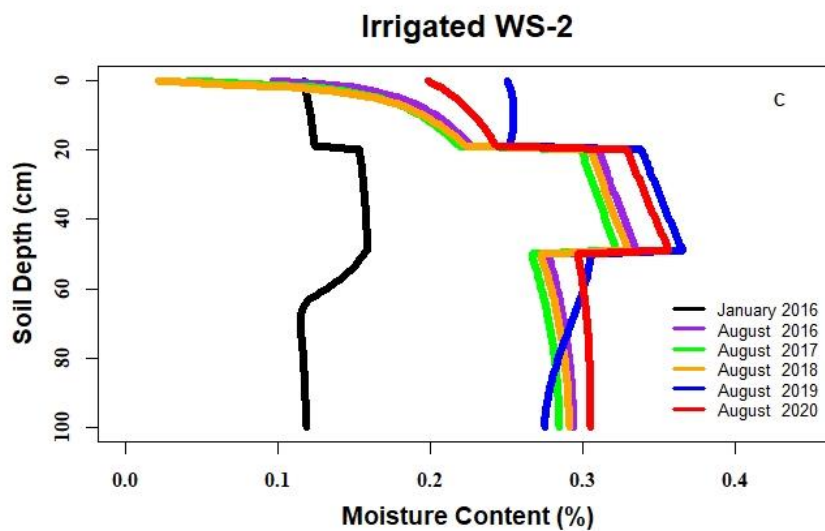


Figure S3.6. Seasonal moisture content for irrigated ATC-1 biochar.



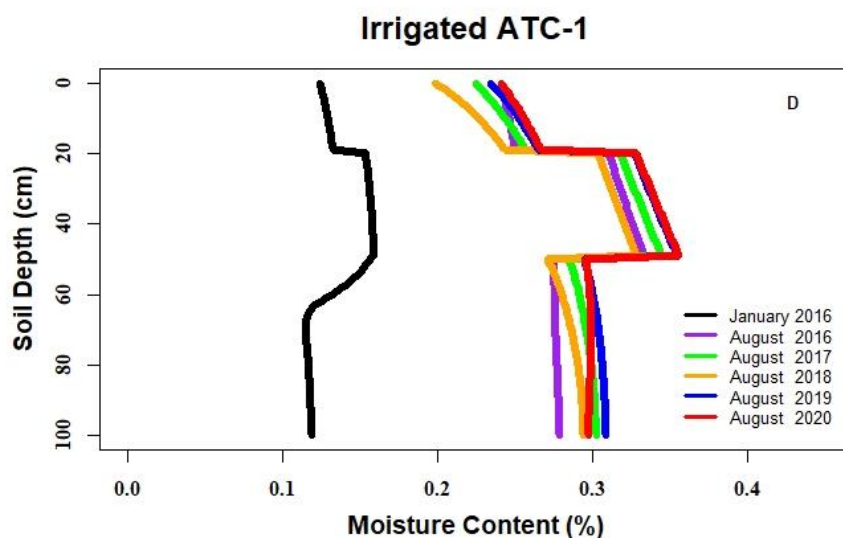


Figure S3.7. Moisture profile over time for irrigated WS-2 (C) and irrigated ATC-2 (D).

**Note: Energy cost of applying water**

Assume a conventional pump with 100 GPM & operation cost of \$7.17/hr (\$0.14/KWH \* 48 KWH/hr + \$0.45 maintenance)

[https://www.eia.gov/electricity/monthly/epm\\_table\\_grapher.php?t=epmt\\_5\\_6\\_a](https://www.eia.gov/electricity/monthly/epm_table_grapher.php?t=epmt_5_6_a)

<https://www.farmprogress.com/compare-costs-irrigation-pumping>

Control = 1,015,570 gal / 100 GPM = 10,156 min / 60 min/hr = 169.3 hrs \* \$7.17 = **\$1,213**

AS-2 = 632,694 gal / 100 GPM = 6,327 min / 60 min/hr = 105.4 hr \* \$7.17 = **\$756**

WS-2 = 692,434 gal / 100 GPM = 6,924 min / 60 min/hr = 115.4 hr \* \$7.17 = **\$827**

ATC-1 = 906,953 gal / 100 GPM = 9,069 min / 60 min/hr = 151.2 hr \* \$7.17 = **\$1,084**

Control vs AS-2 = \$ 457 + \$82 (cost water/AF) = + **\$539**

Control vs WS-2 = \$ 386 + \$69 (cost water/AF) = + **\$455**

Control vs ATC-1 = \$ 129 + \$24 (cost water/AF) = + **\$153**

## Appendix C: Supplemental for Chapter 4

### Summer 2022 Soil Column Experiment: Tomato

**Location:** UCM Greenhouse  
**Latitude:** 37.363991 **Longitude:** -120.422444  
**Experiment Duration:** July 2022 - December 2022

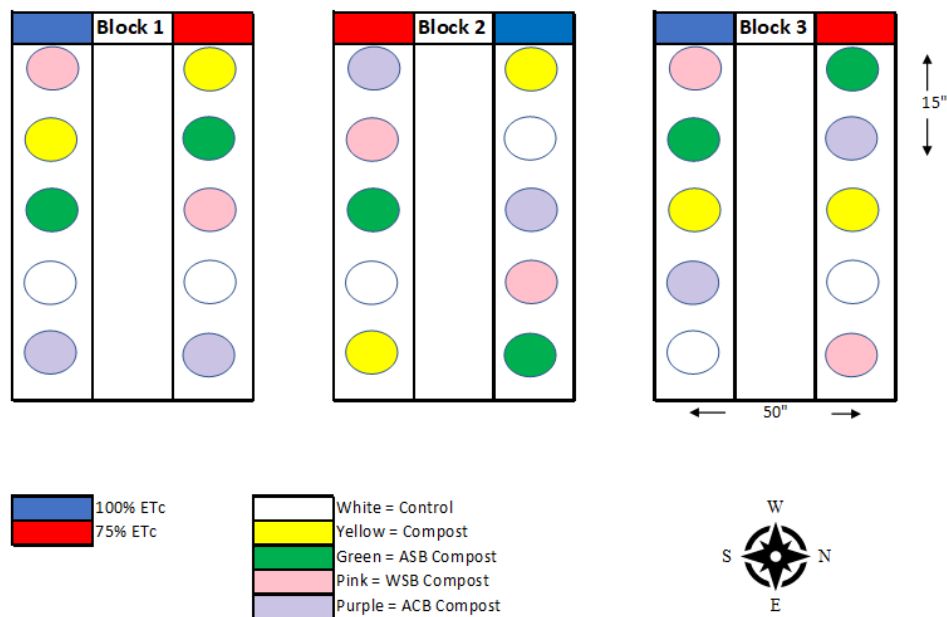


Figure S4.1. Column Experimental Design



Figure S4.2. 1X Mobile Pyrolizer

Table S4-1. Tomato yield. Dataset analyzed using a two-way ANOVA, followed by Tukey-HSD test given statistical significance detected. Value with letter's indicate

statistically significant ( $p < 0.10$ ) among soil treatment, whereas value with the \* asterisk indicate statistical significance across irrigation level.

Yield	WSA	ASB	ACB	Compost	Control
Biomass 100% ET <sub>c</sub> (g)	32.2	47.3	26.3	31.0	66.7
Biomass 75% ET <sub>c</sub> (g)	45.9	35.9	48.1	49.8	54.0
Fruit 100% ET <sub>c</sub> (g)	68.9	52.6	45.9	48.9 *	22.0
Fruit 75% ET <sub>c</sub> (g)	27.0	31.3	37.2	11.3	29.5
Brix 100% ET <sub>c</sub> (%)	5.89 <b>b</b>	8.33 <b>a</b>	7.11 <b>ab</b>	5.89 <b>b</b>	5.50 <b>b</b>
Brix 75% ET <sub>c</sub> (%)	6.50 <b>b</b>	8.22 <b>a</b>	10.0 <b>a*</b>	7.11 <b>b*</b>	9.59 <b>a*</b>

Table S4-2 Water Droplet Penetration Test

Column Treatment	*WDPT (s)	Class
Control	< 1	Non-repellent
Compost	> 3600	Extremely repellent
ASB 5%	> 3600	Extremely repellent
WSB 5%	> 3600	Extremely repellent
ACB 5%	> 3600	Extremely repellent

\*Mean of 9 measurements.

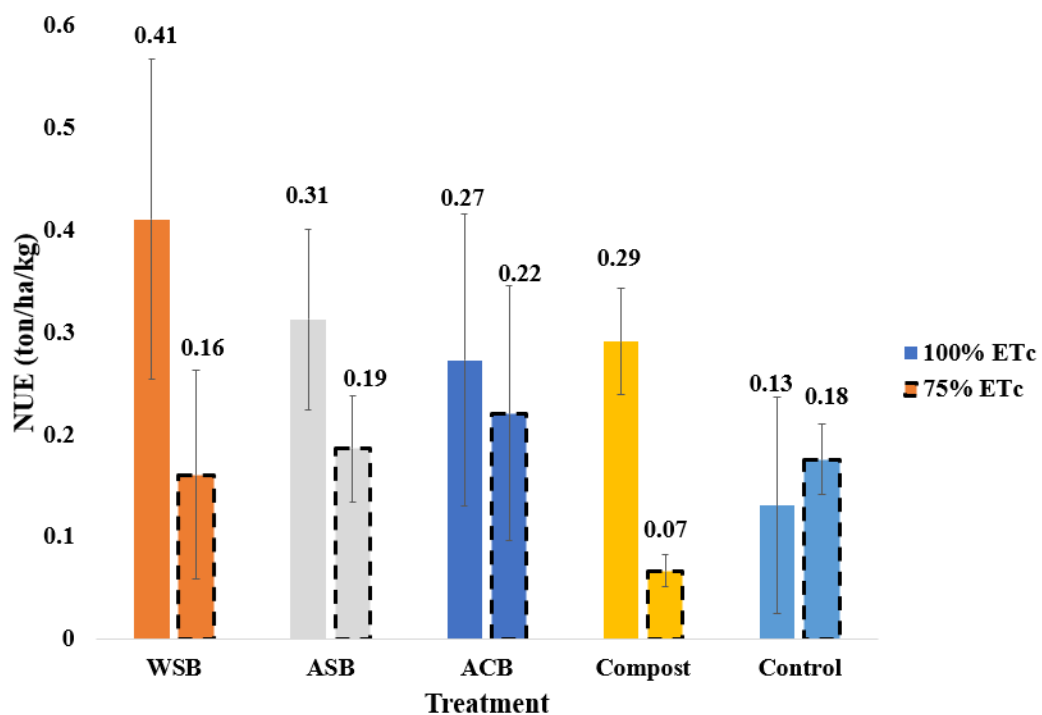
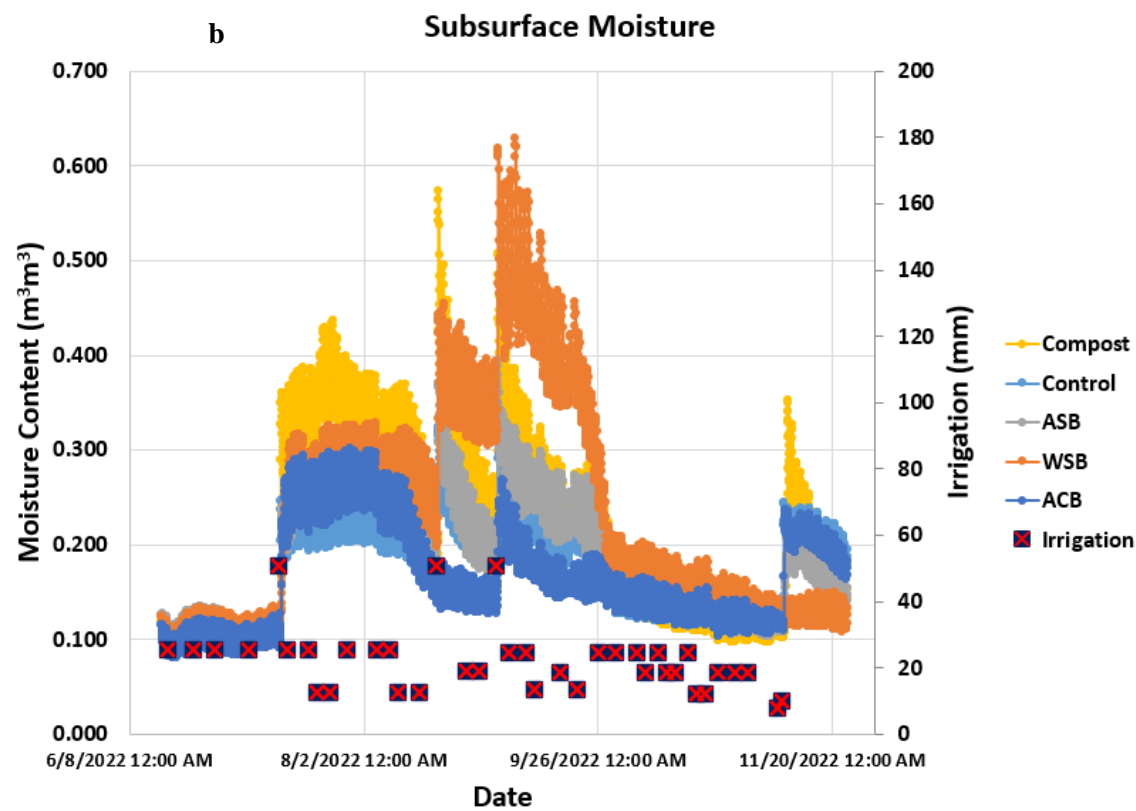
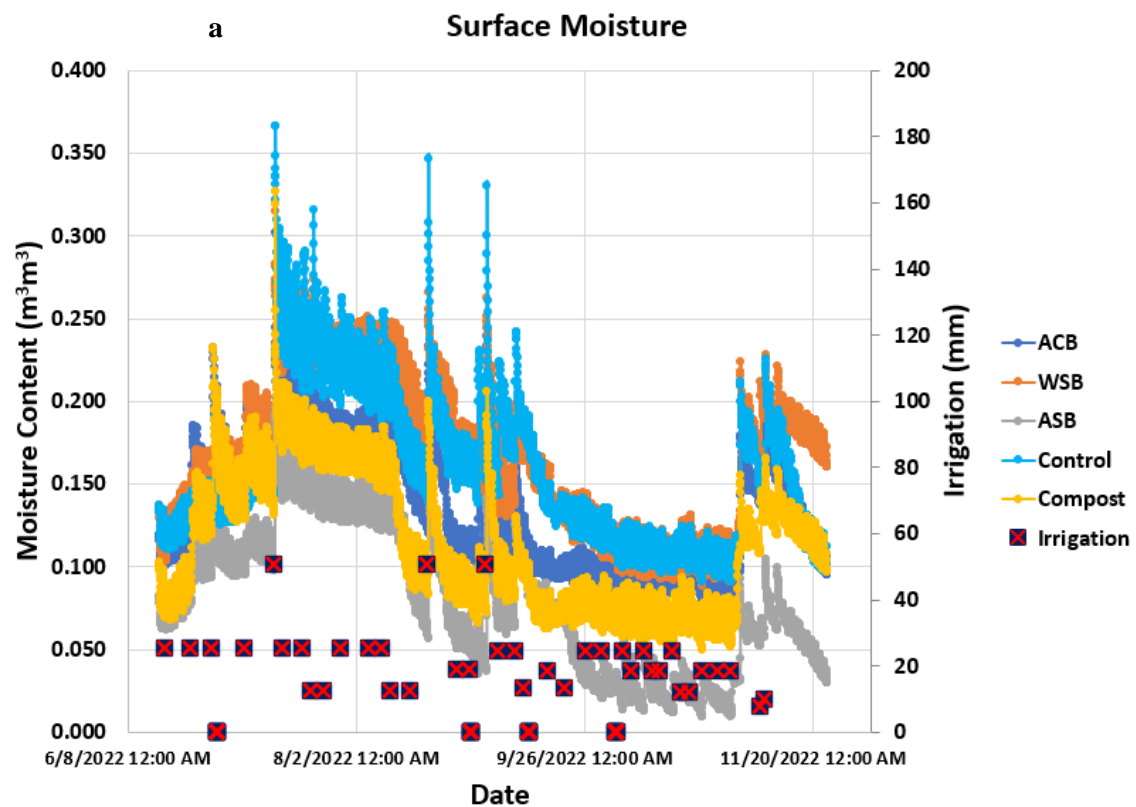


Figure S4.3. Nitrogen Use Efficiency, expressed in ton/hectare/ kg of N applied. Mean of three replications with standard error bar.



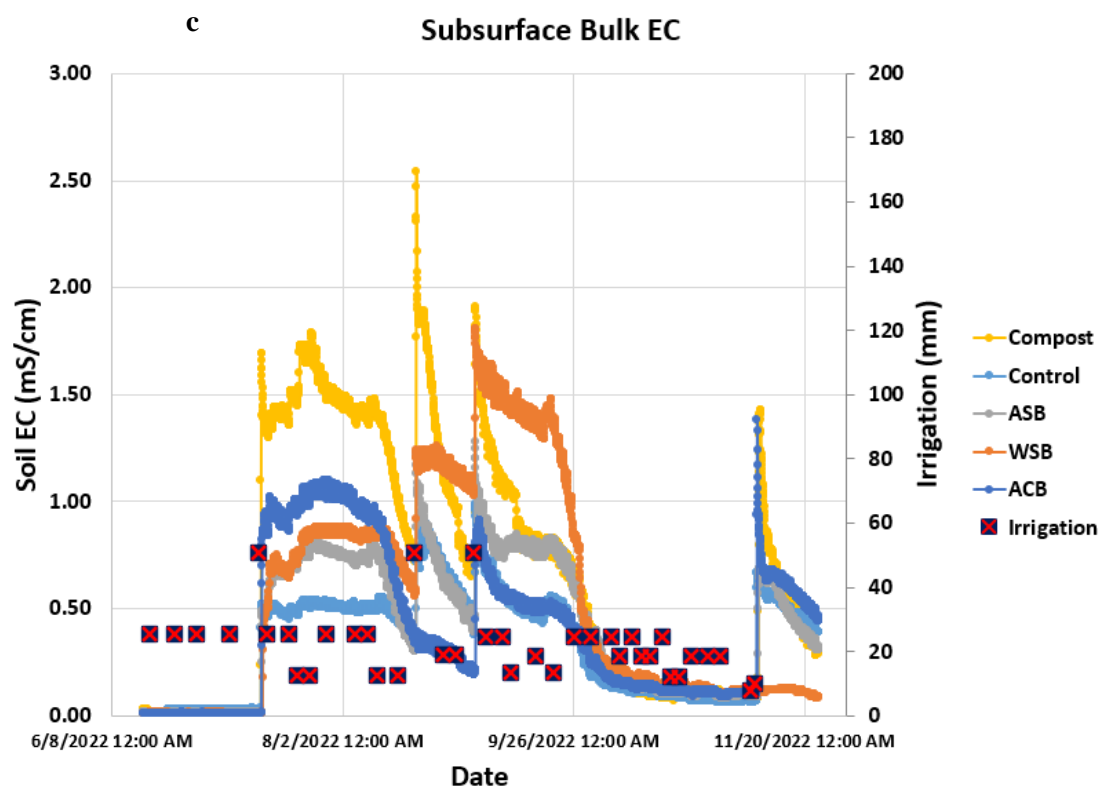


Figure S4.4. Surface, subsurface moisture, and subsurface electrical conductivity in tomato study (a, b, and c)

Table S4-3 Mean fractional groundcover ( $n = 3$ ), measured with the Canopeo Apps. Data analyzed using a two-way ANOVA, followed by Tukey-HSD test given statistical significance detected. Value with the \* asterisk indicate statistical significance across irrigation level.

Date	Irrigation	WSB	ASB	ACB	Compost	Control
		F <sub>c</sub> (%)				
7-25-2022	100% ETc	0.007	0.007	0.007	0.007	0.008
	75% ETc	0.007	0.007	0.007	0.007	0.008
8-19-2022	100% ETc	4.47	5.37	5.15	5.95	4.74
	75% ETc	4.47	5.37	5.15	5.95	4.74
9-14-2022	100% ETc	20.47*	13.16	14.40*	15.72*	14.72*
	75% ETc	7.77	9.57	9.21	10.13	9.44
10-7-2022	100% ETc	28.84	17.42	20.87	23.12	28.15
	75% ETc	20.35	21.14	18.62	24.82	22.81
10-26-2022	100% ETc	30.41	28.15	18.75	27.88	34.88
	75% ETc	30.70	26.78	30.25	36.37	34.23
11-14-2022	100% ETc	17.38	24.51	11.40	15.80	22.53
	75% ETc	16.85	16.09	17.65	13.57	20.04

\*9-14-2022 Irrigation  $p = 0.0123$

Table S4-4. Mean plant chlorophyll content (n = 3) measured throughout the season using the SPAD 502 meter. Data were analyzed using a two-way ANOVA, followed by Tukey-HSD test given statistical significance detected. Value with letter's indicate statistically significant ( $p < 0.10$ ) among soil treatment, whereas value with the \* asterisk indicate statistical significance across irrigation level.

Date	Irrigation	WSB	ASB	ACB	Compost	Control
7-25-2022	100% ETc	49.70	51.15	49.00	49.76	51.35
	75% ETc	49.70	51.15	49.00	49.76	51.35
8-19-2022	100% ETc	59.68 <b>a</b>	61.08 <b>a</b>	55.03 <b>b</b>	59.58 <b>a</b>	57.23 <b>a</b>
	75% ETc	59.68 <b>a</b>	61.08 <b>a</b>	55.03 <b>b</b>	59.58 <b>a</b>	57.23 <b>a</b>
9-14-2022	100% ETc	59.95 <b>a</b>	54.73 <b>ab</b>	55.79 <b>ab</b>	50.27 <b>b</b>	56.31 <b>ab</b>
	75% ETc	57.50 <b>ab</b>	58.02 <b>a</b>	56.18 <b>ab</b>	54.46 <b>b</b>	53.49 <b>ab</b>
10-7-2022	100% ETc	58.98 <b>a</b>	59.88 <b>ab</b>	56.94 <b>ab</b>	53.12 <b>b</b>	56.36 <b>b</b>
	75% ETc	59.79 <b>a</b>	55.93 <b>ab</b>	60.26 <b>ab</b>	58.19 <b>ab</b> *	56.24 <b>b</b>
10-26-2022	100% ETc	58.84	61.20	56.38	60.01	56.52
	75% ETc	65.59 *	64.18	63.74 *	65.27 *	66.50 *
11-14-2022	100% ETc	46.47 <b>ab</b>	54.49 <b>a</b>	44.60 <b>b</b>	45.40 <b>b</b>	46.98 <b>ab</b>
	75% ETc	52.52	51.87	53.82 *	51.21	50.19

\*8-19-2022 Treatment  $p = 0.00438$

\*9-14-2022 Treatment  $p = 0.0186$

\*10-7-2022 Treatment  $p = 0.0083$ , Treatment x Irrigation = 0.0025

\*10-26-2022 Irrigation  $p = 3.01E-011$

\*11-14-2022 Irrigation  $p = 0.0015$ , Treatment x Irrigation = 0.0714